2010

LOCAL SYNAPTIC NETWORK INTERACTIONS IN THE DENTATE GYRUS OF A CORTICAL CONTUSION MODEL OF POSTTRAUMATIC EPILEPSY

Robert F. Hunt III
University of Kentucky, bobby.hunt@uky.edu

Abstract of Dissertation

Robert F. Hunt, III

The Graduate School
University of Kentucky
2010

LOCAL SYNAPTIC NETWORK INTERACTIONS IN THE DENTATE GYRUS OF A CORTICAL CONTUSION MODEL OF POSTTRAUMATIC EPILEPSY

ABSTRACT OF DISSERTATION

A dissertation submitted in partial fulfillment of the requirements for the Doctor of Philosophy in the College of Medicine at the University of Kentucky

By

Robert F. Hunt, III

Lexington, Kentucky

Director: Dr. Bret N. Smith, Associate Professor of Physiology

Lexington, Kentucky

2010

ABSTRACT OF DISSERTATION

LOCAL SYNAPTIC NETWORK INTERACTIONS IN THE DENTATE GYRUS OF A CORTICAL CONTUSION MODEL OF POSTTRAUMATIC EPILEPSY

Posttraumatic epilepsy is a common consequence of brain trauma. However, little is known about how long-term changes in local excitatory and inhibitory synaptic networks contribute to epilepsy after closed-head brain injury. This study adapted a widely used model of experimental brain injury as a mouse model of posttraumatic epilepsy. Behavioral seizure activity and alterations in synaptic circuitry in the dentate gyrus were examined in mice after experimental cortical contusion brain injury. Spontaneous behavioral seizures were observed in 20% of mice after moderate injury and 36-40% of mice weeks after severe injury. In the dentate gyrus, most mice displayed regionally localized mossy fiber reorganization ipsilateral to the injury that was absent in control mice or sections contralateral to the injury. Extracellular field and whole-cell patch clamp recordings were performed in acute brain slice preparations of the dentate gyrus. Dentate granule cells displayed spontaneous and evoked activity that was consistent with network synchronization and the formation of recurrent excitatory network only in slices that had posttraumatic mossy fiber sprouting. The excitability of surviving hilar GABAergic interneurons, which provide important feedback inhibition to granule cells, was examined at similar time points. Cell-attached and whole-cell voltage-clamp recordings revealed increased spontaneous and glutamate photostimulation-evoked excitatory input to hilar GABA neurons ipsilateral to the injury, versus control and contralateral slices. Despite increased excitatory synaptic input to interneurons, whole-cell voltage-clamp recordings revealed a reduction in inhibitory synaptic input to granule cells. These findings suggest that there are alterations in excitatory and inhibitory circuits in mice with posttraumatic mossy fiber sprouting and seizures after cortical contusion head injury.

KEYWORDS: Traumatic brain injury, mossy fiber sprouting, seizure, synaptic excitation, synaptic inhibition.

Robert F. Hunt, III

April 21, 2010

LOCAL SYNAPTIC NETWORK INTERACTIONS IN THE DENTATE GYRUS OF A CORTICAL CONTUSION MODEL OF POSTTRAUMATIC EPILEPSY

By

Robert F. Hunt, III

Dr. Bret N. Smith
Director of Dissertation

Dr. Ok-Kyong Park-Sarge
Director of Graduate Studies

April 21, 2010
Date

RULES FOR THE USE OF DISSERTATIONS

Unpublished dissertations submitted for the Doctor's degree and deposited in the University of Kentucky Library are as a rule open for inspection, but are to be used only with due regard to the rights of the authors. Bibliographical references may be noted, but quotations or summaries of parts may be published only with the permission of the author, and with the usual scholarly acknowledgements.

Extensive copying or publication of the dissertation in whole or in part requires also the consent of the Dean of the Graduate School of the University of Kentucky.

A library that borrows this dissertation for use by its patrons is expected to secure the signature of each user.

NAME	DATE

DISSERTATION

Robert F. Hunt, III

The Graduate School
University of Kentucky
2010

LOCAL SYNAPTIC NETWORK INTERACTIONS IN THE DENTATE GYRUS OF A CORTICAL CONTUSION MODEL OF POSTTRAUMATIC EPILEPSY

DISSERTATION

A dissertation submitted in partial fulfillment of the requirements for the Doctor of Philosophy in the College of Medicine at the University of Kentucky

By

Robert F. Hunt, III

Lexington, Kentucky

Director: Dr. Bret N. Smith, Associate Professor of Physiology

Lexington, Kentucky

2010

For my wife, Courtney,
and my parents, Bob and Dawn Hunt

ACKNOWLEDGEMENTS

I wish to first express great appreciation for my advisor, Dr. Bret Smith, for providing the excellent mentorship, support, and resources that allowed me to carry out this thesis work and to freely pursue research projects. With his extensive knowledge and consistent enthusiasm for my project, he has provided me excellent training in basic neurophysiology of the normal, injured, and epileptic brain. I am also grateful to members of my dissertation committee: Dr. Stephen Scheff, Dr. Kathryn Saatman, and Dr. Steven Estus. Their constructive comments have greatly improved this thesis by challenging me to critically evaluate my work. Moreover, this work would not have been possible without the support and collaboration of Dr. Scheff, for which I am grateful.

I am particularly appreciative of Dr. M. Deepak Bhaskaran and Dr. Andreí Derbenev for their instruction and technical support in slice electrophysiology. Thanks also to Dr. Andrea Zsombok, Dr. Hong Gao, Stephen Springer, Dan Liu, Dr. Kevin Williams, Dr. Peter Gyarmati, and other past and present members of the Smith Lab.

I have greatly enjoyed my time as a graduate student in the Department of Physiology at University of Kentucky. Thanks to the faculty for providing excellent training in systems physiology, and the past and present directors of graduate studies, Dr. Steve Estus and Dr. Ok-Kyong Park-Sarge, for their guidance throughout my graduate training. I would also like to thank Dr. Tom Getchell, Dr. Jim Geddes, Christy Anderson, and members of the grant writing tutorial class for their positive criticism and guidance during the writing of my fellowship applications.

Thanks to the Department of Cell and Molecular Biology, Tulane University; where I initially started graduate school; and the Department of Anatomy and Neurobiology, Medical College of Virginia at Virginia Commonwealth University; for hosting me during Hurricane Katrina. Thanks especially to Dr. John Bigbee for help in getting me into courses after the hurricane and to Dr. Richard Leatherman for providing me a place to live during my semester at VCU.

I greatly appreciate the mentorship and support of Dr. David DeWitt, Dr. Norm Reichenbach, Dr. Paul Sattler, and members of the Department of Biology at Liberty University who encouraged me to pursue a career in research.

Naturally, this project would never have been feasible without the support of my wife, Courtney, who has been patient with me during long work hours; and of course my parents, who have always promoted the pursuit for knowledge and truth. I would also like to thank all of my family and friends who have helped me in numerous ways.

This work was carried out in the Department of Physiology, University of Kentucky Medical College, during the years 2006-2010. The project was financially supported by an Epilepsy Foundation training fellowship and by the National Institutes of Health.

TABLE OF CONTENTS

LIST OF TABLES

LIST OF FIGURES

Chapter 1
Introduction to posttraumatic epilepsy

Posttraumatic epilepsy (PTE) is a common long-term consequence of traumatic brain injury (TBI) for which there is currently no effective treatment. The underlying pathogenesis by which the brain becomes epileptic after TBI is not well understood. This is partially due to a relative lack of experimental models; i.e., animal models of head injury that develop spontaneous seizures (Pitkanen and McIntosh, 2006). This introduction provides a brief review of the functional anatomy associated with the development of acquired epilepsy. That is, the neurophysiological and structural abnormalities that are believed to underly a propensity of the injured brain to generate spontaneous seizures. Emphasis is placed on modifications of synaptic networks in the injured dentate gyrus. The hippocampus has long been recognized as an important structure in epilepsy (Lothman et al., 1991). The dentate gyrus is particularly susceptible to injury, often undergoes time-dependant structural reorganization, and is a widely used model system for altered synaptic circuitry of cortical structures in epilepsy (Dudek and Spitz, 1997; Dudek and Sutula, 2007; Sutula and Dudek, 2007; Nadler, 2003).

1.1 History of epilepsy

Epilepsy is an ancient brain disorder. The earliest written record of seizures is found in the *Sakikku*, an ancient Babylonian medical text, whereby epilepsy was referred to as "the falling disease" (Eadie and Baldin, 2001). The term "epilepsy" is derived from the Greek word *epilavainem*, meaning "to be seized," which describes what was generally believed to be the supernatural act of a god upon an individual. This belief was later refuted by Hippocrates when he wrote "On the Sacred Disease" in 400 B.C., regarding seizures as a disorder of the brain. Some speculate that a boy described in the Gospel of Mark 9:14-29, from whom Jesus expelled an *unclean spirit*, suffered from epileptic seizures. The boy periodically experienced violent convulsions since childhood that included falling to the ground, loss of speech, gnashing teeth, foaming at the mouth, and becoming rigid. However, the modern medical understanding of epilepsy did not

come until the late-1800's when John Hughlings Jackson and colleagues described a seizure as "an occasional, an excessive, and a disorderly discharge of nerve tissue on muscles." Jackson offered detailed descriptions for a number of different epilepsies, especially those with acquired etiologies. Later, in 1929, Hans Berger developed the electroencephalogram (EEG), which allowed electrical field potentials to be recorded from the surface of the brain (Eadie and Baldin, 2001). This invention has proven to be a powerful tool for studying and diagnosing epilepsy.

Henry Gustav Molaison (HM) is perhaps the most famous modern example of PTE (Scoville and Milner, 1957). HM suffered from intractable generalized seizures, presumably from a bicycle accident as a child, and underwent bilateral medial temporal lobe resection. While seizures became less incapacitating after surgery, HM could no longer commit new events to long-term memory. This case emphasized the importance of the hippocampal formation and surrounding limbic areas in seizure generation and normal memory function.

1.2 Definitions

PTE refers to a recurrent, unprovoked, *spontaneous* seizure disorder (i.e., epilepsy) after TBI (Fisher et al., 2005; Agrawal et al., 2006). TBI is to be distinguished from other types of brain insults (e.g., brain tumor) which also carry an increased risk for epilepsy (Herman, 2002). TBI refers to a brain insult produced by a sudden, mechanical force that damages the brain (NINDS, 2010). A seizure is a transient clinical manifestation of abnormal, excessive, and synchronous neuronal activity (Lothman et al., 1991; Fisher et al., 2005). Seizures often involve a change in behavior (McNamara JO, 1994, 2006; Fisher et al., 2005). Epileptogenesis refers to the transformation process by which the normal brain is altered to generate epileptic activity. Structural alterations in neural circuitry – due to progressive neuronal damage and "self-repair" mechanisms – develop through a latent period of variable time and culminate with the emergence of spontaneous, recurrent, seizures (Dudek and Spitz, 1997). Chronic seizures that arise from one or several regions of the temporal lobe are referred to as temporal lobe epilepsy (TLE), which is the most common form of epilepsy (Engel et al., 1997).

1.3 Epidemiology

Greater than one million people are presented for medical care each year in the United States after sustaining a head injury (Faul et al., 2010). The highest rate of TBI occurs in young adults aged 15-24, but children under age 5 and persons older than 75 are also at an increased risk. Additionally, most studies suggest that males are about three times more likely to sustain TBI than females. The leading causes of TBI include falls (28%), motor vehicle accidents (20%), and being struck by objects (19%). While the incidence of epilepsy in the general population is about 1 - 2% (Hauser and Hesdorffer, 1990), the overall incidence of epilepsy is 7-39% after severe closed head injury and as high as 57% after penetrating injury (Caveness et al., 1979; Salazar et al., 1985; Annegers et al., 1998; Asikainen et al., 1999; Herman et al., 2002; Englander et al., 2003). Approximately 20% of all symptomatic (acquired) epilepsies are the result of TBI (Hauser et al., 1991). The latency from insult to seizure onset is variable, but a large majority of patients have onset of spontaneous seizures within one year after injury (Caveness et al., 1979; Salazar et al., 1985; DaSilva et al., 1990; Englander et al., 2003). However, seizure latency may depend on the age at which trauma occurs; children often have a shorter time to seizure onset than adults (Asikainen et al., 1999). PTE occurs as TLE in 35-62% of trauma patients (Diaz-Arrastia et al., 2000; Hudak et al., 2004).

1.4 Risk factors

Injury severity is considered the major determining factor for developing a seizure disorder after brain trauma (Annegers et al., 1998; Herman, 2002; Englander et al., 2003). The severity of TBI is most commonly categorized based on a *Glasgow Coma Scale* (GCS) scoring procedure (Teasdale and Jennett, 1974). This scale relies on information regarding visual, motor, and verbal responses in the acute phase to provide scores that range from 3 (coma state) to 15 (normal function). Head injury severity is often classified based on this system as mild (GCS 13-15), moderate (GCS 9-12), or severe (GCS≤8). Annegers et al (1998) reported that the 30 year cumulative incidence for convulsive seizures was 2.1% for mild, 4.2% for moderate, and 16.7% for severe closed-head TBI.

Englander et al. (2003) found that the cumulative probability for developing spontaneous posttraumatic seizures by 2 years post-injury was 16.8% for mild, 24.3% for moderate, and 8.0% for severe TBI.

Focal brain damage and cortical contusions to the frontal, temporal, or parietal lobes are the next most important risk factor for PTE (D'Alessandro et al., 1982; Englander et al., 2003). Several other risk factors for PTE have been identified, many of which are associated with focal lesions: dural penetration, depressed skull fracture, intraparenchymal hemorrhage, epidural and/or subdural hematomas, reduced brain volume, prolonged impaired consciousness, and injury-induced seizures (Salazar et al., 1985; Annegers et al., 1998; Asikainen et al., 1999; Englander et al., 2003; Frey et al., 2003). It is also likely that genetic background, agent of injury, and acute medical treatments influence the risk of developing PTE; however, the contribution of personal traits and injury dynamics in epilepsy has not been well established (Pitkanen and McIntosh, 2006).

1.5 Classification of neurotrauma

Several classification schemes have been derived for TBI (Saatman et al., 2008). One method is to categorize injuries based on the biomechanical force exerted on the brain (i.e., the physical mechanism of injury) (Goldsmith, 1966; McLean and Anderson, 1997; Saatman et al., 2008). There are two primary types of mechanical loading that produce brain trauma: static and dynamic. Static loading occurs when gradual forces are applied to the brain, e.g., compression of the head by a large object. Dynamic loading is further divided into impact and impulsive loading. Impact loading occurs when contact forces are applied to the brain; e.g., the head strikes or is struck by an object. Impulsive loading is thought to be due to tissue distortion by noncontact (inertial) forces; e.g., a sudden head motion without significant physical contact. Contact forces often produce more focal tissue damage (e.g., cortical contusions, vascular injuries such as epidural or subdural hematomas, and tearing of brain parenchyma), whereas noncontact forces typically produce more diffuse brain damage (e.g., diffuse axonal injury, diffuse brain

swelling, and edema) (Bullock, 1997). Brain injury often involves both focal and diffuse pathologies (McLean and Anderson, 1997; Saatman et al., 2008).

1.6 Classification of posttraumatic seizures

Like TBI, epilepsy is a heterogeneous disorder with many different types and classification schemes (Lothman et al., 1991). Epileptic seizures can be broadly divided into two groups: partial or generalized. Partial (i.e., focal) seizures originate from a localized brain region (the "epileptic focus"), whereas generalized seizures appear throughout the neocortex. Seizures that disrupt normal cognition or consciousness are referred to as complex, and those that do not are referred to as simple. Seizures that originate in the hippocampal formation often spread to other areas of the brain and are thus classified as complex partial with secondary generalization.

Posttraumatic seizures can be additionally classified according to the time of their presentation after injury: immediate or impact (< 24h after injury), early (< 1 week after injury), and late (> 1 week after injury) (Haltiner et al., 1997; Frey, 2003; Agrawal et al., 2006). This classification scheme is thought to represent different pathophysiological processes (Semah et al., 1998; Agrawal et al., 2006). Immediate and early seizures are considered injury-induced seizures (i.e., provoked) and are not epileptic; because they occur as a direct result of neurologic and systemic abnormalities of the acute trauma. Late, spontaneous, seizures are considered to be PTE, because they reflect permanent changes in neuronal function. Spontaneous seizures are often associated with structural reorganization and remodeling of cortical regions susceptible to injury, such as the dentate gyrus (Dudek and Spitz, 1997).

1.7 The hippocampus and dentate gyrus

The hippocampal formation is a neural structure located in the medial temporal lobe of the cerebral cortex (Amaral and Lavenex, 2007). It was originally named by Italian Julius Caesar Arantius in 1587, who analogized its distinct shape as a curved tube that follows the lateral ventricles to that of a seahorse of Greek mythology (ιππος, *hippos*

= horse, καμπος, *kampos* = sea monster) (Olry and Haines, 1998; Amaral and Lavenex, 2007). Later, the surgeon René Jacques Croissant de Garengeot named the hippocampus "Ammon's Horn", a reference to the ram's horns of the Egyptian god of Amun (Lewis, 1922; Amaral and Lavenex, 2007). The general anatomy of the hippocampal formation remains similar across mammalian species (Amaral and Lavenex, 2007). However, in the rodent it is more of a C-shaped structure. An increasingly more complex understanding of the functional organization and plasticity of the hippocampal and parahippocampal regions has emerged in the more than 100 years since first being described in detail by Ramón y Cajal (1995). Its important functional role in learning and memory (Zola-Morgan and Squire, 1993), spatial navigation, and neurological disorders such as epilepsy (Lothman et al., 1991) has long been recognized.

1.7.1 Anatomy of the hippocampal formation

The hippocampal formation contains two distinct subregions: the dentate gyrus and the hippocampus proper, which is further subdivided into *Cornu Ammonis* (CA) areas one through three (Lorente de No, 1934; Rosene and van Hoesen, 1987; Lothman et al., 1991; Amaral and Lavenex, 2007; Figure 1.1). The subiculum and entorhinal cortex are sometimes also included in the term "hippocampal formation" (Amaral and Lavenex, 2007). The cortex of the hippocampal formation is comprised of three layers. The first is a deep polymorph layer that contains fiber tracts and interneurons (i.e., local circuit neurons). In the dentate gyrus, this region is referred to as the hilus. In the hippocampus proper, this region is the stratum oriens. Superficial to the polymorph layer is the principal cell layer. This is the granule cell layer (stratum granulare) of the dentate gyrus, which is a tightly packed layer of 4-8 granule cell somata in thickness. Principal cells of the hippocampus proper are the pyramidal cells of stratum pyramidale. The most superficial layer is referred to as the molecular layer (stratum moleculare). In the dentate gyrus, this region can be subdivided into inner, middle, and outer molecular layers. In CA3, the molecular layer is subdivided into the stratum lucidum; stratum radiatum; and most superficially, the stratum lacunosum-moleculare. The lamination of CA1 and CA2 does not include the stratum lucidum.

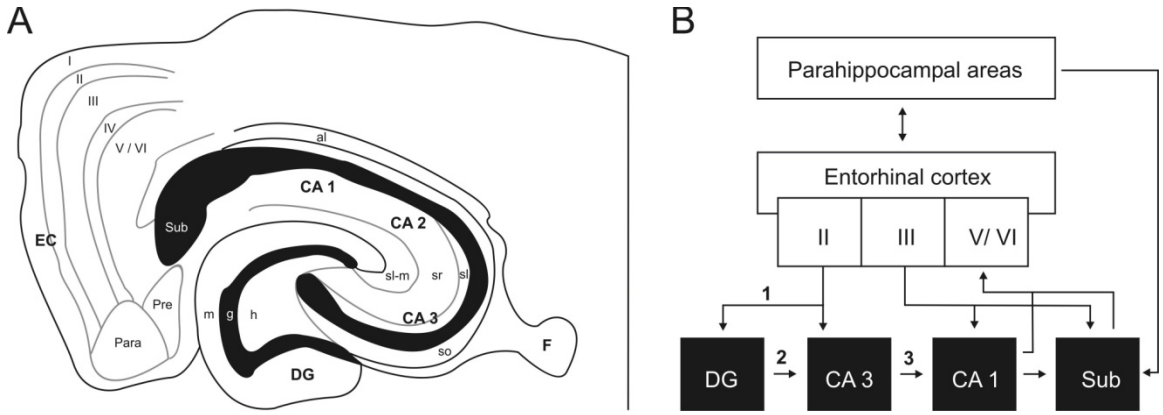

Figure 1.1. Anatomy of hippocampal and parahippocampal regions in the rat brain. A. Anatomical organization of the hippocampus and surrounding regions. **B.** Diagram shows major directional flow of excitatory information through the hippocampus (black boxes). Numbers correspond to pathways in the trisynaptic circuit: 1, perforant pathway; 2, mossy fiber pathway; 3, Schaffer collateral pathway. Abbreviations: EC, entorhinal cortex; DG, dentate gyrus; m, molecular layer; g, granule cell layer; h, hilus (polymorph layer); so, stratum orien; p, pyramidal cell layer; sl, stratum lucidum; sr, stratum radiatum; sl-m, stratum lacunosum-moleculare; al, alveus; Sub, subiculum; Pre, presubiculum; Para, parasubiculum.

1.7.2 Input from entorhinal cortex to the hippocampal formation

The entorhinal cortex contains six cortical layers and forms the main parahippocampal connection to the hippocampus (Lothman et al., 1991; Freund and Busaki, 1996; Amaral and Lavenex, 2007). It is reciprocally connected with the hippocampus as well as other parahippocampal regions, including itself. Superficial layers (I-III) of the entorhinal cortex provide the most prominent input while the deep layers (IV-VI) mainly receive projections from the hippocampus. Entorhinal layer II projections are collectively referred to as the perforant pathway and form synaptic connections with apical dendrites of granule cells and local circuit interneurons throughout the entire extent of the molecular layer of the dentate gyrus. In traditional models, this is the first step of the excitatory polysynaptic entorhinal-hippocampal pathway (Lothman et al., 1991; Freund and Busaki, 1996; Amaral and Lavenex, 2007). Perforant pathway fibers also project to hilar interneurons and to CA3 pyramidal cells, forming connections with pyramidal cell dendrites in the stratum lacunosum-moleculare.

Area CA1 and the subiculum also receive input from the entorhinal cortex, but these inputs arise mainly from layer III.

1.7.3 Connectivity within the hippocampal formation

Transmission of excitatory information between principal neurons of the hippocampal formation is primarily mediated by glutamate binding to ionotropic glutamate receptors. Activation of these receptors increases membrane permeability to positive ions (e.g., Na+) and leads to a depolarizing response of the postsynaptic membrane, i.e., the excitatory postsynaptic potential. The direction of information through the hippocampus is generally considered to be unidirectional (Amaral and Lavenex, 2007). Granule cells in the dentate gyrus project axons, collectively referred to as the mossy fiber pathway, to pyramidal cells and inhibitory interneurons in area CA3. The Schaffer collaterals arise from CA3 pyramidal neurons and project to area CA1 (Andersen et al., 1971). The final step in the polysynaptic pathway is the projection from CA1 pyramidal cells to the subiculum via the alvear pathway. Collectively, the normal flow of excitatory information from entorhinal cortex to dentate gyrus to CA3 to CA1 is commonly referred to as the "trisynaptic pathway" (Andersen et al., 1971; Lothman et al., 1991; Freund and Busaki, 1996). The main hippocampal outputs arise from area CA1 and the subiculum and project to superficial layers of the entorhinal cortex, mainly layers V and VI.

In contrast to the traditional unidirectional model, there are several excitatory backprojections and interconnections within the hippocampus. While granule cells in the dentate gyrus are not normally interconnected, they do form synaptic connections with proximal dendrites of mossy cells in the hilus. Mossy cells, which give rise to associational-commisural fibers, normally project across lamellae to innervate distant granule cells and inhibitory neurons (Amaral, 1978; Ribak et al., 1985; Buckmaster et al., 1996). For this reason, mossy cells have been suggested to be important in regulating lateral inhibition (Buckmaster and Schwartzkroin, 1994). Collaterals of pyramidal cells form an intrinsic recurrent excitatory network in CA3 and, to a lesser extent, CA1. Some reports suggest that CA3 neurons sometimes project back to the hilus and can reach the

inner molecular layer of the dentate gyrus, but these connections are relatively sparse and occur mainly at the most temporal levels of the hippocampus (Scharfman, 2007). Backprojections from CA1 to CA3 have also been described. Additionally, extensive recurrent excitatory connections are also present in the subiculum. Principal cells in all regions of the hippocampal formation form extensive synaptic connections with various types of inhibitory neurons.

1.7.4 $GABA_A$ receptor-mediated inhibition

GABAergic interneurons – i.e., local circuit inhibitory neurons – form robust local synaptic connections with principal cells of the hippocampus and dentate gyrus (Freund and Busaki, 1996). Transmission at these synapses is mediated by γ-aminobutyric acid (GABA), the main inhibitory neurotransmitter of the CNS. GABA primarily acts through ionotropic $GABA_A$ (GABA type A) receptors to increase permeability of chloride and bicarbonate ions (Kaila, 1994). This action leads to a hyperpolarizing response of the postsynaptic membrane, i.e., the inhibitory postsynaptic potential.

Two primary modes of $GABA_A$ receptor-mediated inhibition have been identified: phasic (synaptic) and tonic (extrasynaptic) inhibition (Farrant and Nusser, 2005; Glykys and Mody, 2007; Figure 1.2). Phasic inhibition refers to the transient activation of postsynaptic $GABA_A$ receptors at the synaptic junction following exposure to high concentrations of GABA released from presynaptic vesicles. This form of synaptic communication allows for rapid transmission of information from the presynaptic terminal to the postsynaptic membrane in a spatially and temporally restricted manner. In whole-cell voltage-clamp recordings, synaptic events can be easily identified as inhibitory postsynaptic currents (IPSCs). Small amounts of GABA escape the synaptic cleft and activate high-affinity extrasynaptic $GABA_A$ receptors on the same or adjacent neurons, an event termed “spillover”. Tonic inhibition refers to the persistent activation of these extrasynaptic $GABA_A$ receptors by low concentrations of ambient GABA. Phasic and tonic currents can be blocked by high concentrations of $GABA_A$

receptor antagonists. In whole-cell voltage-clamp recordings the tonic current is reflected by a shift in “holding” current (Figure 1.2 C).

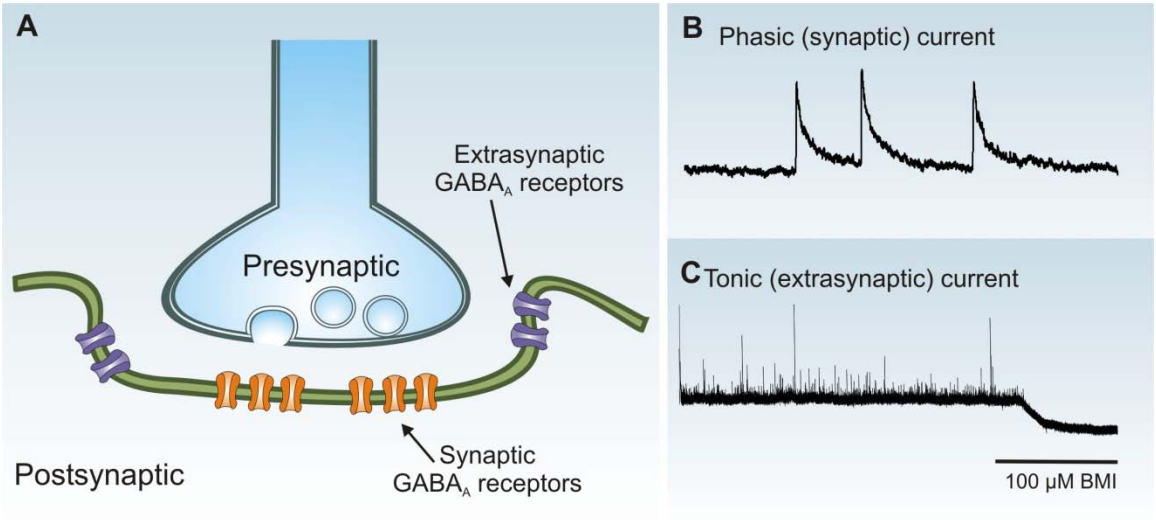

Figure 1.2. Phasic and tonic $GABA_A$ receptor activation. A. Synaptic receptors (orange) are located on the postsynaptic membrane just beneath the presynaptic release site, whereas extrasynaptic receptors (purple) are located away from the synaptic junction. **B.** Phasic (synaptic) IPSCs are rapid events in a whole-cell voltage-clamp recording of a dentate granule cell. **C.** The tonic (extrasynaptic) current in this cell is revealed as a baseline shift after application of the $GABA_A$ receptor antagonist bicuculline methiodide (BMI; 100µM).

1.7.5 Hilar GABAergic interneurons

Inhibitory neurons in the dentate gyrus are diverse and can be identified based on their immunoreactivity for glutamic acid decarboxylase (GAD) – the enzyme that catalyzes the decarboxylation of glutamate to GABA – which is expressed in neurons where GABA is used as a neurotransmitter (Freund and Busaki, 1996; McBain and Fisahn, 2001). Ramon y Cajal (1995) referred to these neurons as “cells with the short axon” and noted that they did not all have the same appearance. Inhibitory neurons can be categorized morphologically, based on their dendritic and axonal arborizations or afferent-efferent connectivity; neurochemically, based on the neuropeptide produced; or physiologically, based on their electrophysiological characteristics (Freund and Busaki,

1996; McBain and Fishan, 2001). Here, interneurons of the dentate gyrus are briefly described based on their morphological characteristics.

Perisomatically-projecting and axo-axonic neurons (Basket and chandelier cells)

Dentate basket cells have somata located in or near the granule cell layer and form divergent perisomatic connections onto cell bodies or proximal dendrites of granule cells (Amaral, 1978; Ribak and Seress, 1983; Han et al., 1993; Kneisler and Dingledine, 1995; Zhang and Buckmaster, 2009). Basket cells are heterogeneous in morphology, afferent input, and neurochemical markers (Freund and Busaki, 1996). A subpopulation of basket cells express the calcium binding protein parvalbumin (Ribak et al., 1990). Studies that combine anterograde tract-tracing with single-cell labeling have suggested these cells receive synaptic contacts from perforant pathway and mossy fiber collaterals (Frostcher and Zimmer, 1983; Ribak and Seress, 1983; Seress and Ribak, 1984; Zipp et al., 1989), and these contacts appear to represent functional connections (Scharfman and Schwartzkroin, 1990; Scharfman et al., 1990). Therefore, basket cells likely participate in both feedforward and feedback inhibition of granule cells. CA3 pyramidal cells have also been shown to occasionally project back to dentate basket cells (Kneisler and Dingledine, 1995).

Chandelier cells (i.e., axo-axonic cells) also have somata located within or near the granule cell layer, and they are distinguished by their preferential projections to axon initial segments of principal neurons (Soriano and Frotscher, 1989; Han et al., 1993; Buhl et al., 1994). Dendrites of chandelier cells concentrate in the outer one-third of the molecular layer (Soriano and Frotscher, 1989; Han et al., 1993; Buhl et al., 1994), which suggests that these neurons mainly receive excitatory input from the perforant pawthway or associational-commisural fibers. Therefore, these neurons likely provide important feedforward inhibition of granule cells.

Dendritically-projecting neurons (HIPP, HICAP, MOPP cells)

Hilar interneurons associated with the perforant pathway (HIPP) have cell bodies located in the hilus subjacent to the granule cell layer (Han et al., 1993; Freund and Busaki, 1996). Their dendrites are mainly restricted to the hilus and their axons localize in the outer-two thirds of the molecular layer where they synapse with distal dendrites of granule cells (Halasy and Somogyi, 1993; Han et al., 1993; Buckmaster and Schwartzkroin, 1995; Freund and Busaki, 1996; Zhang and Buckmaster, 2009). HIPP cells have large axonal arborizations, and it has been estimated that a single neuron may innervate up to one-eighth of the entire dentate gyrus (Han et al., 1993). These neurons can also project across the hippocampal fissure and make contacts with CA1 pyramidal neurons (Han et al., 1993; Buckmaster and Schwartzkroin, 1995). Interneurons that contain the peptide somatostatin have similar afferent-efferent connectivity to HIPP cells (Han et al., 1993), and the terms "somtatostatin-positive interneuron" and "HIPP cell" have been considered synonymous (Freund and Busaki, 1996). However, neuropeptide Y is also sometimes colocalized with somatostatin in these neurons (Acsády et al., 1997; Sík et al., 1997).

Hilar commissural-associational pathway (HICAP) related neurons have somata in the hilus or at the border of the hilus and the granule cell layer (Halasy and Somogyi, 1993; Han et al., 1993; Soriano and Frotscher, 1993; Buckmaster and Schwartzkroin, 1995; Sík et al., 1997). These neurons have dendrites in the hilus and molecular layer (Han et al., 1993; Buckmaster and Schwartzkroin, 1995), suggesting that they participate in feedback and feedforward inhibition of granule cells. Axons of HICAP cells project to the inner molecular layer where they presumably make contacts with granule cell dendrites (Han et al., 1993; Halasy and Somogyi, 1993; Freund and Busaki, 1996; Zhang and Buckmaster, 2009).

Molecular layer interneurons associated with the perforant pathway (MOPP) have cell bodies and dendrites in the molecular layer (Han et al., 1993; Halasy and Somogyi, 1993). Like HIPP cells, these neurons innervate the outer one-third of the molecular layer

where they form synaptic contacts with distal dendrites of granule cells (Han et al., 1993; Halasy and Somogyi, 1993). Thus, MOPP cells are likely to participate in feedforward inhibition of granule cells.

The spatial segregation of GABAergic interneurons innervating granule cells suggests that each cell subtype plays a different functional role in regulating granule cell excitability. Perisomatic inhibition provided by basket and chandelier cells is considered important for controlling and synchronizing principal cell output (Lytton et al., 1991; Cobb et al., 1995; Freund and Buszaki, 1996; Miles et al., 1996; Tamás et al., 2000). Conversely, dendritically projecting GABA neurons (e.g., HIPP cells) are proposed to primarily modulate synaptic efficacy of afferent input to principal cells (Freund and Buszaki, 1996; Miles et al., 1996). However, these cells may also play a role in principal cell synchrony by timing principal cell discharges (Szabadics et al., 2001) Figure 1.3 shows the relative location of somata and the target zone for each of the main GABAergic interneuronal subtypes in the dentate gyrus.

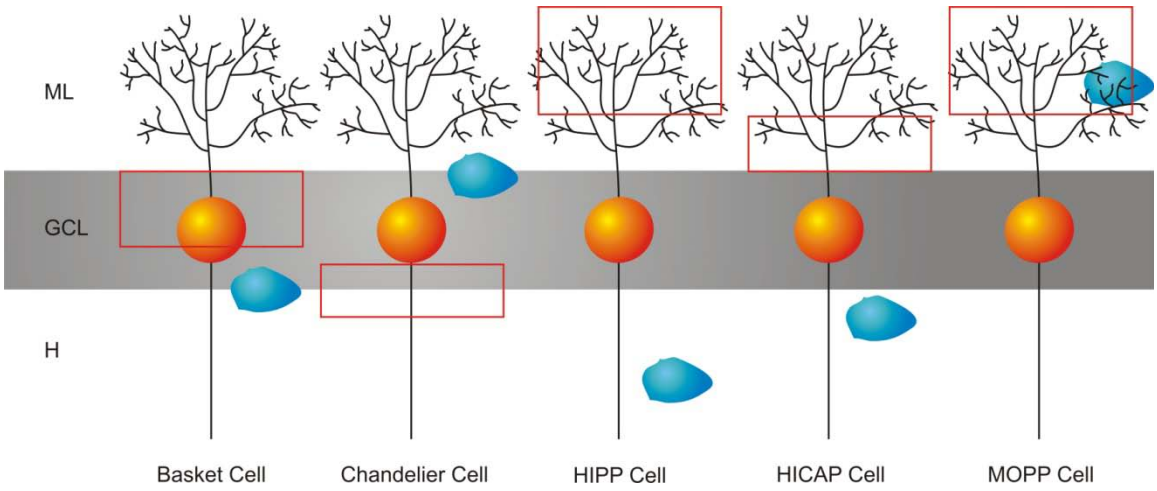

Figure 1.3. Domain specific innervation of granule cells by GABAergic interneurons in the dentate gyrus. The relative location for somata of each inhibitory interneuron subtype (blue) is shown. Each of the interneuronal subtypes has a spatially segregated terminal zone (red box) where they make domain specific synaptic contacts onto dentate granule cells (orange). Abreviations: ML, molecular layer; GCL, granule cell layer; H, hilus. Adapted from Freund and Buszaki (1996).

1.7.6 The dentate "gate"

The dentate gyrus has long been hypothesized to function as a tightly regulated "filter" or "gate" that limits the propagation of excessive excitatory activity between the entorhinal cortex and the hippocampus (Hsu, 2007). This concept is due to the seemingly strategic anatomical location of the dentate gyrus for controlling the flow of information into the hippocampus; i.e., it contains the first cell layer in the "trisynaptic loop." In acute brain slices, dentate granule cells are normally resistant to the spontaneous generation of repetitive synchronous discharges, even in the presence of $GABA_A$-receptor antagonists (Schwartzkroin and Prince, 1978; Cronin et al., 1992; Wuarin and Dudek, 1996; Patrylo and Dudek, 1998). Moreover, previous studies have used electrical stimulation of the entorhinal cortex or perforant pathway to demonstrate that evoked activity can penetrate the normal hippocampus only after high frequency stimulation (Alger and Teyler, 1976; Teyler and Alger, 1976; Lothman et al., 1992; Heinemann et al., 1992; Stringer and Lothman, 1992) or in the presence of $GABA_A$-receptor antagonists (Iijima et al., 1996; Coulter and Carlson, 2007).

The resistance of the dentate gyrus to synchronous activity and propagated discharges from the entorhinal cortex is due, in part, to the intrinsic synaptic circuitry of the dentate gyrus and passive properties of granule cells. Granule cells normally have a relatively negative resting membrane potential in the range of -65 to -85mV (Fricke and Prince, 1984; Staley et al., 1992). This hyperpolarized state creates a relatively high threshold for granule cell activation. Moreover, these cells are resistant to repetitive action potential firing (i.e., they have high spike accommodation during maintained depolarization) (Staley et al., 1992). Granule cells are not normally interconnected, preventing synchronized granule cell discharges, and inhibitory interneurons in the molecular layer and hilus provide robust GABA-mediated inhibition (Freund and Busaki, 1996; Coulter and Carlson, 2007). In contrast, CA3 pyramidal cells have resting membrane potentials of -55mV to -65mV, normally form an interconnected excitatory network (Miles et al., 1984; Miles and Wong, 1986, 1987), and are prone to synchronous activity after blocking GABA-mediated inhibition (Schwartzkroin and Prince, 1978; Miles et al., 1984; Miles and Wong, 1986, 1987). Therefore, these cells are widely

hypothesized to act as an “amplifier” of activity transmitted through the “dentate gate” (Hsu, 2007). Whether the dentate gyrus acts as a “gate,” where electrical activity is blocked in an all-or-none manner (Stringer et al., 1989; Lothman et al., 1992; Stringer and Lothman et al., 1992), or as a “filter,” where electrical activity is blocked only under certain conditions (Hsu, 2007), remains controversial and not fully understood.

1.8 Pathophysiology of acquired epilepsy

For decades, the central dogma in epilepsy research has been that seizures occur due to some type of imbalance between excitatory and inhibitory neurotransmission (Dudek and Spitz, 1997; McCormick and Contreras, 2001; Nadler, 2003). Within this framework, models typically rely on mechanisms whereby excitatory influences are increased and inhibitory influences are decreased, usually in the presence of recurrent excitatory circuits.

1.8.1 Epileptiform activity

Epileptiform activity broadly describes the abnormal electrical activity associated with a seizure. Abnormal fluctuations in cortical field potentials can be recorded from the scalp or dura by EEG in patients and animal models with focal epilepsy (Engel, 1987). These electrical potentials represent synchronized discharges of a population of cortical neurons. Abnormal synchronous discharges that occur as a single event; i.e., a brief (< 250 ms), large amplitude potential observed in the presence of otherwise normal background activity; are referred to as interictal (between seizure) spikes (Matsumoto and Ajmone-Marsan, 1964a; Ayala et al., 1973). In extracellular recordings, synchronous cortical discharges appear as population activity (i.e., a group of neurons that discharge simultaneously). At the level of a single neuron, this activity consists of sustained depolarization and a burst of action potentials (Ayala et al., 1973; Dichter and Ayala, 1987; Lothman et al., 1991; McCormick and Contreras, 2001), often referred to as a paroxysmal depolarizing shift (PDS) in membrane potential. Interictal spikes are used clinically to diagnose epilepsy and identify active regions of epileptic foci (Engel, 1987;

Staley and Dudek, 2006). However, they may not always represent the primary focus from which seizures originate, because EEG can only detect synchronous activity of cortical neurons that are tightly packed together.

Ictal (i.e., seizure) actvity consists of repetitive and rhythmic deflections in the EEG and reverberating depolarizations and action potential firing in single-cell recordings at the "epileptic focus" (Matsumoto and Ajmone-Marsan, 1964b; Ayala et al., 1973; McCormick and Contreras, 2001). Factors underlying the transition from interictal to ictal activity are unclear. However, interictal activity is proposed to drive synaptic networks toward a synchronous state (McCormick and Contreras, 2001; Staley and Dudek, 2006). Recurrent excitatory circuits – which form when principal cells are sufficiently interconnected – have long been proposed as the cellular basis for pathologically synchronous activity (i.e., seizures) (Traub and Wong, 1982; McCormick and Contreras, 2001; Dudek and Spitz, 1997).

1.8.2 Network synchronization

Cellular mechanisms of network synchronization are derived from a basic operation of recurrent excitatory circuits. Glutamate receptor activation leads to a depolarization of cortical neurons. This triggers action potentials and increases in intracellular calcium (i.e., the PDS). The PDS drives repetitive action potentials down the axon which leads to sustained glutamate release and activation of postsynaptic neurons via recurrent collaterals that connect the neurons in a network. The network transition into a synchronized state depends on the probability that excitatory activity will trigger an action potential in postsynaptic cells and whether activity in these neurons is sufficiently strong to propagate excitatory synaptic activity throughout the network.

The functional relationship between recurrent excitatory circuits and network synchronization was first demonstrated in the hippocampus. CA3 pyramidal cells have robust axonal arborizations that connect neighboring pyramidal cells in a recurrent excitatory network (Ramon y Cajal, 1995; Lorente de No, 1934; Nowlin and Babb, 1983; MacVicar and Dudek, 1980; MacVicar and Dudek, 1982; Miles et al., 1984; Miles and Wong, 1986). In normal medium, CA3 neurons are capable of intrinsic bursting, (i.e.,

firing a series of action potentials when sufficiently depolarized), but they normally do not generate this activity spontaneously or in synchrony (Wong et al., 1977; Wong and Prince, 1978; Miles and Wong, 1983). When inhibition is suppressed, the balance between excitation and inhibition is shifted towards excitation. Under these conditions and after surgical isolation from afferent input, pyramidal cells spontaneously generate bursts of action potentials with synchronized onset and offset (Miles et al., 1984; Miles and Wong, 1986, 1987). Dual intracellular recordings from pyramidal cells have demonstrated that a burst of presynaptic action potentials can elicit a burst of action potentials in a postsynaptic neuron (Miles and Wong, 1986, 1987). Connections between two cells which appear to be unconnected in normal medium can be revealed when inhibition is suppressed (Miles and Wong, 1987). Moreover, population activity can be initiated by activation of just a single neuron (Miles and Wong, 1983). This suggests that polysynaptic activity can spread throughout the network by activating recurrent excitatory synapses from just one cell. Therefore, groups of highly interconnected principal cells have the ability to synchronize their output, but synchrony is regulated (or masked) by intrinsic mechanisms and synaptic inhibition.

These types of experiments demonstrated basic characteristics of functional recurrent excitatory circuits. 1) Spontaneous burst activity can be generated after surgical isolation from afferent input. 2) Evoked activity in one group of cells can elicit activity in distant cells of the same interconnected network. Modeling suggests that these events are only observed when there are sufficient excitatory interconnections between cells (Traub and Wong, 1982). Moreover, recurrent excitatory circuits are only revealed when recurrent inhibition is overcome.

A consequence of the interconnectivity of excitatory neurons is the possibility for “runaway” excitation if recurrent excitatory networks are left unchecked by inhibitory networks. If recurrent excitatory circuits are exposed, they can synchronize, and a seizure can occur.

Network changes in epilepsy have been best described in the context of injury by electrical stimulation or repeated seizures. For example, status epilepticus induced by systemic administration of kainic acid or pilocarpine in rodents is followed by the emergence of spontaneous seizures after a short latency of several weeks (Hellier et al.,

1999; Shibley and Smith, 2002). In these models and human TLE, the generation of epileptic activity is associated with specific patterns of neuron loss and the formation of new recurrent excitatory circuits in the dentate gyrus (Dudek and Spitz, 1997; Dudek et al., 2002; Nadler, 2003; Dudek and Sutula, 2007). These changes in neural circuitry are thought to render the brain more susceptible to abnormal network synchronization and seizures after injury.

1.9 Synaptic reorganization of the epileptic dentate gyrus

1.9.1 Mossy fiber sprouting

Excitatory axon sprouting is a defining feature of the injured dentate gyrus in experimental and human TLE. Dentate granule cells, which are not normally interconnected, sprout axon collaterals into the inner molecular layer (i.e., mossy fiber sprouting), which is normally devoid of mossy fiber terminals (Figure 1.4). These dramatic changes in local mossy fiber circuits are relatively easy to detect by Timm's histochemistry and are consistently reproduced in human tissue (de Lanerolle et al., 1989; Sutula et al., 1989; Houser et al., 1990; Babb et al., 1991; Zhang and Houser, 1999) and experimental models of TLE (Nadler et al., 1980; Ben-Ari et al, 1985; Tauk and Nadler, 1985; Cronin and Dudek, 1988; Buckmaster et al., 2002; Buckmaster and Dudek 1997b; Shibley and Smith, 2002). Quantitative anatomical analyses have provided much evidence that sprouted mossy fibers in the inner molecular layer predominantly form new synaptic connections with dendrites of nearby granule cells, versus inhibitory interneurons (Frotscher and Zimmer, 1983; Okazaki et al., 1995; Zhang and Houser, 1999; Wenzel et al., 2000; Buckmaster et al., 2002). These new axon collaterals that sprout into the inner molecular layer typically remain within the normal septotemporal span of granule cell axon collaterals in the hilus, ~600 µm (Buckmaster and Dudek, 1999).

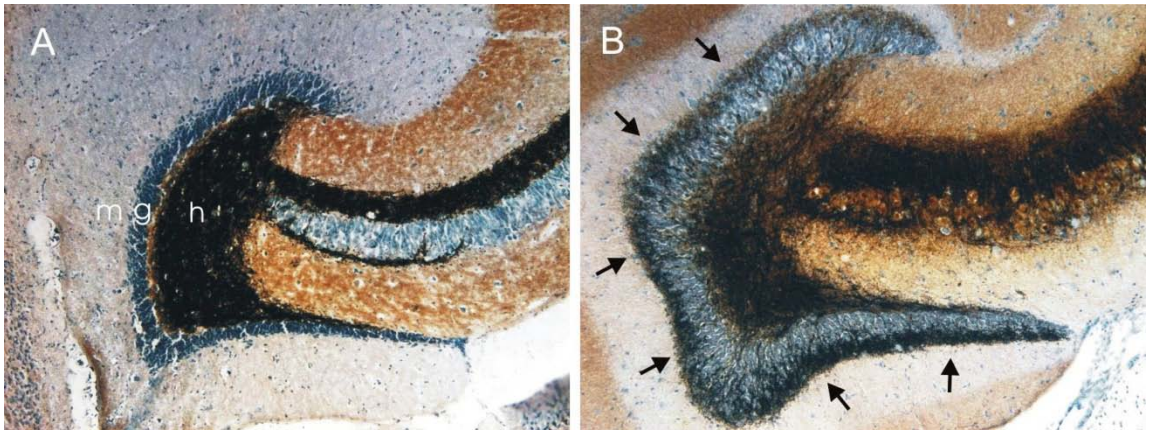

Figure 1.4. Granule cell axons (i.e., mossy fibers) sprout collaterals to dendrites of nearby granule cells after epileptogenic insult. A. Photomicrograph of Timm and Nissl staining in a horizontal section from a control mouse. **B.** Photomicrograph of Timm and Nissl staining in a horizontal section from a mouse that sustained pilocarpine-induced status epilepticus and developed spontaneous seizures. Note the presence of a dense band of Timm staining in the inner molecular layer (arrows), which represents mossy fiber axons and terminals. Abreviations: m, molecular layer; g, granule cell layer; h, hilus.

Several laboratories have independently demonstrated that functional effects of mossy fiber sprouting include the emergence of new recurrent excitatory circuits that are not present in the normal dentate gyrus (Cronin et al., 1992; Wuarin and Dudek, 1996; 2001; Patrylo and Dudek, 1998; Lynch and Sutula, 2000; Winokur et al., 2004). These new circuits have been proposed to form the basis from which synchronous network activity can periodically arise in the dentate gyrus. Recurrent excitatory circuits are normally masked by recurrent inhibitory circuits and can be experimentally revealed by altering the extracellular environment to increase excitation (e.g., elevated $[K^+]_o$) and/or reduce inhibition by blocking $GABA_A$ receptors (Wuarin and Dudek, 1996, 2001; Patrylo and Dudek, 1998; Lynch and Sutula, 2000; Winokur et al., 2004). When surgically isolated from afferent input (i.e., entorhinal cortex) under these conditions, spontaneous and evoked reverberating burst discharges, indicative of synchronous network activation, are repeatedly observed by single-cell and extracellular field potential recordings from granule cells in slices of epileptic rodents with mossy fiber sprouting (Cronin et al., 1992; Patrylo and Dudek, 1998; Winokur et al., 2004; Winokur et al., 2003). Studies using dual whole-cell patch-clamp recordings and localized glutamate stimulation have suggested

monosynaptic granule cell – granule cell connections in slices with mossy fiber sprouting that are absent in the normal dentate gyrus (Molner and Nadler, 1999; Wuarin and Dudek, 1996; 2001; Lynch and Sutula, 2001; Scharfman et al., 2003). Therefore, mossy fiber sprouting may provide a means for granule cell network synchronization that may be "unmasked" if inhibitory control is impaired.

1.9.2 Hilar cell loss

Specific patterns of hilar neuron loss are present in clinical and experimental epilepsy. The loss of certain populations of hilar interneurons is also a histopathological feature in experimental TBI (Lowenstein et al., 1992; Hall et al., 2005; Santhakumar et al., 2000; Grady et al., 2003) and in human posttraumatic epilepsy (Kharatashivilli et al., 2006; Swartz et al., 2006). However, whether neuron loss is a necessary component of acquired epilepsy is controversial (Maglóczky, 2010). Nevertheless, excitatory mossy cells and inhibitory interneurons are both vulnerable to cell death (Cavazos et al., 1994; Buckmaster and Jongen-Rêlo, 1999; Houser, 1999; Kobayashi and Buckmaster, 2003). Status epilepticus and repeated seizures induce mossy cell loss, degeneration of these inputs, and the formation of mossy fiber sprouting. Therefore, mossy cell loss has been hypothesized to play a major role in triggering abnormal mossy fiber synapse formation onto granule cells (Nadler et al., 1980; Cavazos and Sutula 1990; Babb et al., 1991; Okazaki et al. 1995; Buckmaster et al., 1996; Nadler, 2003). However, Maglóczky (2010) speculated that cell loss is not necessary for excitatory axon sprouting in epilepsy, because robust axon sprouting was observed in sclerotic and non-sclerotic resected tissue from TLE patients. Additionally, mossy cells can make contacts onto distant GABAergic interneurons and have been proposed to drive lateral inhibition (Buckmaster and Schwartzkroin, 1994). Their loss may be associated with reduced excitatory input to inhibitory interneurons (Sloviter, 1987, 1991, 1994). However, lateral inhibition appears to remain intact in the dentate gyrus of rats after pilocarpine-induced TLE (Buckmaster and Jongen-Rêlo, 1999).

While the majority of GAD-positive hilar interneurons are preserved in TLE (Babb et al., 1989; Buckmaster and Jongen-Rêlo, 1999), a selective loss of certain

populations of GABAergic interneurons is observed in human (Babb et al., 1989; de Lanerolle et al., 1989; Cavazos et al., 1994; Mathern et al., 1995; Zhu et al., 1997; Houser, 1999; Maglóczky et al., 2000; Andrioli et al., 2007) and experimental (Obenaus et al., 1993; Buckmaster and Dudek, 1997; Buckmaster and Jongen-Rêlo, 1999; Kobayashi and Buckmaster, 2003; Sun et al., 2007) epilepsy. The pattern and extent of hilar GABAergic neuron loss is variable, but fewer somatostatin- and neuropeptide Y-positive hilar interneurons are the most consistent finding, suggesting a preferential loss of HIPP cells.

1.9.3 Alterations in synaptic inhibition associated with epilepsy

Two main hypotheses have emerged concerning the possible relationship between hilar neuron loss and dysfunction of synaptic inhibition in epilepsy. The first hypothesis proposes that reduced synaptic inhibition of granule cells is due to excitatory denervation of intact inhibitory interneurons, possibly due to the loss of excitatory mossy cells (e.g., the “dormant basket cell” hypothesis; Sloviter 1987, 1991, 1994). This hypothesis was later revised to propose that excitatory drive to basket cells is restored by mossy fiber sprouting weeks later (i.e., at the time of spontaneous seizures) (Sloviter, 2003). Therefore, this hypothesis proposes that mossy fiber sprouting has mainly an antiepileptogenic effect and predicts that mossy fibers sprout mainly to dentate GABAergic interneurons. The main electrophysiological evidence relies on two phenomena in an electrical stimulation model. In this model, mossy cells are lost but inhibitory basket cells remain intact. Perforant pathway stimulation evokes an increase in extracellular excitability of granule cells days after injury, which is interpreted as a decrease in synaptic inhibition. Weeks later, enhanced extracellular paired-pulse inhibition is observed in the granule cell layer after stimuli applied to the perforant pathway, which is interpreted as enhanced synaptic inhibition.

The “dormant basket cell” hypothesis is controversial, because causal relationships between extracellular paired-pulse responses and synaptic inhibition have not been established (Bernard et al., 1998). Moreover, sprouted mossy fibers in the molecular layer predominantly form new synaptic connections with dendrites of granule

cells, not inhibitory interneurons (Frotscher and Zimmer, 1983; Okazaki et al., 1995; Zhang and Houser, 1999; Wenzel et al., 2000; Buckmaster et al., 2002). Whole-cell patch-clamp recordings from putative GABAergic interneurons also suggest that excitatory drive to GABA neurons is reduced in experimental TLE. Doherty and Dingledine (2001) showed reduced excitatory drive onto hilar border interneurons after pilocarpine-induced status epilepticus. Zhang and Buckmaster (2009) demonstrated that basket cells receive less excitatory input 3-7d after pilocarpine-induced status epilepticus, and excitatory drive to basket cells remains low for several weeks, after the onset of spontaneous seizures. These findings suggest that excitatory denervation of basket cells may contribute to reduced inhibitory synaptic drive to granule cells after injury, but it is unlikely that mossy fiber sprouting restores excitatory input to these cells.

The second hypothesis proposes that a reduction in the total number of inhibitory interneurons in the dentate gyrus after injury is associated with a net reduction in synaptic inhibition of granule cells. This hypothesis is more widely accepted and has yielded more consistent results. Loss of hilar GABA neurons is associated with a permanent loss of inhibitory synaptic input to granule cells (Kobayashi and Buckmaster, 2003; Shao and Dudek, 2005b; Sun et al., 2007; Williamson et al., 1995; 1999). This is consistent with fewer synaptic contacts, and it is associated with a reduction in the number of inhibitory interneurons (Kobayashi and Buckmaster, 2003). It is important to note that a reduction in synaptic inhibition by itself may not be sufficient for network synchronization in the dentate gyrus. For example, burst discharges are not observed in control tissue, even in the presence of $GABA_A$-receptor antagonists. Moreover, interneuron loss and the subsequent reduction in synaptic inhibition occur within the first few days after brain insult by pilocarpine treatment (Kobayashi and Buckmaster, 2003; Sun et al., 2007), and this finding cannot explain why seizure generation emerges after a latent period of several days to weeks.

There are “compensatory” mechanisms for GABA cell loss that have emerged, providing a more complex understanding of how GABAergic inhibition is altered in epilepsy. Surviving hippocampal GABA interneurons have been reported to spout new axon collaterals in human and experimental TLE (Babb et al., 1989; Mathern et al., 1995; Cossart et al., 2001; Thind et al., 2009; Zhang et al., 2009). Axon sprouting of inhibitory

neurons may partially restore inhibitory synaptic input to principal cells, but this may be complicated by alterations in synaptic efficacy at GABAergic synapses (Hirsch et al., 1999; Kobayashi and Buckmaster, 2003; Zhang and Buckmaster, 2009). Increased mossy fiber collaterals onto hilar interneurons has been proposed to occur during epileptogenesis (Chang and Lowenstein, 2003; Sloviter, 2003), but functional evidence for this hypothesis has not been established.

1.10 Animal models of posttraumatic seizures and hyperexcitability

The experimental limitations of human studies make appropriate animal models an invaluable tool for identifying basic mechanisms of epileptogenesis after TBI. Moreover, experimental models are necessary for developing and testing new treatments for PTE. The ideal model is one whereby the behavioral, anatomical, and physiological aspects of human PTE are easily and efficiently reproduced. Unfortunately, there are relatively few clinically relevant experimental models of PTE (Pitkanen and McIntosh, 2006).

1.10.1 Fluid percussion injury (FPI)

The fluid percussion injury (FPI) model has been the best characterized in terms of epilepsy after closed-head TBI (Pitkanen and McIntosh, 2006). Injury is delivered through a craniotomy by rapid fluid injection which first strikes the intact dura and then moves into the epidural space (Lifshitz, 2009). The height at which a pendulum hammer is dropped determines the pressure of the fluid pulse transmitted through a fluid-filled cylinder. This pressure can be used to estimate injury severity. Injury severities that have been investigated with regard to long-term changes in excitability can be categorized into two groups: severe injuries, with fluid pressure typically >3 atm; and moderate injuries, with impact forces of 2 - 2.2atm. Craniotomies can be applied centrally to the midline to produce more diffuse injuries or laterally to produce mixed focal and diffuse injury (Lifshitz, 2009; Pitkanen and McIntosh, 2006).

Several studies have reported electrographic seizures in rats after *severe* FPI (D'Ambrosio et al., 2004, 2005, 2009; Kharatashivilli et al., 2006). Depth-electrode recordings have inferred that seizures are sometimes initiated in hippocampal structures (D'Ambrosio et al., 2005; Kharatashivilli et al., 2006). Spontaneous seizures are present in 50% of rats by 12 months after severe lateral FPI (Kharatashivilli et al., 2006). In this study, rats with posttraumatic seizures after severe injury were accompanied by bilateral mossy fiber sprouting and hilar neuron loss. Mossy fiber sprouting and hilar neuron loss after FPI is apparently associated with the frequency and extent of electrographic abnormalities (Kharatashivilli et al., 2006, 2007). Little to no mossy fiber sprouting is detectable at time points less than 6 months post-injury (Kharatashivilli et al., 2006, 2007). Unfortunately, the functional effects of mild to moderate posttraumatic mossy fiber sprouting on network synchrony have not been directly examined. D'Ambrosio and colleagues (2004, 2005) reported that 100% of rats develop seizure-like epileptiform activity by 9 weeks after severe rostral perisagittal FPI, but tonic-clonic convulsive seizures are typically not observed. These electrographic abnormalities were accompanied by subtle changes in behavior (e.g., behavioral arrest). However, similar electrographic events were observed in nearly 40% of sham-control rats by 21 weeks post-injury (D'Ambrosio et al., 2005). It is unclear why control rats had epileptiform activity, but this may be due to how a seizure is defined (D'Ambrosio et al., 2009). D'Ambrosio et al. (2009) proposed that electrographic abnormalities with $\geq$ 2 second duration are ictal events. This is different from Kharatashivilli et al. (2006) who defined a seizure as electrographic events $\geq$ 5s duration with obvious behavioral abnormalities defined by a widely used behavioral scale for rodent seizures (Racine, 1979).

Spontaneous seizures have not been detected after *moderate* FPI (Kharatashivilli, 2007; Echegoyen et al., 2009). However, seizure susceptibility is increased after moderate FPI after injection of pentylenetetrazol (PTZ) (Kharatashivilli et al., 2007), kainic acid (Echegoyen et al., 2009), and pilocarpine (Gurkoff et al., 2009). Few Timm granules are detected in the inner molecular layer months after moderate FPI (Shumate et al., 1995; Santhakumar et al., 2001). In the hilus, there are fewer mossy cells (Toth et al., 1997; Santhakumar et al., 2000) and GABAergic interneurons (Lowenstein et al., 1992; Toth et al., 1997; Santhakumar et al., 2000) one-week after moderate FPI. Hilar cell loss

is accompanied by reduced mIPSCs in granule cells (Toth et al., 1997; Witgen et al., 2005). Lowenstein et al. (1992) reported an injury severity-specific increase in the number of population spikes evoked in the granule cell layer by high frequency perforant path stimulation one-week post-FPI *in vivo*. Abnormal electrophysiological responses were associated with the degree of hilar neuron loss and were interpreted as evidence for an early reduction in synaptic inhibition after FPI. The reduction in hilar interneurons persists for at least 5 months (Toth et al., 1997), but long term changes in inhibitory synaptic input to granule cells after TBI have not been established.

There are several benefits and limitations to using FPI to model PTE. The injury produced by this model reflects both focal and diffuse pathologies, which is common to human TBI (Graham et al., 2006; Pitkanen and McIntosh, 2006). However, FPI has a large diffuse injury component, especially at more moderate injury severities. Seizures and mossy fiber sprouting presumably only develop in 50% of rats after lateral FPI of sufficient severity to produce 30-40% mortality (>3atm). Mortality after severe FPI has been attributed to disproportionate injury to the brainstem (Shima and Marmarou, 1991). Moreover, seizures do not develop in significant numbers of rats until 7-12 months after severe injury. This makes long-term studies unrealistic. Brain injury produced by FPI can be variable due to fluid dispersion through the epidural space. A relatively long latency to seizure onset and epileptic pathology combined with high injury mortality and variability makes studies of PTE in this model labor-intensive.

1.10.2 Weight drop

The weight drop model, also referred to as the impact-acceleration model, has been examined as a model of posttraumatic hyperexcitability (Golarai et al., 2001). Trauma is delivered to the neocortex by dropping a large blunt weight through a tube to impact the skull. Injury severity is managed by adjusting the height at which the weight is dropped (Marmarou et al., 2009). This injury produces large and extensive damage to cortical and subcortical structures, including the dentate gyrus and hippocampus (Golarai et al., 2001). Seizures have not been reported in this model. However, increased seizure susceptibility to PTZ is observed 15 weeks after injury (Golarai et al., 2001). Bilateral

mossy fiber sprouting develops by 16 weeks post-injury (Golarai et al., 2001). While the presence of mossy fiber sprouting is associated with lowered seizure threshold, whether the increase in seizure susceptibility is associated with sprouting is unclear. The lack of demonstrated spontaneous seizures after weight drop is an obvious limiting factor in using this injury to model PTE. There are several other limitations and complications. Impact is delivered to the intact skull, not directly to the brain via craniotomy as in FPI. Therefore, there is an increased risk for skull fracture, and injury dynamics can depend somewhat on skull thickness (Marmarou et al., 2009). By using gravitational forces to produce head injury, there can also be a risk for secondary "rebound" injury. Weight drop injury can also be difficult to perform on mice, limiting the use of transgenic animals and genetic manipulation with this model (Marmarou et al., 2009).

1.10.3 Controlled cortical impact (CCI) injury

Controlled cortical impact (CCI) injury is a widely used experimental model of closed-head injury that has not yet been identified as a model of injury-induced epilepsy. First developed by Lighthall (1988), this model often utilizes an electronically controlled pneumatic impactor to apply a focal contusion injury to the brain surface through a craniotomy (Dixon et al., 1991; Scheff et al., 1997; Hall et al., 2005, 2008; Saatman et al., 2006; Dixon and Kline, 2009; Figure 1.5). Injury severity is managed by adjusting the depth of tissue compression. This model is unique, because it allows for good control over biomechanical parameters such as force, velocity, duration, and depth of deformation. This allows for a consistent and reproducible focal injury with minimized risk for inaccuracy or secondary "rebound" injury. Moreover, several risk factors for PTE are modeled by CCI injury including intraparenchymal hemorrhage accompanied by epidural and subdural hematomas (Lighthall, 1988; Dixon, 1991); cell loss in the neocortex, hippocampus, and dentate gyrus (Goodman et al., 1994; Smith et al., 1995; Fox et al., 1998; Anderson et al., 2005; Hall et al., 2005, 2008); neurogenesis in the dentate gyrus (Rola et al., 2006); and increases in morphologically identified synapses in the hippocampus (Scheff et al., 2005). Interestingly, early seizures within 24h have sometimes been reported in this model (Nilsson et al., 2004; Kochanek et al., 2006).

However, no data currently exists regarding chronic changes in excitability within the dentate gyrus after CCI.

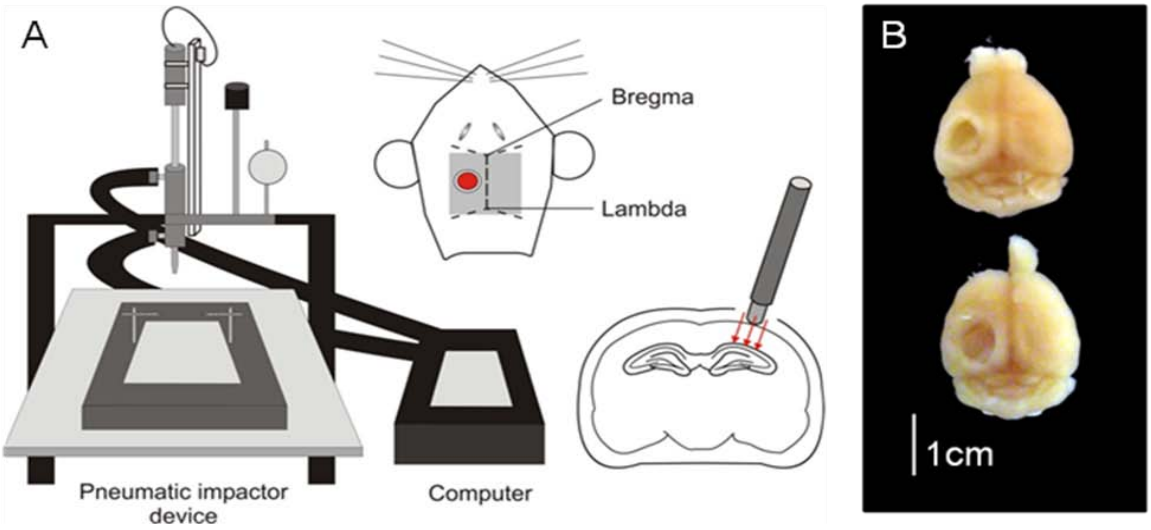

Figure 1.5. CCI injury produces a unilateral cortical contusion over the left somatosensory cortex. A. Illustration of CCI injury device. Insets show relative impact location (red circle and arrows). **B.** Shown are brains of two mice 9 weeks post-TBI that received severe cortical contusion injuries.

1.11 Study aims and significance

The overall objectives of the present work were: 1) adapt an experimental model of TBI as an experimental model of PTE, and 2) investigate chronic alterations in synaptic circuitry in the dentate gyrus that may contribute to the generation of epileptic activity after closed-head TBI. The CCI injury model was selected for use, because it has not yet been adapted as an experimental model of PTE (Pitkänen and McIntosh, 2006), it reproduces many risk factors for epilepsy after closed-head injury, and it is a commonly used experimental model of cortical contusion TBI (Dixon and Kline, 2009).

Synaptic network changes leading to PTE likely involve modifications to excitatory and inhibitory circuitries. Mossy fiber sprouting and dysfunction of synaptic inhibition are defining characteristics of the injured dentate gyurs in TLE. Previous reports in clinical (Swartz et al., 2006) and experimental (Kharatashivilli et al., 2006) PTE suggest that these features are also likely relevant markers of TBI-induced epilepsy.

Extracellular field and whole-cell patch-clamp electrophysiology in acute brain slices provide a simple but relatively direct approach to investigating neuronal activity and network synchronization after TBI. These techniques also allow for comparisons to be made with the abundant literature describing altereations in excitatory and inhibitory circuits in the dentate gyrus of models of pharmacologically- or electrically-induced TLE. Therefore, emphasis is placed on using these techniques in the dentate gyrus after CCI injury in mice.

The following specific aims were addressed:

1. Determine whether injured mice develop posttraumatic seizures. The presence of spontaneous seizures is a fundamental characteristic of any experimental epilepsy model. Seizures were detected in mice by periodic behavioral monitoring after CCI.

2. Determine whether mossy fiber sprouting develops after cortical contusion injury. Mossy fiber sprouting is a well-described characteristic of the injured dentate gyrus, and it is a marker of the reactive plasticity of excitatory circuits in epilepsy. Timm's staining was performed in brain sections of injured and control animals to visualize zinc containing mossy fibers.

3. Evaluate whether mossy fiber sprouting is associated with increased neuronal activity and the formation of a new recurrent excitatory circuit. Formation of new functional recurrent excitatory circuits – which form the basis from which synchronous neuronal discharges arise – have not been demonstrated after TBI. Whole-cell patch-clamp and extracellular field recordings of dentate granule cells were performed to investigate whether posttraumatic mossy fiber sprouting is associated with increased and synchronous granule cell activity after TBI.

4. Determine whether excitability of surviving GABAergic interneurons is altered. Increased excitatory innervation of hilar GABAergic neurons is a proposed compensatory mechanism to enhance synaptic inhibition in epilepsy (Chang and Lowenstein, 2003; Sloviter, 2003), but evidence for this hypothesis is lacking. Therefore, whole-cell patch-

clamp recordings of visually identified hilar GABAergic cells were performed to determine whether excitatory drive to these neurons was enhanced after TBI.

5. Determine whether a change in synaptic inhibition can be detected in the dentate gyrus after TBI. Alterations in synaptic inhibition may have critical implications in the regulation of excitatory networks after TBI. Moreover, whether synaptic inhibition is reduced or enhanced in PTE remains to be established. Whole-cell patch-clamp recordings were performed in granule cells to examine whether synaptic inhibition is altered in the injured dentate gyrus after TBI.

Chapter 2
Materials and methods

Animals. Six to ten week old adult male CD-1 (Harlan) or GIN (eGFP-expressing Inhibitory Neurons; FVB-Tg(GadGFP)4570Swn/J; The Jackson Laboratory; Oliva et al., 2000) mice weighing 28-35g were housed under a normal 12h/12h light/dark cycle. Water and food were available *ad libitum*. Mice were housed for a minimum of 7d prior to experimentation, and all procedures were first approved by the University of Kentucky Animal Care and Use Committee and adhered to NIH guidelines for the care and use of laboratory animals. All experiments were performed on mice 6-13 weeks post-injury.

Head injury. Young-adult mice were subjected to a unilateral cortical contusion by CCI injury as previously described (Scheff et al., 1997). Mice were anesthetized by 2% isoflurane inhalation and placed in a stereotaxic frame. The skull was exposed by a midline incision, and a 4-5mm craniotomy was made lateral to the sagittal suture and centered between bregma and lambda. The skull cap was removed without damage to the exposed underlying dura. The contusion device consisted of an electronically controlled, pneumatically driven impactor fitted with a beveled stainless steel tip 3mm in diameter (Precision Systems and Instrumentation, Fairfax, VA). Brain injury was delivered using this device to compress the cortex to a depth of 0.5mm (mild injury) or 1.0mm (severe injury) at a velocity of 3.5m/sec and 400-500ms duration. The hemostatic agent Surgicel (Johnson & Johnson, Arlington, TX) was placed over the dura after injury, the incision sutured, and the animal was allowed to recover.

Seizure monitoring. Injured animals were monitored for immediate seizures (i.e., injury-induced) and spontaneous seizures. Observation periods occurred during the light phase of the light/dark cycle, and seizures were rated from 1 to 5, with 5 being the most severe, according to a modified Racine rating scale (Racine, 1972; Shibley and Smith, 2002; Figure 2.1). Posttraumatic seizures were classified based on the time post-injury in which they occurred: immediate, first 90 minute monitoring session; early, 1 - 7d post-injury; and late, > 7d after injury.

Figure 2.1. Modified racine rating scale classification of behavioral seizures (Racine, 1979). **A.** Seizure category scale and definitions for each seizure category. **B.** Seizure classification scheme. **C.** Representative examples for each seizure category are shown in the same mouse after pilocarpine-injection.

Slice preparation. Mice were deeply anesthetized by isoflurane inhalation and decapitated. The brain was removed and stored for < 1 min in ice-cold (2-4^{o}C) oxygenated artificial cerebrospinal fluid (ACSF) containing in mM: 124 NaCl, 3 KCl, 1.3 $CaCl_2$, 26 $NaHCO_3$, 1.3 $MgCl_2$, 1.4 NaH_2PO_4 and equilibrated with 95% O_2-5% CO_2 (pH 7.2-7.4). Brains were blocked, glued to a sectioning stage, and 400 µm-thick horizontal or coronal slices were cut in cold, oxygenated ACSF using a vibrating microtome (Vibratome Series 1000; Technical Products International, St. Louis, MO). The hippocampus was isolated from surrounding tissue, making sure to completely remove the entorhinal cortex. The order of slices was maintained so that the location along the septotemporal axis of each hippocampi was known.

Whole-cell patch-clamp electrophysiology. After an equilibration period of at least 1h, slices were transferred to a recording chamber on an upright, fixed-stage microscope equipped with infrared differential interference contrast (Olympus BX50WI). Recordings were performed on granule cells and hilar eGFP neurons identified by fluorescent illumination. Patch pipettes were pulled from borosilicate glass (1.65 mm outer diameter and 0.45 mm wall thickness, Garner Glass Co., Claremont, CA) with a P-87 puller (Sutter Instruments). The intracellular solution contained (in mM): 130–140 K^+ or Cs^{2+} gluconate, 1 NaCl, 5 EGTA, 10 HEPES, 1 $MgCl_2$, 1 $CaCl_2$, 3 KOH or CsOH, 2 ATP, and 0.2% biocytin (pH 7.15 – 7.3). QX-314 bromide (5mM) was added to the intracellular solution for electrical stimulation recordings. Open tip resistance was 2-7 MΩ. Recordings were obtained with an Axopatch 200B or Multiclamp 700B amplifier (Axon Instruments, Foster City, CA), low-pass filtered at 2-5 kHz, and digitized at 88 kHz (Neuro-corder; Cygnus Technology, Delaware Water Gap, PA). Cell attached recordings of spontaneous action potentials were recorded in voltage-clamp mode at -60mV. For whole-cell patch-clamp recordings, cells were first voltage-clamped for ~5 min at -60 or -70mV (i.e., near resting membrane potential) to allow equilibration of intracellular and recording pipette contents. Resting membrane potentials were determined by removing the voltage clamp. Spontaneous-, miniature-, and evoked- excitatory postsynaptic currents (s-, m-, and eEPSCs) were examined at a holding potential of -60 mV (inhibitory interneurons) or -70 mV (granule cells), and inhibitory postsynaptic currents (s-, m-, and eIPSCs) were examined at a holding potential of 0 mV. Current-clamp (*i.e.*, voltage) recordings were performed at resting membrane potential (I= 0pA). Series resistance was monitored throughout the recordings, and data was only used for analysis if the series resistance remained less than 25 MΩ and ≤ 20% change during the recordings.

Glutamate photostimulation. Slices were perfused with γ-(carboxy-2-nitrobenzyl) ester, trifluoroacetic acid salt (i.e., CNB-caged glutamate, 250μM; Molecular Probes, Eugene, OR) added to recirculating ACSF or Mg^{2+}-free ACSF and 100μM picrotoxin (PTX). Brief pulses of fluorescent light (30ms exposure, UV filter, Chroma Technology, Rockingham, VT) were directed into the slice through the 40x objective used to obtain recordings. The objective was initially positioned to “uncage” glutamate directly over the

recorded cell. This resulted in a large inward current in voltage-clamp with superimposed sodium spikes or a large depolarization in current clamp with superimposed action potentials. The objective was then moved away from the recorded cell by manually moving the microscope until a direct inward current after stimulation was no longer observed. This effective diameter of stimulation (~100 μm) was set by apertures in the light path. Photostimulations were applied along the entire extent of the granule cell layer and in the hilus/CA3 region. A series of at least five stimuli were applied per stimulation location at 0.1Hz stimulation frequency.

Extracellular field potential recordings. Field potential recordings were obtained from the granule cell layer in the dentate gyrus 42-71d post-CCI. For electrophysiological recording, slices were placed in recording chambers that allowed positioning of both stimulating and recording electrodes, and perfused with oxygenated ACSF. Slices were visualized under an upright microscope (Olympus Bx-51W1) for electrode placement. Extracellular recording electrodes were filled with 1M NaCl and placed near the apex of the granule cell layer for recordings. A concentric bipolar stimulating electrode made of platinum-iridium wire (125 μm diameter; FHC, Inc, Bowdoinham, ME) was used to apply stimuli to fiber pathways at 0.1Hz. Stimulus intensity was adjusted to produce a population spike of ~50% of maximum amplitude. For antidromic stimulation experiments, a single stimulus was delivered to the hilus. For orthodromic activation experiments, pairs of stimuli were delivered to the perforant path at interpulse intervals (IPI) of 20, 40, 80, and 160ms respectively and the ratio of the second population spike to the first (PS2/PS1) was calculated. An increase in the paired pulse ratio (PPR) of PS2/PS1 in slices from injury versus control groups was interpreted as a reduction in synaptic inhibition, and a reduction in the PPR was interpreted as an increase in synaptic inhibition (Reeves et al., 1997). Electrical signals were recorded using an Axopatch 200B amplifier (Axon Instruments), low-pass filtered at 2-5 kHz, digitized at 88 kHz (Neurocorder), stored on videotape, and analyzed on a PC computer using pClamp programs (Axon Instruments). In some experiments, slices were perfused with Mg^{2+}-free ACSF containing picrotoxin (100μM) to block $GABA_A$-receptor mediated recurrent inhibition and unmask NMDA-receptor mediated excitatory synapses at resting

membrane potential (Smith and Dudek 2001, 2002; Lynch and Sutula, 2000; Winokur et al., 2004).

Electrical stimulation. A concentric bipolar stimulating electrode made of platinum–iridium wire (125 μm diameter; FHC, Inc., Bowdoinham, ME) was used to apply paired stimuli to the hilus. Stimulus intensity was adjusted to produce an eIPSC at 50% of maximum amplitude. Pairs of stimuli were delivered to the perforant path at pairing intervals of 30, 60, 90, 120 and 200 ms. Eight to 10 consecutive recordings were made at 0.1Hz for each pairing frequency, averaged, and the ratio of the second eIPSC to the first (eIPSC2/eIPSC1) was calculated to establish the PPR.

Pharmacology. The following agents were added to the ACSF for some experiments: bicuculline methiodide (BMI; 30-100 μM), picrotoxin (PTX; 100 μM), kynurenic acid (1 mM), (2*R*)-amino-5-phosphonovaleric acid (APV; 50 μM), tetrodotoxin (TTX; 2 μM).

Timm's histochemistry. Hippocampal slices were placed in 0.37% sodium sulfide solution in 0.1M $NaHPO_4$ for 20 min, followed by 4% paraformaldehyde in 0.15M phosphate buffer overnight to fix the slices. Slices were then rinsed three times with phosphate buffered saline (PBS; 0.01 M; pH 7.4) and placed in a 30% sucrose solution in PBS overnight or until they sank for cryoprotection. The slices were sectioned at 20μm on a cryostat, rinsed, mounted on charged slides (Superfrost Plus; Fisher Scientific), and dried overnight. Sections were treated according to previous protocols using Timm's stain to reveal mossy fibers and Nissl counterstained by cresyl violet to visualize cell bodies (Tauck and Nadler, 1985; Shibley and Smith, 2002). To quantify the regional distribution of mossy fiber sprouting after CCI, sections from the ipsilateral and contralateral hemispheres were examined by an investigator who was blind to the electrophysiological outcomes. Scores for sprouting were assigned based on the following scale of Tauck and Nadler (1985): 0, little to no Timm granules in the granule cell layer; 1, mild staining in the granule cell layer with occasional puncta the inner molecular layer; 2, moderate continuous staining through the granule cell layer with discontinuous, punctuate staining in the inner molecular layer; and 3, continuous band of dense staining throughout the

inner molecular layer. At least three sections from each slice were examined and the median score reported if variability between sections existed. If Timm's staining between the blades of the granule cell layer was variable, an averaged score was used (e.g., if the lower blade had a score of 1 while the upper blade had a score of 2, the slice would be given an overall grade of 1.5). Timm scores were assigned based on the region of the granule cell layer in which recorded cells were obtained (i.e., inner blade, apex, or outer blade) in Chapter 3, because Timm's staining between the blades of the granule cell layer was almost always asymmetric. Timm scores >1 were considered to reflect an abnormal degree of mossy fiber sprouting as previously described (Patrylo and Dudek, 1998; Shibley and Smith, 2002). The degree of structural damage to the dentate gyrus was analyzed at the injury site in the same Timm scored sections by switching the filter from bright field to fluorescence. Cresyl violet is a red fluorescent under a TRITC filter as previously described (Alvarez-Buylla et al., 1990).

Biocytin labeling. Prior to cryoprotection, slices in which a recording from an eGFP neuron was obtained were examined for biocytin labeling and eGFP content. Slices were immersed in avidin conjugated to Texas Red (1:400; Vector Laboratories, Burlingame, CA) in PBS containing 0.5% Triton X-100 and incubated for 3 to 4h at room temperature to identify biocytin-filled neurons and confirm the location of the recorded cell. Slices were then rinsed three times with PBS, mounted on slides, covered with Vectashield containing DAPI (Vector Laboratories), and cover-slipped. Images were taken with an Olympus BX40 microscope and captured with a Spot RT camera (Diagnostic Instruments). Slices were then washed in PBS, placed in 30% sucrose solution, and Timm and Nissl stained.

Data analysis and statistics. Data analysis was performed using pClamp 10.2 (Clampfit, Axon Instruments), MiniAnalysis 6.0 (Synaptosoft, Leonia, NJ), Instat (GraphPad software, San Diego, CA), and IBM SPSS Statistics 18 (SPSS Inc., Chicago, Il) programs. A two minute sample recording per cell was used for measuring synaptic event frequency, amplitude, and kinetics. Events characterized by a typical fast rising phase and exponential decay phase were manually detected using MiniAnalysis, and only currents

with amplitudes greater than three times the root mean square (RMS) noise level were included for analysis. Event frequency, mean amplitude, and kinetics were averaged across neurons (i.e., *n*= neurons) and groups were compared by one-way ANOVA followed by a Tukey's *post hoc* test or two-tailed t-test. Paired-pulse responses were analyzed by two-way (treatment group x pairing interval) repeated measures (pairing interval) ANOVA. For photostimulation experiments, EPSC frequency was analyzed every 100ms for 500ms prior to and after each stimulation trial and averaged for each stimulation site (i.e., *n*= stimulation sites). A response at a given location was considered to be positive (i.e., a local synaptic connection was evoked) if the number of EPSCs in at least one of the first three 100ms segments after stimulation was greater than the mean number of events per 100ms prior to stimulation + 3SD and a response was observed in at least 3 of 5 trials time locked to the stimulus, demonstrating that the response was repeatable. Direct photostimulation responses (i.e., due to postsynaptic activation of the recorded neuron) could be easily distinguished from synaptic responses based on a lack of onset latency and slower rise time, and they were revealed by addition of 2µM TTX (see Chapter 5, Figure 5), which blocked evoked synaptic events but not direct currents (Callaway and Katz, 1993; Dantzker and Callaway, 2000; Waurin and Dudek, 2001). All stimulation sites in which the selection criteria were not met were considered to have a negative response. The number of eEPSCs for each stimulation site was calculated by subtracting the number of EPSCs in the first 300ms before stimulation from the number of EPSCs in the first 300ms after stimulation. This relatively short time window was chosen to limit confounding effects of polysynaptic activation, because field potential bursts indicative of recurrent excitatory connections between granule cells occur within the first 300ms after an initial antidromically evoked population spike (see Chapter 2), and because granule cells remain depolarized and fire most of their action potentials during this timeframe using identical photostimulation parameters (see Chapter 3). To analyze differences in evoked activity after glutamate stimulation, data from control and contralateral slices, which acted as an internal control, were combined and compared to responses ipsilateral to the injury by two-tailed Fisher's exact test or Mann-Whitney U. Data are expressed as mean ± SD unless otherwise stated, and significance was set at $P < 0.05$.

Any variation to these methods is described in an additional methods section for the chapter in which they pertain.

Chapter 3

Posttraumatic epilepsy after controlled cortical impact injury in mice

This chapter was published in *Exp Neurol.* Feb 2009; 215 (2):243-45.

3.1 Introduction

TBI is often accompanied by the delayed development of PTE (Caveness et al., 1979; Annegers et al., 1998; Englander et al., 2003), and PTE is manifested as TLE in as many as 62% of trauma patients (Diaz-Arrastia et al., 2000; Hudak et al., 2004). However, prophylactic treatment for PTE has been largely unsuccessful and patients often do not qualify for surgery (Temkin et al., 1998, 2001). Thus, a clinical association between TBI and epilepsy is well documented, but the cellular and molecular mechanisms by which trauma leads to the development of seizures remain poorly understood.

The dentate gyrus has long been regarded as a model system for studying alterations in synaptic circuitry associated with TLE (Tauck and Nadler, 1985; Sutula et al, 1989; Waurin and Dudek, 1996; Buckmaster et al., 2002; Shibley and Smith, 2002). Experimental animal models and human TLE are characterized by hippocampal cell loss and mossy fiber sprouting in the dentate gyrus (Ben-Ari et al., 1985; Tauck and Nadler, 1985; Buckmaster et al., 2002; Shibley and Smith, 2002; Winokur et al., 2004; Jiao and Nadler, 2007). New recurrent excitatory circuits emerge after mossy fiber sprouting, and these changes are accompanied by increased excitability of the dentate gyrus and other limbic regions (Cronin and Dudek, 1988; Wuarin and Dudek, 1996, 2001; Smith and Dudek, 2001; Winokur et al., 2004). However, responses in TLE models may not reflect more subtle changes seen in human PTE. For example, status epilepticus induced by systemic administration of kainic acid or pilocarpine in rodents results in bilateral mossy fiber sprouting that is often much more robust than in hippocampi from surgical patients. Identifying experimental models of TBI that also display the pathophysiology of human TLE is necessary for understanding fundamental aspects of injury-induced epileptogenesis.

Several rodent models of TBI exist, but most are used to study acute or cognitive effects of brain injury and few have been adapted as animal models of TLE. Of these models, fluid percussion injury (FPI) and weight drop have been the most widely investigated as models of posttraumatic hyperexcitability. Studies performed in rats have suggested model-specific changes in seizure susceptibility, mossy fiber organization, and excitability after head injury that may also be related to injury severity and location (Golarai et al., 2001; Santhakumar et al., 2001; D'Ambrosio et al., 2004, 2005; Kharatishvili et al., 2006; Griesemer and Mautes, 2007). Controlled cortical impact (CCI) is a widely used experimental model of closed head injury that has not yet been identified as a model of injury-induced TLE. Several risk factors for epilepsy after trauma are modeled by lateral CCI including intraparenchymal hemorrhage accompanied by epidural and subdural hematomas (Lighthall, 1988; Dixon, 1991); cell loss in the neocortex, hippocampus, and dentate gyrus (Goodman et al., 1994; Smith et al., 1995; Fox et al., 1998; Anderson et al., 2005; Hall et al., 2005); neurogenesis in the dentate gyrus (Rola et al., 2006); and increases in morphologically identified synapses in the hippocampus (Scheff et al., 2005). Interestingly, early seizures within 24h have sometimes been reported in this model (Nilsson et al., 2004; Kochanek et al., 2006). However, no data currently exists regarding chronic changes in excitability within the dentate gyrus after CCI.

In this chapter, the hypothesis that CCI can induce TLE and synaptic reorganization in the dentate gyrus in mice was tested. Specifically, I focused on three main questions: (1) Do mice develop spontaneous seizures; (2) does injury induce mossy fiber sprouting; and (3) are there long-term changes in excitability in the dentate gyrus after CCI injury?

3.2 Methods

Seizure assessment. Control and injured animals were monitored for seizures during 11 random 1–2h intervals beginning 42 days post injury until the day of experimentation (by 71d). Five to eight mice were monitored per session for a total of 18h. Each observation period included ~50% of mice from both mild and severe injury groups. Observation periods occurred during the light phase of the light/dark cycle, and seizures were rated from 1 to 5, with 5 being the most severe, according to a modified Racine scale as previously described (Racine, 1972; Shibley and Smith, 2002; see Chapter 2). To minimize subjectivity in seizure assessment, category one seizures (i.e. facial automatisms, increased grooming behaviors) were excluded since abnormalities of these behaviors are often difficult to distinguish.

Histology. At least three sections from each slice were examined and the median score reported if variability between sections existed. If Timm's staining between the blades of the granule cell layer was variable, an averaged score was used (e.g., if the lower blade had a score of 1 while the upper blade had a score of 2, the slice would be given an overall grade of 1.5). Timm scores >1 were considered to have an abnormal degree of mossy fiber sprouting (Patrylo and Dudek, 1998; Shibley and Smith, 2002).

Data analysis. Numerical data are presented as the mean ± S.E.M. Timm scores are represented as relative ranges. The nonparametric Kruskal-Wallis test with Dunn *post hoc* was used to analyze for differences between groups of Timm scores.

3.3 Results

Mice were subjected to either mild (0.5mm injury depth; *n*= 10) or severe (1.0mm injury depth; *n*= 24) CCI injury and compared to age-matched controls (*n*=5). Cortical contusion produced a consistent and reproducible focal lesion in the ipsilateral somatosensory cortex (Figure 1A). This cortical site underwent substantial cell loss, as described in detail previously (Tang et al., 2002; Hall et al., 2005; Saatman et al., 2006). All injured mice survived and remained otherwise healthy until the day of experimentation (Table 3.1).

Table 3.1

Development of seizures in CD-1 mice after controlled cortical impact

	Days post-injury	Survival rate (%)	Percent mice with seizures	Highest seizure category observed
Control	–	5/5 (100%)	0/5 (0%)	–
Mild injury (0.5 mm)	65.70±5.8[a]	10/10 (100%)	2/10 (20%)	2
Severe injury (1.0 mm)	61.18±8.55[a]	24/24 (100%)	4/11 (36%)	3

[a] Denotes mean±SD.

3.3.1 Spontaneous seizures

Early posttraumatic seizures within 24h after head-injury and acute increase of interstitial glutamate have previously been reported after CCI (Nilsson et al., 1994; Kochanek et al., 2006). However, delayed spontaneous seizures after CCI have not been described. Mice were passively monitored for spontaneous seizures beginning 42d post-CCI until the day of experimentation (see Methods). Category 2 generalized seizures that included tail and neck stiffness, head nodding, and freezing up to 90s or longer were observed in 20% (n= 2 of 10) of mice that received mild injury and 36% (n= 4 of 11) of mice that received severe injury (Table 3.1). Spontaneous tonic-clonic seizures that included single forelimb myoclonus (category 3) were also observed in two of 11 mice (18%) that sustained a severe injury.

3.3.2 Posttraumatic mossy fiber sprouting

Unprovoked generalized seizures after experimental brain trauma indicate limbic involvement (D'Ambrosio et al. 2005; Kharatishvili et al., 2006) and are associated with mossy fiber sprouting in murine models of TLE (Shibley and Smith, 2002). Timm's staining was performed on horizontal sections 7d and 42-71d after CCI to compare mossy fiber organization in septal and temporal hippocampal sections contralateral and ipsilateral to the lesion (see Methods). None of the 14 septal or temporal sections from 5 control animals contained abnormal mossy fiber organization (i.e. all Timm scores were < 1; Figure 3.1B, E). A Kruskal-Wallis test did not indicate a significant difference in Timm score distributions between groups at 7d after severe injury (n= 6 animals) in either septal ($H_{(2, 29)} = 5.262$, $P > 0.05$) or temporal ($H_{(2, 29)} = 0.954$, $P > 0.05$) dentate gyrus (Figure 3.2A, B). However, two of the 6 mice (33%) examined had aberrant mossy fiber sprouting (i.e. Timm scores > 1) in septal sections of the dentate gyrus ipsilateral to the injury after 7d. Mossy fiber sprouting was not observed in temporal sections or the contralateral hemisphere.

A Kruskal-Wallis test demonstrated a significant difference in Timm score ranges between groups 42-71d after severe injury in both the septal ($H_{(2, 52)} = 23.453$, $P < 0.0001$) and temporal ($H_{(2, 52)} = 8.675$, $P < 0.01$) dentate gyrus (Figure 3.2 C, D). A Dunn's post hoc test demonstrated that Timm scores for ipsilateral slices were statistically different from controls at both septal and temporal locations ($p<0.001$). Of 18 mice, 10 (55%) contained mossy fiber sprouting in more septal sections (i.e. Timm score >1; Figure 3.1D, G), and in two mice (11%) the sprouting was also observed in the temporal dentate gyrus. Only one mouse (6%) had a Timm score >1 in contralateral dentate gyrus 42-71d post-injury (Figure 3.1 E, F). A small but significant difference in Timm score ranges was also found 42-71d after mild injury in septal ($H_{(2, 36)} = 6.415$, $P < 0.05$) and temporal ($H_{(2, 37)} = 7.035$, $P < 0.05$) locations (Figure 3.2 D, E). However, a Dunn's post hoc test failed to find significant differences between groups. One mouse (10%) that received mild injury had moderate mossy fiber sprouting in the septal dentate gyrus, and one mouse (10%) contained moderate sprouting in the temporal dentate gyurs. None of these 10 mice were found to have abnormal mossy fiber organization in the

contralateral hemisphere. The two mice that sustained severe injury and were observed to have spontaneous convulsive seizures also displayed robust mossy fiber sprouting (i.e. Timm scores > 2.0) in the ipsilateral dentate gyrus after CCI. In all cases, the degree of sprouting decreased with temporal progression along the hippocampal axis.

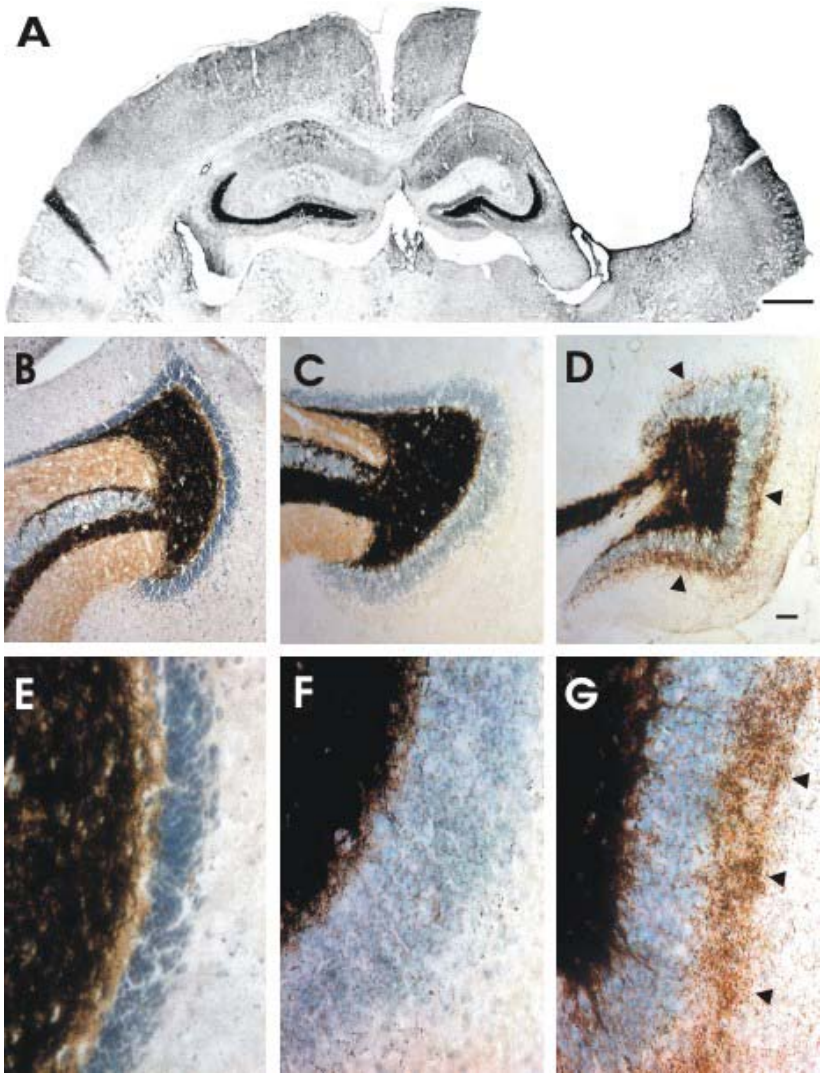

Figure 3.1. Reorganization of mossy fiber projections after severe injury. A. Representative Timm and Nissl counter-stained coronal section (~Bregma -2.0mm) from a mouse after severe controlled cortical impact TBI. **B.** Timm and Nissl stained horizontal section from a control mouse. **C.** Timm and nissl stained section from the contralateral hemisphere of an injured mouse 42d post CCI. **D.** Staining in the septal dentate gyrus ipsilateral to the lesion revealed mossy fiber sprouting into the inner molecular layer (arrows) at the same septotemporal level and in the same mouse as in **C**. **E-G.** Higher power images of **B-D**. Scale bars: 500µm in **A**, 100µm in **B-D**, 25µm **E-G**.

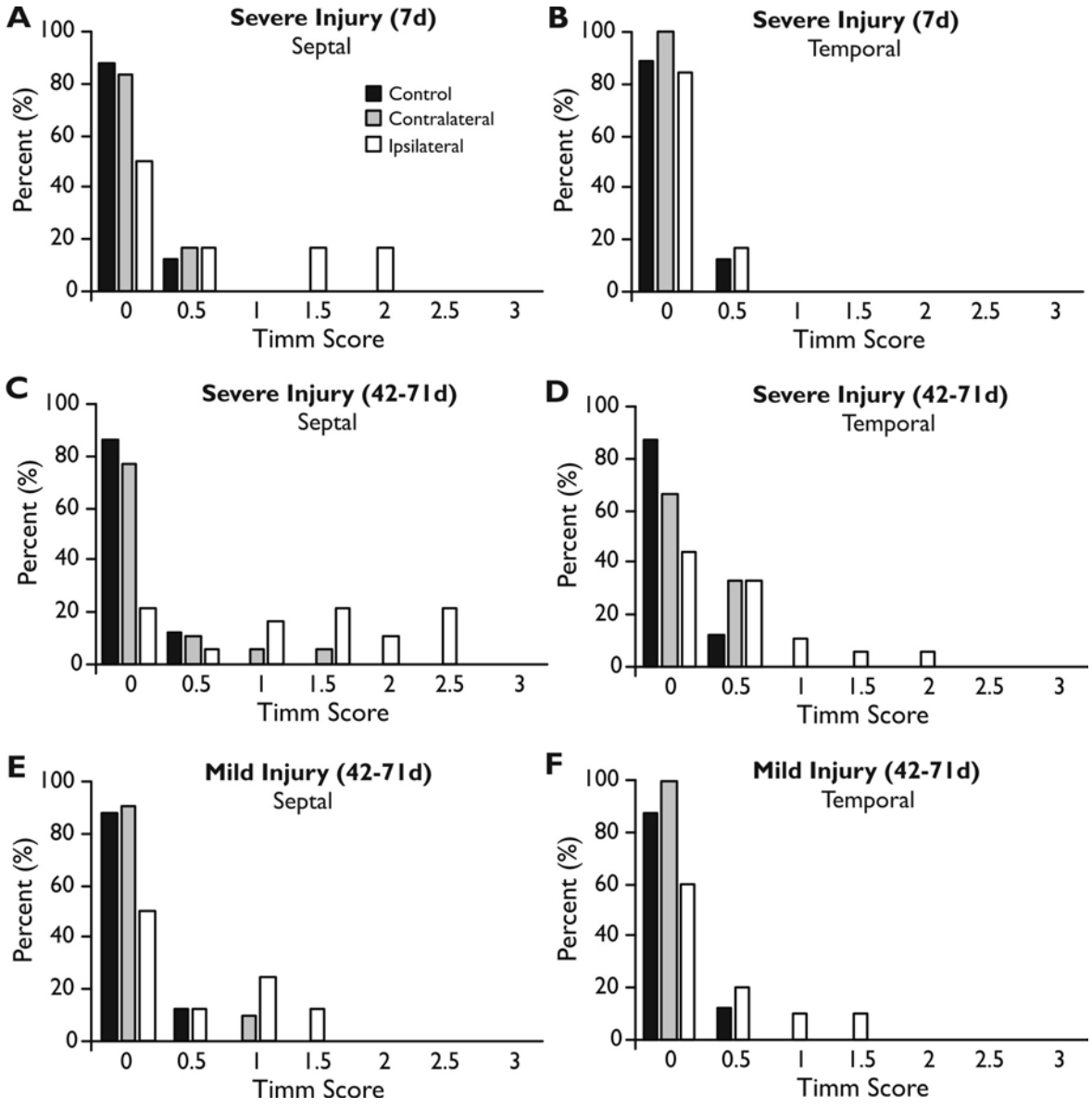

Figure 3.2. Mossy fiber sprouting progresses with time after CCI injury. Sprouting was typically confined to the septal dentate gyrus of the ipsilateral hemisphere. Timm score ranges are given for three groups (controls, injured ipsilateral hemisphere, and injured contralateral hemisphere) from septal (A) and temporal (B) dentate gyrus 7d after severe injury, septal (C) and temporal (D) dentate gyrus 42-71d after severe injury, and septal (D) and temporal (E) dentate gyrus 42-71d after mild injury.

3.3.3 In vitro electrophysiology

Responses to paired-pulse stimulation

Extracellular field recordings of perforant path input to dentate granule cells were used to assess the strength of synaptic inhibition in the dentate gyrus 42-71d after CCI. Paired electrical stimuli were delivered to the perforant path at pairing intervals of 20, 40, 80, and 160ms. The strength of inhibition was determined by measuring PPR - the amplitude of the second population spike as a percentage of the first (PS2/PS1) - of four experimental groups (septal and temporal slices of the dentate gyrus, ispilateral and contralateral to the lesion) after mild and severe injury compared to similarly located slices from controls. Responses in 14 hippocampal slices from 5 control animals revealed facilitation of the second population spike at all intervals (Figure 3.3); a t-test confirmed no significant difference between septal-most and temporal slices from controls and the data were therefore combined for analysis. A one-way ANOVA demonstrated no significant change in PPR between the groups at any of the tested IPIs after either mild ($F_{(4, 59)} = 0.39$, $P>0.05$, 20ms; $F_{(4,57)} = 0.89$, $P>0.05$, 40ms; $F_{(4,65)} = 1.04$, $P>0.05$, 80ms; $F_{(4,56)} = 0.64$, $P>0.05$, 160ms) or severe ($F_{(4, 50)} = 0.66$, $P>0.05$, 20ms; $F_{(4,48)} = 1.00$, $P>0.05$, 40ms; $F_{(4,64)} = 1.71$, $P>0.05$, 80ms; $F_{(4,47)} = 2.36$, $P>0.05$, 160ms) CCI injury. No change in PPR was detected by selecting for injury only.

However, to determine whether granule cell responses were selectively altered in slices with mossy fiber sprouting, I further analyzed the PPR in slices of four different groups: (1) ipsilateral dentate gyrus with Timm scores ≥ 1.5 (n=15 slices); (2) ipsilateral dentate gyrus with Timm scores ≤ 1 (n=42 slices); (3) contralateral dentate gyrus (Timm scores ≤ 1; n=46 slices); and (4) control dentate gyrus (Timm scores < 1). A one-way ANOVA demonstrated a significant difference in PPR between groups at early IPIs of 20ms and 40ms ($F_{(3, 95)} = 4.13$, $P<0.01$, 20ms; $F_{(3, 93)} = 2.74$, $P<0.05$, 40ms) but not at 80ms or 160ms ($F_{(3. 118)} = 1.34$, $P>0.5$, 80ms; $F_{(3, 92)} = 0.67$, $P>0.05$, 160ms). Post hoc comparisons revealed that PPR was significantly reduced by 47% at the 20ms interval and 59% at the 40ms interval in ipsilateral slices that had mossy fiber sprouting ($P<0.01$), suggesting an increase in the strength of inhibition (Figure 3.3A, B). Interestingly, PPR in

slices from the ipsilateral hemisphere in injured animals that did not contain mossy fiber sprouting was not statistically different from controls at any IPI. Population spike amplitude ratios from the contralateral dentate gyrus, which also did not display mossy fiber sprouting, were also not different from controls (Figure 3.3A, B).

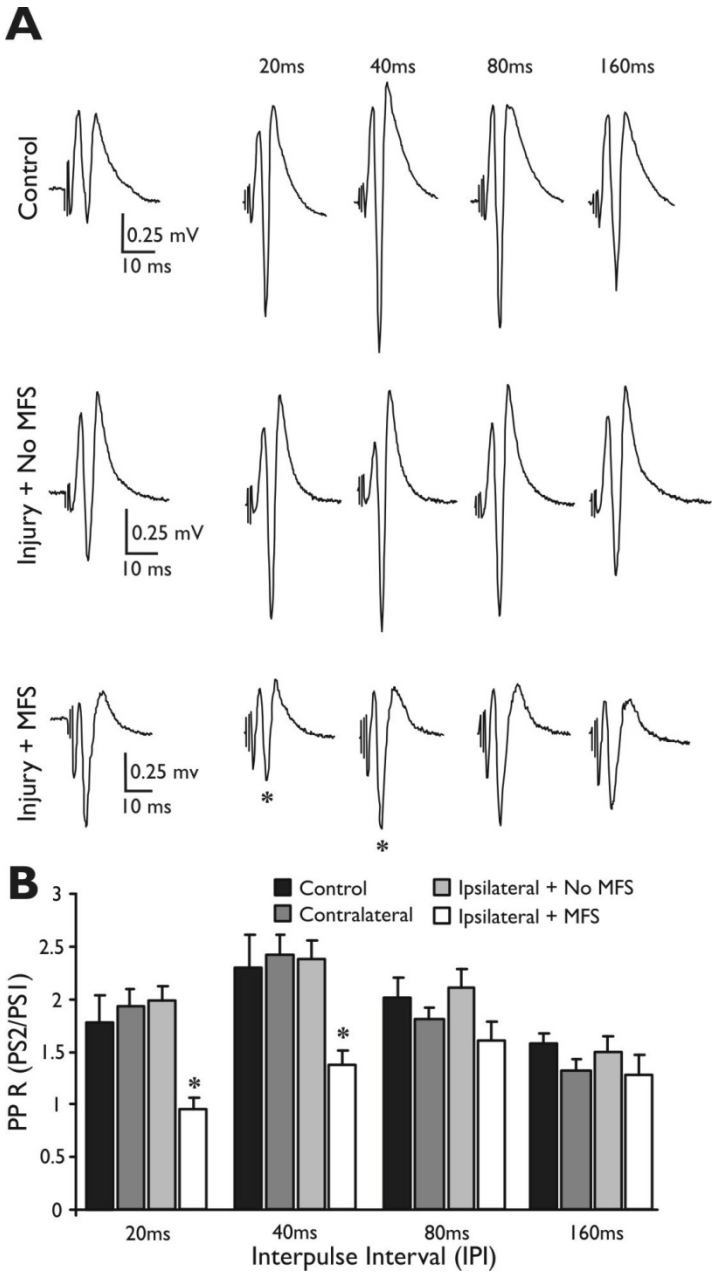

Figure 3.3. **Paired-pulse ratios in the dentate gyrus are reduced in slices from injured mice with mossy fiber sprouting 42-71d after injury. A.** Representative field-potential recordings evoked by paired-pulsed stimulation of perforant path input to the dentate gyrus at 20, 40, 80, and 160ms interpulse intervals in controls, CCI injured mice with no mossy fiber sprouting (MFS), and CCI injured mice with MFS. Facilitation of the second population spike was observed at all intervals in controls and injured mice without mossy fiber sprouting. Paired-pulse ratios were significantly decreased in slices from injured mice with mossy fiber sprouting at early (20ms and 40ms) but not later (80ms and 160ms) intervals. **B.** Bar graph showing the mean PPR for all slices at 20, 40, 80, and 160 ms (n=15-46). Bars represent means ± S.E.M. Asterisks (*) represent a significant reduction in paired-pulse ratios as determined by one-way ANOVA with Tukey's post hoc analysis ($P < 0.01$).

Hyperexcitability in slices with mossy fiber sprouting

Hilar-evoked field potentials were examined in the same slices used to obtain paired-pulse data. These experiments were first performed in "normal" ACSF and then in Mg^{2+}-free ACSF containing 100μM PTX. In "normal" ACSF, electrical stimulation consistently elicited a single population spike in nearly all hippocampal slices from controls and injured animals (Figure 3.4, 3.5A). Two ispilateral slices (one each from a mild and severe injury) had 2-3 population spikes. In Mg^{2+}-free ACSF containing PTX, a single population spike was elicited in all slices (n= 14) from control animals (Figure 3.4A). When hilar-evoked responses under these conditions were compared among injured animals, 98% (n= 45 of 46) of contralateral slices without mossy fiber sprouting and 87.5% (n= 35 of 40) of ipsilateral slices without mossy fiber sprouting had a single population spike (Figure 3.4B). Three of 15 (20%) ipsilateral slices with mossy fiber sprouting had a single population spike similar to controls. Increased excitability or epileptiform activity was observed in the remaining slices, which almost exclusively included the ipsilateral dentate gyrus. The increase in excitability was observed in the form of multiple population spikes in 1 (2%) contralateral slice, 5 (12.5%) ipsilateral slices without mossy fiber sprouting, and 12 (80%) ipsilateral slices with mossy fiber sprouting (Figure 3.4C). In three (20%) of the slices from the ipsilateral dentate gyrus, hilar stimulation evoked prolonged negative-going field potentials and secondary

population spikes with long and variable latency to the stimulus (Figure 3.4D). Slices with the latter, most robust response, contained the highest degree of mossy fiber sprouting (Timm scores$\geq$ 2). Timm score ranges associated with a single population spike, multiple population spikes, and prolonged negative field shifts were compared and found to be statistically different by Kruskal-Wallis test ($H_{(2, 107)} = 27.77$, $P < 0.00001$; Figure 3.5B). A Dunn's post hoc test confirmed that Timm scores associated with slices containing a single hilar-evoked population spike were significantly different from Timm scores of slices that had multiple population spikes ($P<0.01$) and prolonged negative field shifts ($P<0.001$). In both cases of hyperexcitability the secondary activity could be completely and reversibly blocked by 50μM APV. The relative range of hilar-evoked responses observed in Mg^{2+}-free ACSF containing PTX for each experimental group are given in Figure 3.5C.

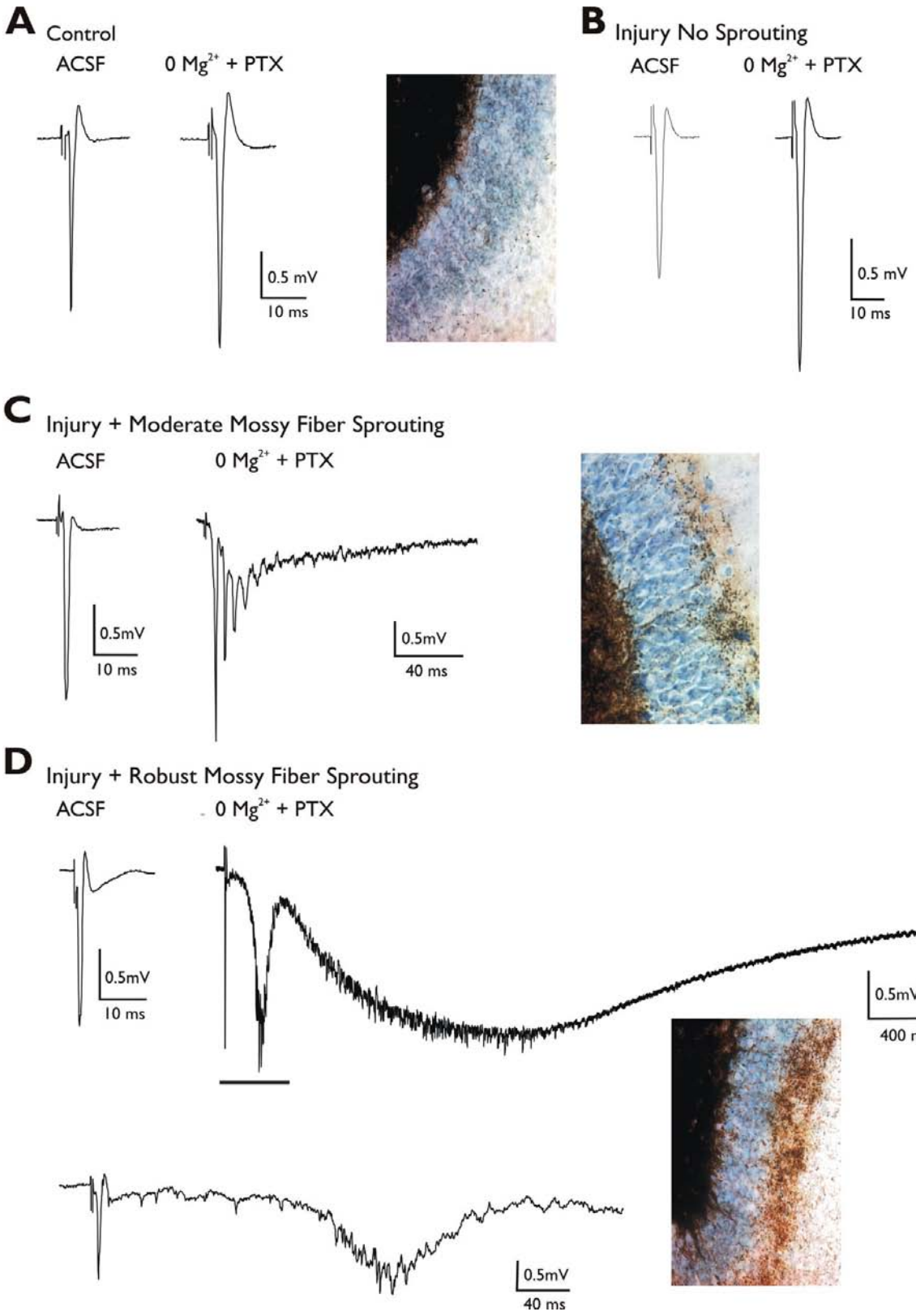
A
Control
ACSF
0 Mg2+ + PTX
0.5 mV
10 ms
B
Injury No Sprouting
ACSF
0 Mg2+ + PTX
0.5 mV
10 ms
C
Injury + Moderate Mossy Fiber Sprouting
ACSF
0 Mg2+ + PTX
0.5mV
10 ms
0.5mV
40 ms
D
Injury + Robust Mossy Fiber Sprouting
ACSF
0 Mg2+ + PTX
0.5mV
10 ms
0.5mV
400 ms
0.5mV
40 ms

Figure 3.4. Electrical stimulation of mossy fibers in the hilus evokes increased population responses in the dentate gyrus of mice with mossy fiber reorganization 42-71d after CCI injury. A, B. Hilar-evoked responses in controls and injured mice without mossy fiber sprouting consisted of a single population spike in normal ACSF and in Mg^{2+}-free ACSF containing PTX. **C**. Evoked responses in a slice from a CCI-injured mouse with moderate mossy fiber sprouting. A single population spike was evoked in normal ACSF. Multiple population spikes were evoked in Mg^{2+}-free ACSF containing PTX. **D.** Hilar stimulation evoked a single population spike in normal ACSF in a slice with robust mossy fiber sprouting. In Mg^{2+}-free ACSF containing PTX, a prolonged negative field-potential shift with secondary population activity was evoked. The underlined portion of the trace in **D** is expanded below to demonstrate the initial population spike followed by secondary activity. Insets provide representative Timm's stains demonstrating the level of mossy fiber sprouting typical of slices that produced each response.

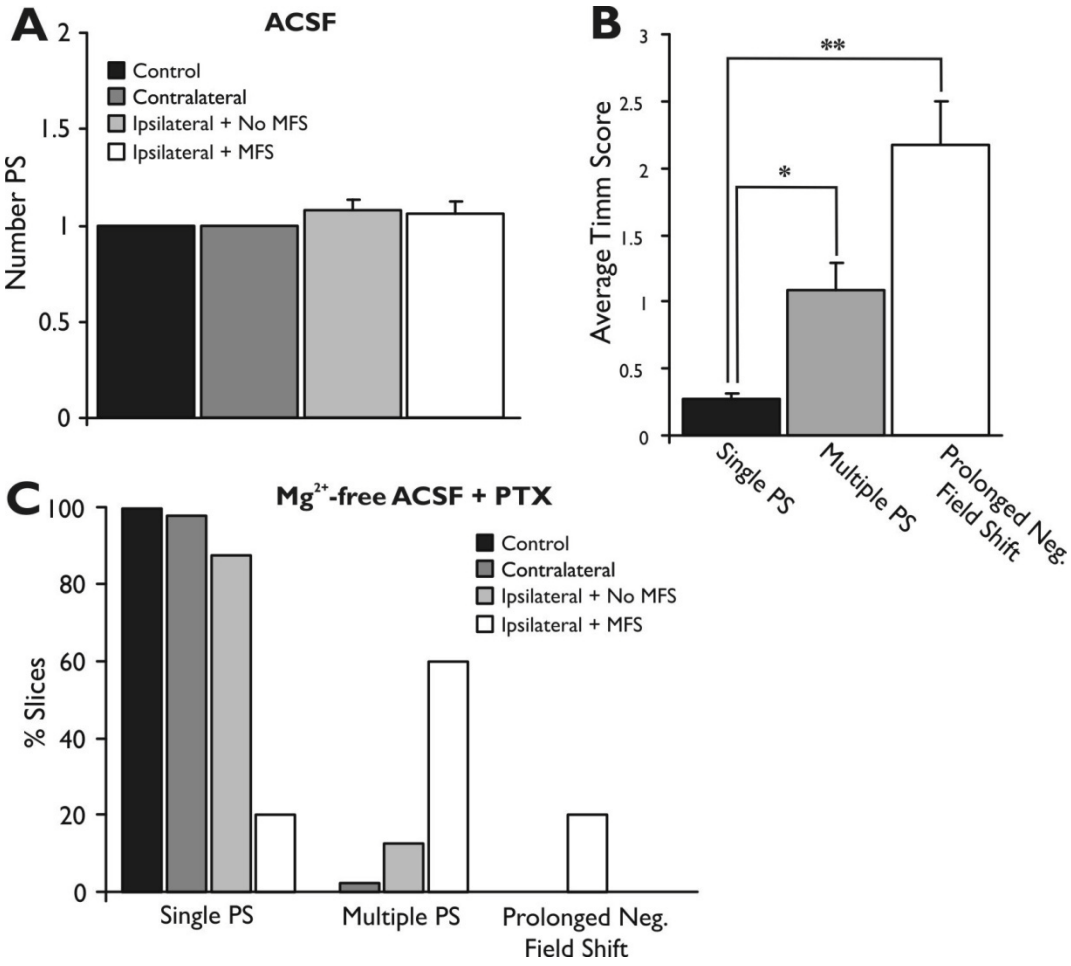

Figure 3.5. Increased excitability is revealed in the dentate gyrus of CCI-injured mice during disinhibition. A. Hilar stimulation in normal ACSF evoked a single population spike in nearly all slices from injured and control animals. **B**. Average Timm scores for slices in which a single population spike, multiple population spikes, or prolonged negative field shifts were evoked in the presence of Mg^{2+}-free ACSF containing PTX. Bars represent means ± S.E.M. Single asterisks (*) represent $P < 0.01$ and double asterisks (**) represent a $P < 0.001$ as determined by Kruskal-Wallis with Dunn's post hoc analysis. **C.** Relative range of hilar-evoked population responses in Mg^{2+}-free ACSF containing PTX.

Spontaneous epileptiform activity in slices with robust mossy fiber sprouting

The susceptibility to generation of spontaneous epileptiform activity in the presence of Mg^{2+}-free ACSF containing PTX was also examined. Three ipsilateral slices that contained robust mossy fiber reorganization (i.e. Timm scores ≥ 2) exhibited spontaneous bursts of population spikes and large amplitude negative-going field potential shifts of variable frequency in the granule cell layer (Figure 3.6B). Small amplitude positive-going shifts, but not epileptiform burst discharges, were regularly observed in all other slices from injured and control animals (Figure 3.6A).

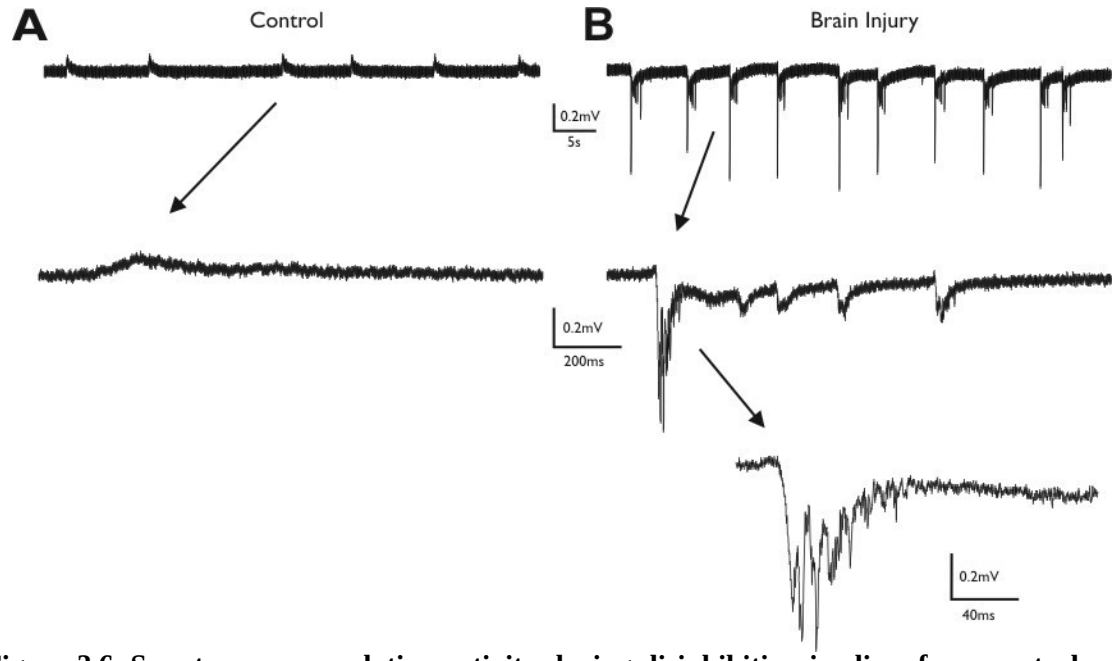

Figure 3.6. Spontaneous population activity during disinhibition in slices from control and injured mice. A. Field-potential recordings in the dentate gyrus of a control mouse demonstrate spontaneous positive-going field potential deflections. **B.** Spontaneous epileptiform activity consisting of large amplitude negative going field shifts and spontaneous population spikes observed in the dentate gyrus of a mouse with mossy fiber sprouting. Arrows in **A** and **B** indicate expanded portions of the respective traces.

3.4 Discussion

The results of this study suggest that the dentate gyrus of injured mice with mossy fiber sprouting became epileptogenic. Mice developed spontaneous seizures by 42-71d after mild or severe CCI injury, an important extension of previous studies that suggested this model of TBI induced early seizures (Nilsson et al, 2004; Kochanek *et al.*, 2006). In addition, I found evidence for regionally localized structural reorganization of mossy fibers in the dentate gyrus ipsilateral to the injury that was accompanied by reduced PPR and increased spontaneous and hilar-evoked recurrent excitability. These long-term behavioral, anatomical, and functional changes are consistent with TLE development in humans and rodents.

3.4.1 Spontaneous seizures after mild and severe CCI

Several characteristics of seizures in injured mice resembled seizures observed in other rodent models of TLE and PTE (Shibley and Smith, 2002; D'Ambrosio et al., 2004, 2005; Kharatishvili et al., 2006). In the present study, 20-36% of mice were observed to have unprovoked seizures weeks after injury. This is comparable to clinical studies that indicate as many as 39% of patients sustaining severe TBI with intact dura develop PTE (Caveness, 1976; Annegers et al., 1998). While increased seizure susceptibility to electrical stimulation and proconvulsant drug exposure has been noted after CCI and weight drop (Golarai et al., 2001; Statler et al., 2008), spontaneous seizures have only been reported in rats after severe FPI (Kharatishvili et al., 2006; Griesemer and Mautes, 2007). Previous studies have suggested that limbic involvement typically does not evolve in rats until several months after FPI (D'ambrosio et al., 2004, 2005; Kahratishvili *et al.*, 2006), but many mice in this study developed seizures and hippocampal pathology by 10 weeks post-injury. A shorter time period from injury to TLE makes studies of injury-induced epileptogenesis more feasible. Since animals in the present study were observed periodically, I presumably underestimated the number of mice that developed spontaneous seizures and the frequency of seizures. However, I was mainly concerned with the qualitative assessment of seizure development after CCI. Continuous video-

EEG or longer periods of seizure monitoring may increase the yield for seizure detection. It also remains to be elucidated whether a gradual shift in seizure type from partial to secondarily generalized over time also occurs after CCI as has been reported after FPI (D'Ambrosio et al., 2005; Kharatishvili et al., 2006).

3.4.2 Posttraumatic mossy fiber sprouting

Mossy fiber reorganization is a phenomenon repeatedly observed in TLE patients and animal models, is well developed by 2-4 weeks after an epileptogenic insult in rodents, and persists throughout life (Dudek and Spitz, 1997). Mossy fiber sprouting may only be one of many anatomical factors such as neuron loss, neurogenesis, gliosis, or morphological changes associated with epileptogenesis (Pitkanen and Sutula, 2002). However, I examined changes in mossy fiber organization because of its traditional consistency and reliability as a marker of the epileptic dentate gyrus. Mossy fiber sprouting after CCI was most prominent in dorsal regions of the ipsilateral dentate gyrus and resembled sprouting observed in humans and animal models of TLE (Tauck and Nadler, 1985; Shibley and Smith, 2002). Previous reports in rats have indicated minimal sprouting in the dentate gyrus ipsilateral to the injury at 3 months post-FPI (Santhakumar et al., 2001) and dense sprouting in the septal dentate gyrus ipsilateral to the injury in rats that display spontaneous seizures by 12 months (Kharatishvili et al., 2006). However, I detected minimal axon reorganization near the injury site as early as 7d post-injury, and the number of animals with mossy fiber sprouting increased with time post-injury such that 55% of mice were found to have locally abnormal mossy fiber organization by 10 weeks after severe CCI. Even in animals with spontaneous seizures, mossy fiber sprouting was mainly localized to areas ipsilateral and proximal to the lesion. Thus, sprouting may not need to be as widespread as is often observed in status epilepticus-induced TLE models to contribute to seizures.

Injury severity likely contributes to the degree of mossy fiber sprouting after TBI. Similar to the observation that severe lateral FPI is necessary to induce sprouting in rats (Santhakumar et al., 2001), more mice developed mossy fiber sprouting after severe CCI. Several previous studies have described in detail the extent, variability, and progression

of cortical and hippocampal damage after mild or severe CCI in mice (Hannay et al, 1999; Tong et al., 2002; Hall et al., 2005; Saatman et al., 2006). Previous reports in rats and mice indicate greater cortical lesion volume after severe vs mild injury that is due to an increase in injury depth but not rostral-caudal distribution (Goodman et al., 1994; Hannay et al., 1999; Saatman et al., 2006). The present electrophysiological experiments utilized mainly horizontal slices, which allowed recordings to be made from approximately the temporal two-thirds of the hippocampal formation (i.e., from just ventral to the lesion to near the temporal pole), so the lesion site itself was not analyzed. Since the present methods of CCI were identical to those used in previous studies (Hall et al., 2005), the assumption is that the initial lesion was similar in dimension and variability to that described previously. Despite reports that indicate severe injury in the CCI model can occasionally produce bilateral damage to structures that are especially susceptible to injury, such as the thalamus and hippocampus (Goodman et al., 1994; Smith et al., 1995), nearly all slices from the contralateral dentate gyrus appeared devoid of mossy fiber sprouting in the inner molecular layer, even in mice with generalized seizures. Thus, it is possible to observe a full range of Timm scores - from no sprouting to robust sprouting - in slices from a single mouse after CCI.

The presence of regionally robust mossy fiber sprouting in mice that displayed category 3 seizures suggests an association between axon sprouting and seizure severity and/or frequency after TBI. However, it is difficult to establish whether injury-induced mossy fiber reorganization precipitates limbic seizures, seizures induce mossy fiber sprouting, a combination of the two occur, or even to be confident that sprouting is a necessary accompaniment of limbic seizures. Studies aimed at determining causality are complicated by the myriad cellular and molecular alterations occurring concurrent with axon sprouting, several of which may also contribute to the development of seizures after brain injury. Synaptic reorganization in other damaged structures such as CA1, amygdala, and neocortex could additionally contribute to seizure development after injury but are more difficult to detect. For example, increases in synaptic connections and excitability of CA1 pyramidal cells have been reported after focal injury (i.e. CCI and weight drop), are also seen in TLE models, and could further contribute to seizures (Smith and Dudek, 2001; 2002; Scheff et al., 2005; Griesemer et al., 2007). Moreover,

Buckmaster and Dudek (1997b) reported no direct association between seizure frequency and the degree of mossy fiber sprouting after kainate-treatment. In the present study sprouting was more prevalent at 42-71d versus 7d after severe CCI injury, suggesting progressive development of new excitatory connections in the dentate gyrus. However, mice were not monitored for seizures at the earlier time points, and the relationship between structural damage, axon sprouting, and seizure development was beyond the scope of this study. Further investigations using continuous EEG in combination with cellular techniques that compare animal models with variable levels of mossy fiber sprouting (i.e., TBI, status epilepticus, etc.) may provide insight into any causal relationships between axon sprouting, epileptogenesis, and the onset of limbic seizures.

3.4.3 Increased synaptic inhibition after CCI

Reduced PPR has been repeatedly demonstrated in the dentate gyrus of epileptic patients and animal models of TLE (Tuff et al., 1983; Buckmaster and Dudek, 1997a; Swanson et al., 1998). One view is that mossy fiber sprouting after an epileptogenic insult plays a restorative role by enhancing excitatory synaptic input onto GABAergic interneurons in the hilus (Sloviter, 1991, 1992). However, other studies have demonstrated decreased inhibitory input onto granule cells that is possibly related to the loss of GABAergic interneurons in epileptic animals (Buckmaster and Dudek, 1997a; Kobayashi and Buckmaster, 2003). Previous reports of paired-pulse data in rats after TBI have been conflicting. Reeves et al. (1997) reported reduced PPR in the ipsilateral dentate gyrus at early IPIs (20ms-100ms) up to 15d post-FPI *in vivo*. Other studies have suggested no change or even increased PPR weeks to months after TBI (Lowenstein et al., 1992; Golarai et al., 2001). In the present study, PPR at all IPIs from ipsilateral and contralateral slices without mossy fiber sprouting was similar to controls. I found that PPR was selectively reduced at earlier (20ms and 40ms) but not later (80ms and 160ms) IPIs in slices with mossy fiber sprouting (Timm scores >1) after injury. This is an interesting finding that suggests a long-term increase in synaptic inhibition after TBI associated with mossy fiber reorganization. Previous studies of posttraumatic hyperexcitability have not differentiated between slices with and without sprouting.

Perforant path stimulation did not consistently evoke paired pulse inhibition at low IPIs (i.e., 20ms) in control slices as is commonly observed. However, other reports demonstrated paired-pulse inhibition in control slices at low IPIs (Kirby et al., 1995; Hirota and Roth, 1997). Differences in stimulation frequency, intensity, inter-pulse interval, time post-injury, ACSF composition, and/or animal model could all contribute to discrepancies among studies. Moreover, variations in stimulus parameters have been reported to have inconsistent effects on paired-pulse inhibition, particularly at high stimulation frequencies and/or intensities (Waldbaum and Dudek, 2005, 2007). In the present study all experimental conditions remained constant; control data were obtained alongside data from injured animals, and different slices from injured animals were treated identically within an experiment. Field-potential experiments are limited in that perforant path stimulation is not a direct measure of GABA-mediated inhibition. I found that interval-specific changes in PPR were associated with mossy fiber sprouting, consistent with the hypothesis that sprouting may increase synaptic inhibition in these slices, but it remains possible that other injury-induced changes of dentate gyrus networks could produce similar effects. Alternative interpretations of the present paired-pulse data could include the possibility of a presynaptic effect such that transmitter release probability is altered, inhibitory cells may sustain damage and undergo functional changes as a result of TBI, and/or hilar mossy cells may be driving synaptic inhibition in the injured mice. Future experiments that use cellular approaches to assess excitatory and inhibitory drive onto both granule cells and GABAergic interneurons may better clarify the effect of TBI on recurrent inhibition in the dentate gyrus. Regardless, these data suggest an interval-specific and selective reduction of PPR in slices containing mossy fiber sprouting after TBI.

3.4.4 Epileptiform activity after CCI

Numerous *in vitro* studies have suggested that mossy fiber reorganization contributes to epileptiform activity and seizures by forming a positive-feedback network among granule cells (Cronin and Dudek, 1988; Molnar and Nadler, 1999; Lynch and Sutula, 2000; Buckmaster *et al.*, 2002; Scharfman et al., 2003; Winokur et al., 2004).

The present data are consistent with this view. An increased susceptibility to spontaneous and evoked epileptiform activity in the ipsilateral dentate gyrus of slices with mossy fiber sprouting were revealed in the presence of Mg^{2+}-free ACSF containing PTX. These epileptiform discharges were not observed in slices from injured or control animals that did not display mossy fiber sprouting. Spontaneous positive shifts in slices from controls and negative field shifts in slices from kainate treated rats and reeler mutant mice during disinhibition have previously been described (Cronin et al, 1992; Waurin and Dudek, 1996; Buckmaster and Dudek, 1997a; Patrylo et al., 2006). Hilar stimulation evoked prolonged negative-going field-potential shifts and secondary population spikes in slices with robust levels of sprouting and multiple population spikes in many but not all slices with more moderate levels of mossy fiber sprouting. These responses are qualitatively similar to those observed in animal models of TLE (Tauck and Nadler, 1985; Cronin et al., 1992; Waurin and Dudek, 1996; Patrylo et al., 1999; Winokur et al., 2004). Multiple population spikes were observed in a small percentage of ipsilateral and contralateral slices that did not have robust mossy fiber sprouting. This may indicate that mossy fiber reorganization is not solely responsible for the enhanced excitability in some slices. However, one obvious limitation to electrical stimulation is that cell bodies and other axons of passage can be activated concurrent with mossy fibers making it an indirect measurement of synaptic connectivity. The possibility that neurons in the hilus (e.g., excitatory mossy cells) play a role in the increased excitability observed in this preparation cannot be excluded. Caged glutamate microstimulation (Molnar and Nadler, 1999; Waurin and Dudek, 2001; Winokur et al., 2004) or dual intracellular recordings (Scharfman et al., 2003) could provide a more direct assessment of synaptic connections between granule cells after CCI. Even so, these data indicate that mossy fiber reorganization in slices from injured animals is associated with increased susceptibility for epileptiform activity.

3.4.5 Additional comparisons between CCI and other experimental models of TBI-induced epilepsy

Distinct strengths and limitations exist with any experimental model. Currently, FPI and weight drop are the most widely used trauma models that have also been adapted as models of post-traumatic hyperexcitability. CCI offers potential advantages over these other models. Perhaps the most important advantage is that CCI has been adapted to mice (Smith et al., 1995; Sullivan et al., 1999), rats (Dixon et al., 1991; Scheff et al., 1997), and even larger animals such as sheep (Anderson et al., 2003). To date, studies of TBI-induced epilepsy using FPI and weight drop have been nearly exclusively performed in rats. The ability to perform CCI in mice provides an invaluable experimental tool for studying the contribution of genetic background in PTE development. CCI produces a consistent and reproducible focal injury in each animal, and mechanical parameters (i.e., injury velocity, depth, and tissue deformation) are easily managed. There is minimized risk for inaccuracy or secondary "rebound" injury as can be seen with other focal TBI models (i.e., weight drop). On the other hand, lateral FPI produces a mixed focal *and* diffuse injury making it impossible to determine the contribution of each injury type to epileptogenesis. A more focused and consistent injury produced in CCI may have behavioral and/or functional implications. One commonality among the abovementioned TBI models is that all produce a degree of focal injury. This suggests that focal injury may play a more critical role in epileptogenesis than diffuse injury. Thus, the highly focal lesion produced by CCI may reflect a more relevant aspect of PTE. A potential limitation of the CCI model is that increasing injury severity does not achieve increased mortality; this contradicts clinical observations. Severity of lateral FPI must be increased such that mortality rate is ~50% in order to induce TLE in rats (Kharatishvili et al., 2006). Mortality after severe FPI may be due to disproportionate injury to the brainstem and/or the more diffuse nature of the model. Weight drop is another highly focal model of severe TBI after which nearly all animals have been similarly reported to survive (Griesemer and Mautes, 2007). Therefore, the injury-induced sequence of events leading to mortality may be different from those leading to TLE.

In conclusion, CCI reproduced key behavioral, anatomical, and functional features common to human PTE and TLE in mice. Development of specific hippocampal pathology often associated with TLE development occurred at earlier time points than described in some other TBI models. Therefore, CCI not only provides a useful model of TBI but is also effective in inducing PTE in mice.

Chapter 4

Regionally localized recurrent excitation in the dentate gyrus of a cortical contusion model of posttraumatic epilepsy

This chapter was published in *J Neurophysiol.* Mar 2010; 103(3):1490-1500.

4.1 Introduction

In patients and experimental models of temporal lobe epilepsy, the generation of epileptic activity is associated with axon sprouting and reorganization of neuronal circuitry (Tauk and Nadler, 1985; Sutula et al., 1989; Dudek and Spitz, 1997; Buckmaster et al., 2002; Shibley and Smith, 2002; Hunt et al., 2009). The dentate gyrus, which is particularly susceptible to injury, often undergoes structural reorganization, and it is a widely used model system for studying altered synaptic circuitry in epilepsy. Several studies suggest that dentate granule cells, which are not normally interconnected, sprout axon collaterals into the inner molecular layer (i.e., mossy fiber sprouting) to form functional recurrent excitatory connections with nearby granule cells during epileptogenesis and may contribute to network synchronization (Cronin and Dudek, 1988; Cronin et al., 1992; Waurin and Dudek, 1996, 2001; Lynch and Sutula, 2000; Winokur et al., 2004; Hunt et al., 2009). Mossy fiber sprouting has been reported weeks to months after experimental TBI in rodents (Santhakumar et al., 2001; Golarai et al., 2001; Kharatishvili et al., 2006; Hunt et al., 2009) and in temporal lobe epilepsy patients with a history of head injury (Swartz et al., 2006), but the functional implications of injury-induced regional alterations in neuronal circuitry after TBI have not been well described.

The degree of mossy fiber sprouting after experimental TBI is qualitatively less than the robust, bilateral sprouting observed weeks after experimental status epilepticus. While less widespread axon reorganization is a more typical representation of the clinical setting, computational models have suggested that synchronous network activity may only occur if robust recurrent synaptic connections are present (Traub and Wong, 1981; 1982). Studies using extracellular field recordings to examine network excitability in the

dentate gyrus after experimental head injury have not consistently demonstrated epileptiform activity after TBI (Reeves et al., 1997; Santhumakar et al., 2001; Golarai et al., 2001; Hunt et al., 2009). Moreover, Santhakumar and collegues (2001) reported a recovery within a month after fluid percussion injury from an early increase in extracellular excitability of the granule cell layer that may be related to mossy fiber sprouting. Therefore, mossy fiber sprouting may play a different functional role in the dentate gyrus after mechanical injury than in pharmacologically induced temporal lobe epilepsy models. The persistence of recurrent excitatory connections between granule cells after TBI has not been well established. Understanding how synaptic circuit reorganization may contribute to seizures or chronic changes in excitability after TBI should help to elucidate the importance of these cellular mechanisms in PTE.

Here, I tested the hypothesis that mossy fiber sprouting forms an excitatory feedback circuit between granule cells after CCI head injury. I specifically focused on three main questions: (1) can an increase in excitatory synaptic input onto individual granule cells be detected after injury; (2) do granule cells in slices with posttraumatic mossy fiber sprouting exhibit spontaneous epileptiform activity; and (3) can excitatory synaptic events be elicited by local glutamate photostimulation at distant locations within the granule cell layer?

4.2 Methods

Seizure monitoring. Injured animals were monitored for immediate seizures (i.e., injury-induced) during a 90 minute interval that began ~90 minutes after CCI injury. I chose this time for practical reasons (i.e., to allow animals to fully recover from anesthesia and surgery) and based on a previous report that behavioral manifestations are not observed until at least 1h post-CCI (Kochanek et al., 2006). Control and injured mice were subsequently observed 4-6 hr/wk for spontaneous seizures during random 1–2h intervals until 10 weeks post-injury. Observation periods occurred during the light phase of the light/dark cycle, and seizures were rated from 1 to 5, with 5 being the most severe, according to a modified Racine scale (Racine, 1972; Shibley and Smith, 2002). To minimize subjectivity in seizure assessment, category one seizures (i.e. facial automatisms, increased grooming behaviors) were excluded from analysis. Posttraumatic seizures were classified based on the time post-injury in which they occurred: immediate, first 90 minute monitoring session; early, 1 - 7d post-injury; and late, > 7d after injury.

4.3 Results

4.3.1 Posttraumatic seizures

Mice were monitored for behavioral seizures from the time of injury until 10 weeks post-injury. During the first 90 minute monitoring period following injury, 5 of 33 mice (15%) were observed to have at least one injury-induced seizure. The majority of these mice had only one or two seizures; one mouse had three category 3-5 seizures during this period. One mouse (3%) that did not have immediate seizures had a category 3 seizure at 3d post-injury (i.e., early seizure). Spontaneous category 2-4 seizures were observed in 12 of 30 mice (40%), and category 3-4 seizures were observed in 4 of 30 mice (13%) (Figure 4.1). The average latency from injury to first observed spontaneous seizure was 6.5 ± 1.3 weeks after injury. This latent period is considered to be an estimate, since I did not monitor continuously. Of the 5 mice that had immediate seizures, 3 (60%) were observed to have spontaneous seizures.

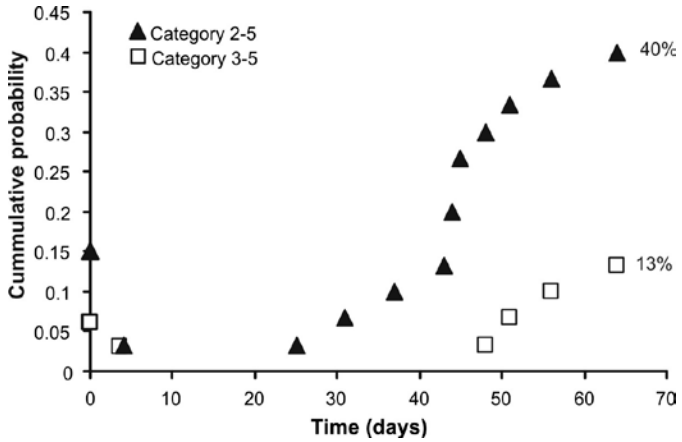

Figure 4.1. Mice develop injury-induced and spontaneous seizures after severe CCI injury. Cumulative probability plot of the first observed seizure after CCI injury (time 0). Seizure counts were reset after 1d and 7d to separate immediate, early, and spontaneous seizures.

4.3.2 Injury-induced mossy fiber reorganization

Coronal brain sections of the dorsal hippocampus used for recordings in 21 mice were examined for gross anatomical damage in the hippocampus and mossy fiber sprouting at the injury site. Damage through the entire depth of the cortex directly below the impact site and hippocampal distortion were observed in all injured mice examined 8-12 weeks post-TBI, as previously described (Tong et al., 2002; Hall et al., 2005; Saatman et al., 2006). In 20 of 21 mice (95%), the cortical cavitation at the injury site extended into the hippocampus and a separation of the dorsal and ventral blades of the granule cell layer was visible. Mossy fiber sprouting was observed in sections ipsilateral to the injury in all 20 mice. One mouse had hippocampal and granule cell layer distortion, but cavitation was restricted to the cortex. Mossy fiber sprouting was not present in this mouse. Figure 4.2 shows the range of lesion to the dentate gyrus and degree of mossy fiber sprouting under the injury. No gross structural damage was observed in any section contralateral to the injury (n= 21) or in control mice (n= 15 animals), and these sections were also devoid of abnormal mossy fiber organization (i.e., all Timm's scores ≤ 1).

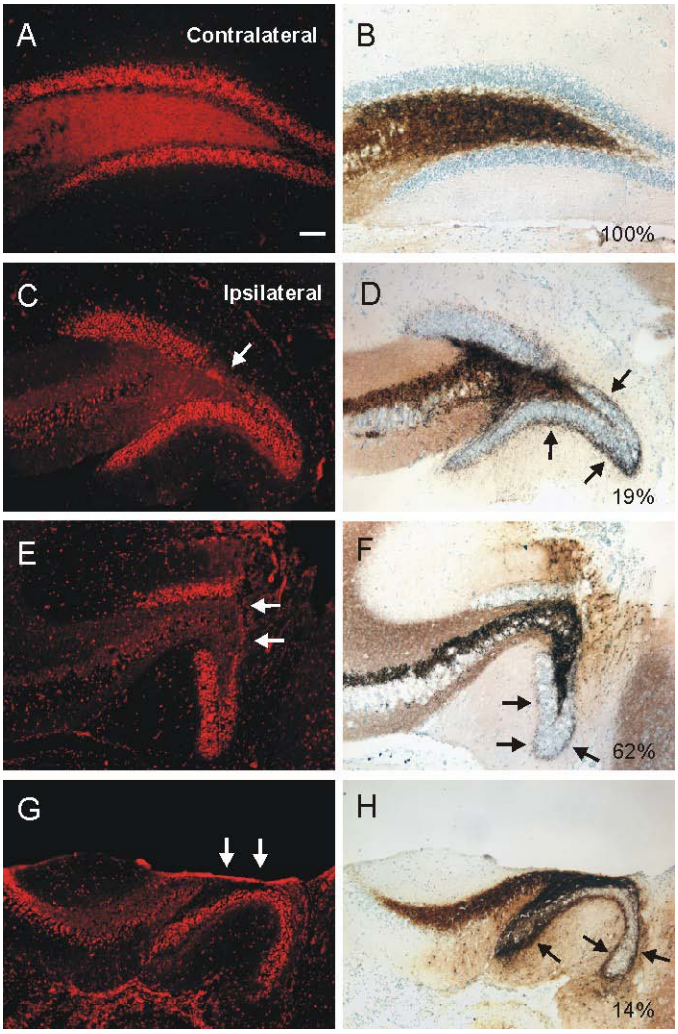

Figure 4.2. Cavitation into the hippocampus and posttraumatic mossy fiber sprouting 8-12 weeks after severe CCI injury. A. Representative Nissl stain of the dentate gyrus contralateral to the injury site. **B.** Timm's stain of the same section in **A** shows the absence of mossy fiber sprouting in the inner molecular layer. **C, E, G.** Representative Nissl stain images of the ipsilateral dentate gyrus at the injury site. Arrows indicate severe thinning of the granule cell layer. **D, F, H.** Timm's stain of the same sections in **C, E, G.** Note the presence of moderate mossy fiber sprouting in all sections (arrows). Percentage of mice with each type of lesion/Timm stain at the injury site is indicated. Scale bar is 100µm.

4.3.3 Excitatory input to dentate granule cells

To analyze whether excitatory synaptic input to dentate granule cells was increased after CCI injury, whole-cell voltage-clamp recordings of sEPSCs were obtained from granule cells in four treatment groups based on post hoc identification of mossy fiber sprouting: 1) ipsilateral slices with mossy fiber sprouting (n= 23 cells in 20 slices from 13 animals), 2) ipsilateral slices without mossy fiber sprouting (n= 22 cells in 18 slices from 14 animals), contralateral slices (n= 9 cells in 8 slices from 7 animals), and uninjured controls (n= 10 cells in 9 slices from 6 animals). Recordings were made from cells in the apex or outer blade regions of the granule cell layer where Timm's staining was typically most robust. The average resting membrane potential for these cells was: controls, -75 ± 3.8 mV; contralateral, -76 ± 2.9 mV; ipsilateral with no MFS, -75 ± 5.3 mV; and ipsilateral with MFS, -79 ± 4.4 mV. These values are consistent with previously reported ranges of -65mV to -85mV (Fricke and Prince, 1984; Staley et al., 1992; Waurin and Dudek, 1996), and one-way ANOVA found no difference between groups ($F_{(3,64)}$=2.03, P >0.05).

Spontaneous EPSCs were recorded at a holding potential of -70mV. At this potential, outward currents were not typically present. Application of 1mM kynurenic acid blocked inward events, indicating that these currents were mediated by glutamate receptors. Representative recordings for each group are shown in Figure 4.3A-D. As shown in table 4.1, EPSC kinetics (i.e., 10-90% rise time and decay time constant) were comparable to previous reports (Keller et al., 1991; Staley and Mody, 1992), and significant differences were not observed between groups (P>0.05). A significant difference in the mean event frequency between treatment groups was detected by one-way ANOVA (control: 0.64 ± 0.3Hz, contralateral: 0.66 ± 0.4Hz, ipsilateral without MFS: 0.65 ± 0.4Hz, ipsilateral with MFS: 2.2 ± 0.9Hz; $F_{(3,64)}$= 27.1, P<0.001; Figure 4.3E). Post hoc comparisons revealed that granule cells from ipsilateral slices with mossy fiber sprouting had a significantly higher frequency of sEPSCs versus other groups. To determine whether EPSC frequency was associated with the density of Timm's staining, a Timm score was obtained for each slice in which a recording was obtained. The average sEPSC frequency for each cell in slices ipsilateral to the injury was plotted as a function

of Timm score (Figure 4.3F), and a Spearman's rank correlation analysis indicated a significant positive relationship between EPSC frequency and Timm's score (r_s= 0.82, P < 0.001). This is consistent with previous reports that suggest a relationship between EPSC frequency and degree of mossy fiber sprouting in kainate treated rats (Waurin and Dudek, 2001). The mean amplitude of sEPSCs for each treatment group was: control, -7.4 ± 3.0pA; contralateral, -6.8 ± 1.7pA; ipsilateral without MFS, -7.1 ± 1.7pA; and ipsilateral with MFS, -9.4 ± 5.4pA. One-way ANOVA did not indicate significant differences between groups ($F_{(3, 64)}$= 1.9, P > 0.05; Figure 4.3G).

TABLE 1. *Passive membrane properties of granule cells after CCI injury*

	Average Timm Score	RMP, mV	10–90% EPSC RT (ms)	EPSC Decay τ (ms)
Control	0	−75 ± 3.8	1.8 ± 0.1	7.6 ± 0.6
Contralateral	0	−76 ± 2.9	1.8 ± 0.2	7.8 ± 0.5
Ipsilateral (No MFS)	0.4 ± 0.5	−75 ± 5.3	1.9 ± 0.4	7.9 ± 1.2
Ipsilateral (MFS)	2.4 ± 0.5	−79 ± 4.4	1.7 ± 0.3	7.3 ± 1.3

Values are means ± SD; RMP, resting membrane potential; RT, rise time; MFS, mossy fiber sprouting.

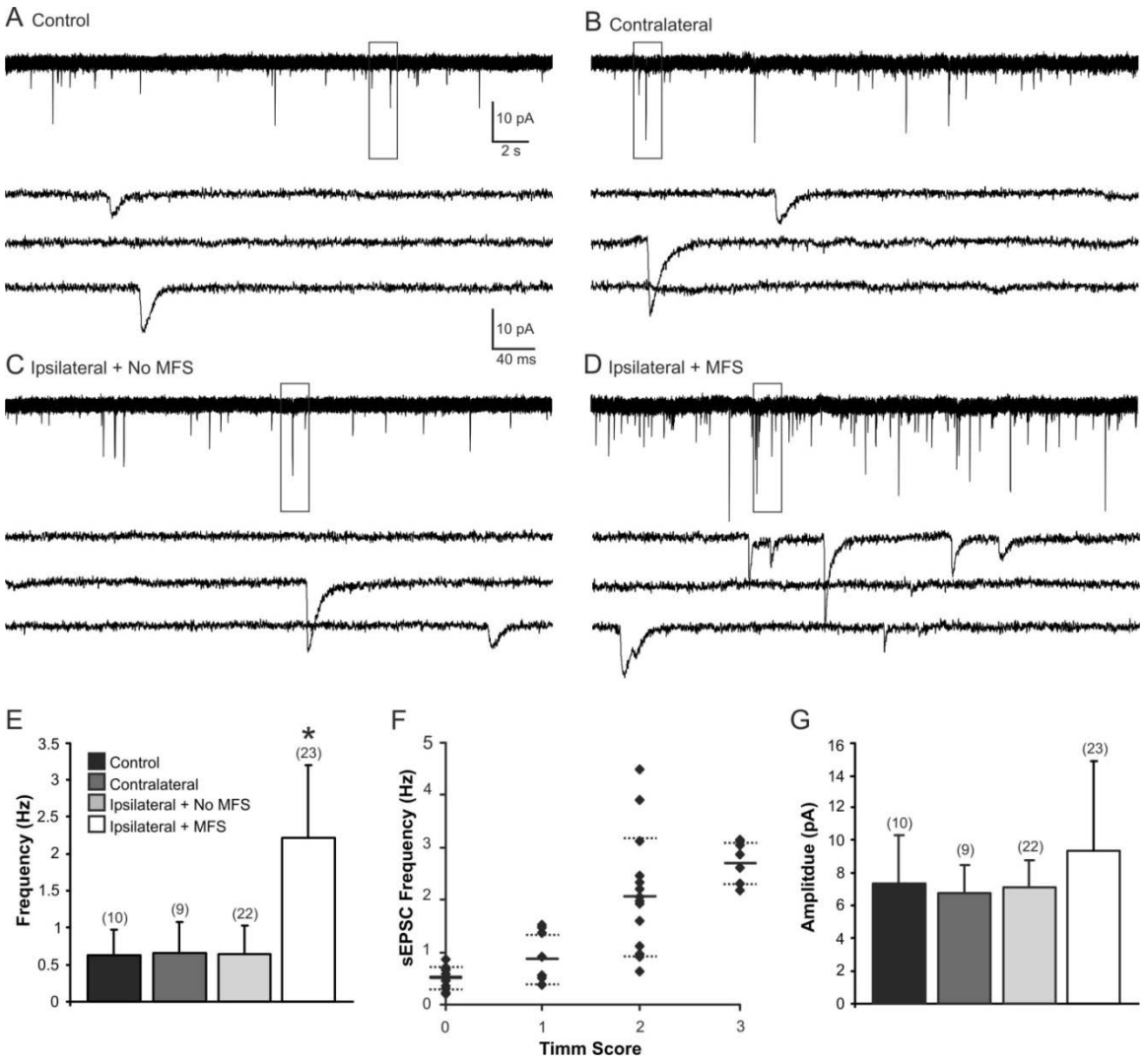

Figure 4.3. Increased sEPSCs in slices of the ipsilateral dentate gyrus with mossy fiber sprouting (MFS). A-D. Representative whole-cell patch-clamp recordings of granule cells in slices from **A**) control, **B**) contralateral, **C**) ipsilateral without MFS, and **D**) ipsilateral with MFS. Boxed areas of each trace are enlarged below. **E.** Average EPSC frequency for cells in each treatment group. The number of cells are indicated in parentheses above each bar. **F.** EPSC frequency plotted as a function of Timm score. Solid lines represent mean EPSC values and dotted lines respresent ±SD. **G.** Average amplitude for cells in each of the four treatment groups. Error bars indicate mean ± SD. Asterisk (*) indicates P<0.001.

4.3.4 Spontaneous epileptiform burst activity in slices with mossy fiber sprouting

When surgically isolated from afferent input, dentate granule cells normally do not fire spontaneous bursts of action potentials at resting membrane potential, even when inhibition is depressed (Fricke and Prince, 1984; Cronin et al., 1992, Waurin and Dudek, 1996). However, in conditions of reduced inhibition and increased excitability, spontaneous burst responses can be observed in slices from kainate-treated rats with mossy fiber sprouting, but not in controls (Cronin et al., 1992). I tested whether spontaneous epileptiform burst activity occurred in granule cells after injury. Slices were perfused with Mg^{2+}-free ACSF containing 100μM PTX to unmask NMDA receptor-mediated excitatory synapses and block $GABA_A$-mediated inhibition. Recordings were first obtained from granule cells in voltage-clamp at a holding potential of -70mV. Spontaneous bursts of repetitive or compound EPSCs were never observed in 42 granule cells in slices from injured and control slices without mossy fiber sprouting (n= 5, control; n= 14, contralateral; and n= 23, ipsilateral without mossy fiber sprouting). In contrast, 34 of 51 cells (67%) in 34 slices with mossy fiber sprouting from 19 injured animals had spontaneous bursts of large amplitude compound EPSCs (Figure 4). This difference was found to be significant ($P<0.001$; Fisher's exact test). Some of the cells examined for EPSCs were also examined for spontaneous epileptiform bursts of action potentials by switching to current-clamp mode and recording activity at resting membrane potential. Action potentials were not observed in any of 17 cells from slices without mossy fiber sprouting from injured and control animals (n=5, control; n= 5, contralateral; and n=7, ipsilateral without mossy fiber sprouting). In contrast, 65% of cells in slices with mossy fiber sprouting displayed bursts of action potentials (n= 17 of 26, Figure 4.5). This difference was statistically significant ($P<0.001$; Fisher's exact test). Action potential bursts were only observed in cells that also had bursts of EPSCs. Spontaneous burst activity was therefore only observed in granule cells of slices with mossy fiber sprouting from injured animals and was never observed in slices without mossy fiber sprouting from control or injured animals.

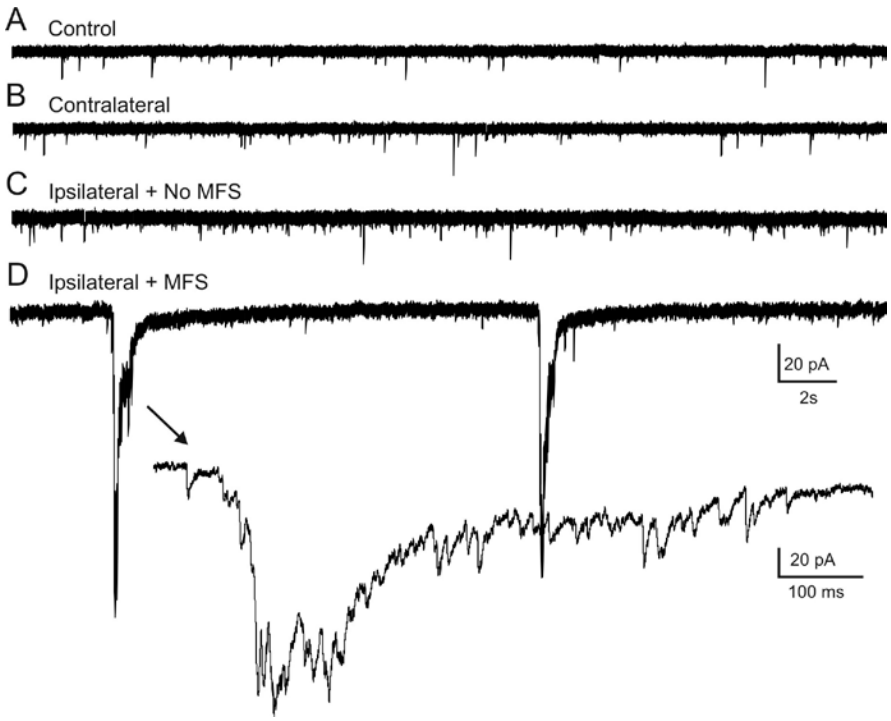

Figure 4.4. Spontaneous bursts of compound EPSCs in cells from slices with mossy fiber sprouting ipsilateral to the injury. Representative whole-cell voltage-clamp recordings of granule cells in **A**) a slice from an uninjured control mouse, **B**) a contralateral slice in an injured mouse, **C**) a slice ipsilateral to the injury without MFS, and **D**) a slice ipsilateral to the injury with MFS. Arrow indicates expanded portion of the trace in **D**. Slices were incubated with Mg^{2+}-free ACSF and 100μM PTX; V_m= -70mV for all recordings.

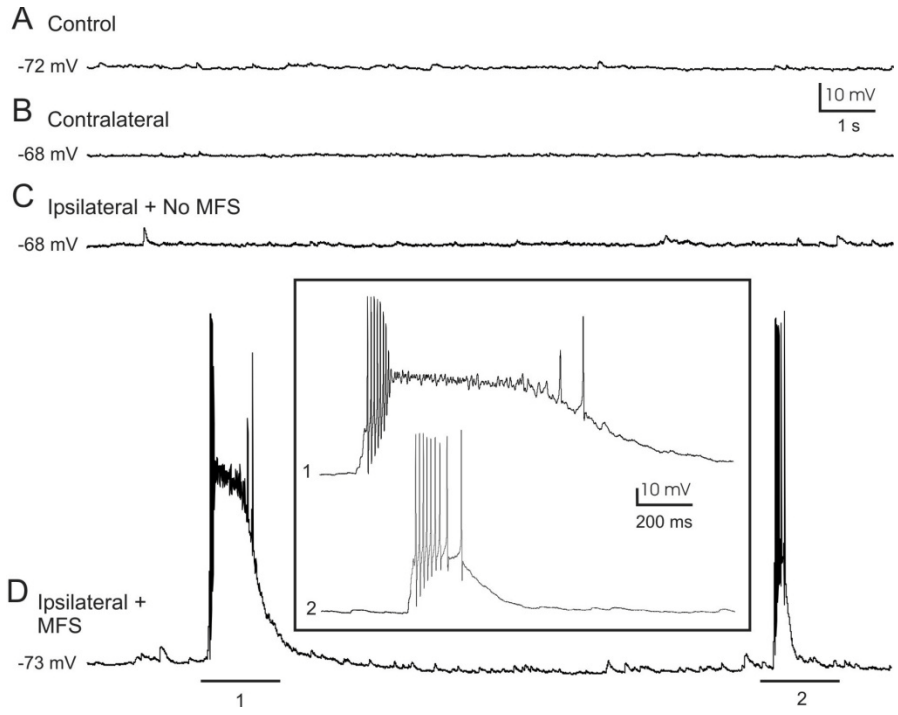

Figure 4.5. Spontaneous epileptiform bursts of action potentials in cells of slices with mossy fiber sprouting ipsilateral to the injury. Representative whole-cell current-clamp recordings of granule cells in **A**) a slice from an uninjured control mouse, **B**) a contralateral slice in an injured mouse, **C**) a slice ipsilateral to the injury without mossy fiber sprouting (MFS), and **D**) a slice ipsilateral to the injury with MFS. Inset shows expanded sections of the underlined portions of the trace in **D** labeled **1** and **2**. Resting membrane potential is indicated for each trace.

4.3.5 Excitatory synaptic connections between granule cells after CCI

Localized glutamate stimulation has been used to elicit responses that reflect synaptic connections between granule cells in slices with mossy fiber sprouting after pilocarpine or kainate treatment (Waurin and Dudek 1996, 2001; Lynch and Sutula, 2000; Winokur et al., 2004). I used glutamate photolysis to test the hypothesis that synaptic connections between granule cells can be evoked in slices with mossy fiber sprouting ispilateral to the injury and not in the contralateral dentate gyrus where mossy fiber sprouting was absent. The presence (or absence) of synaptic connections was assessed by examining two postsynaptic responses: 1) photolysis-evoked EPSCs were first recorded at a holding potential of -70mV and 2) photolysis-evoked action potentials were recorded at resting membrane potential. Stimuli applied directly to the recorded cell

evoked a large amplitude inward current with occasional superimposed sodium currents (voltage-clamp) or a large depolarization with superimposed action potentials (current-clamp), confirming that the stimulation parameters were capable of evoking action potentials in the recorded cells (Figure 4.6A,B).

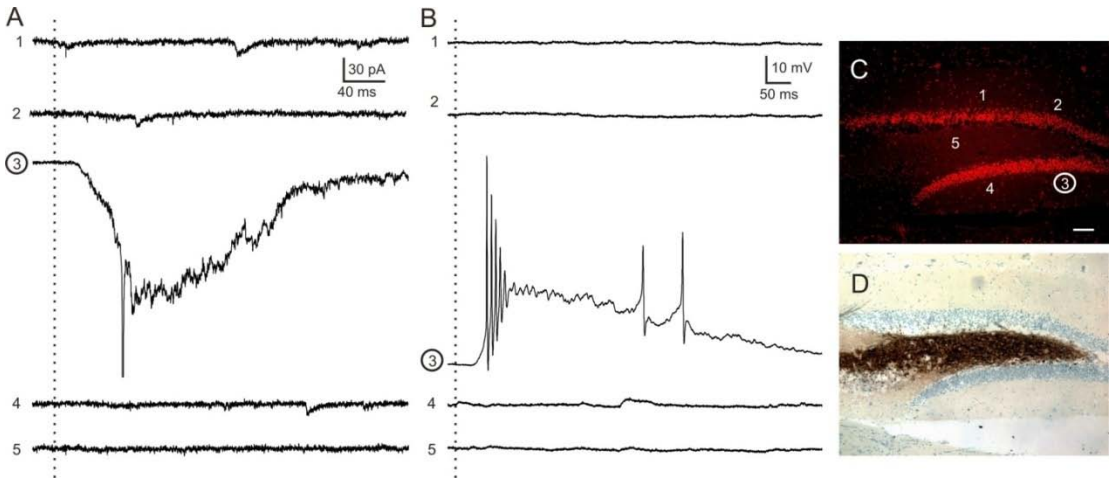

Figure 4.6. Granule cell - granule cell connections are not detected by glutamate photostimulation in cells from slices contralateral to the injury. A. Voltage-clamp recordings at -70mV from a granule cell. **B.** Current clamp recordings at resting membrane potential from the same cell as **A.** Dotted vertical lines indicate the time of stimulation. Numbers to the left of each trace indicate corresponding stimulus position shown in **C**. **C.** Nissl stain image of the slice from which the recorded cell was obtained. Numbers correspond to the approximate locations along the granule cell layer that photostimulation was applied to give the numbered responses recorded in **A** and **B**. Stimulation position **3** (circled) is the approximate location of the recorded cell. Note that direct activation of the recorded cell induced an inward current and burst of action potentials. **D.** Timm's stain image of the same section in **C** indicating no MFS into the inner molecular layer.

An increase in evoked synaptic activity was not observed in cells from slices contralateral to the injury (Figure 4.6); i.e., the average number of EPSCs in any given 100ms segment after stimulation was not greater than the average number of EPSCs before stimulation + 3SD at any stimulation site contralateral to the injury (n= 42 stimulus locations in 5 cells from 3 animals). In current-clamp recordings, photostimulation at the same locations did not evoke EPSPs or action potentials at any

site, except when applied directly to the recorded neuron. Therefore, glutamate photostimulation failed to elicit a synaptically-mediated response at any location along the granule cell layer or in the hilus/CA3 region in slices contralateral to the injury.

In contrast, photostimulation of the granule cell layer evoked a synaptic response and an increase in activity in 6 of 8 cells (75%) from 8 ipsilateral slices with mossy fiber sprouting (n= 66 stimulus locations, 5 animals; Figure 4.7). A total of 18 stimulation locations (1 to 6 locations per cell) were determined to give a positive response to photostimulation. Figures 4.8 and 4.9 show the variability of evoked responses in the granule cell layer ipsilateral to the injury site. A frequency histogram was constructed to show the distribution of the average number of eEPSCs for locations that had a positive response to photostimulation (Figure 4.8E). In current-clamp mode, EPSPs were consistently evoked and often reached action potential threshold (66%). Photostimulation evoked action potentials in nearly all trials (96%) at locations that had ≥ 4 eEPSCs in voltage-clamp mode. Only 24% of stimulations evoked action potentials at locations that had < 4 eEPSCs. The remaining stimulus locations (n= 48), including all 17 locations in the hilus and CA3, had no response to photostimulation. An increase in the number of EPSCs after stimulation was not observed and EPSPs were not evoked by photostimulation at these locations.

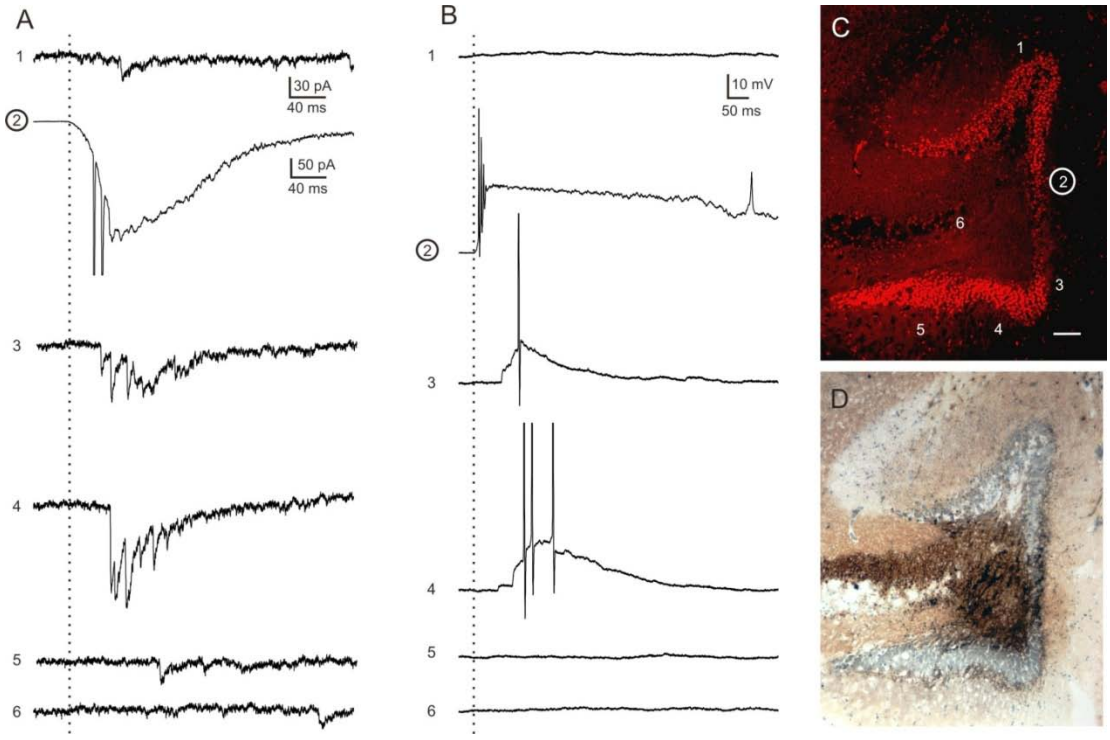

Figure 4.7. Granule cell - granule cell connections are detected by glutamate photostimulation in cells from slices ipsilateral to the injury with mossy fiber sprouting. A. Voltage-clamp recordings at -70mV from a granule cell. **B.** Current-clamp recordings at resting membrane potential from the same cell as **A.** Dotted vertical lines indicate the time of stimulation. **C.** Nissl stain image of the slice from which the recorded cell was obtained. Numbers correspond to the approximate location along the granule cell layer that photostimulation was applied to give the responses recorded in **A** and **B**. Stimulation site number **2** (circled) is the approximate location of the recorded cell. Note that direct photoactivation of the recorded cell induced an inward current and burst of action potentials (**A2**, **B2**). Activity induced in neurons at locations **3** and **4** resulted in synaptic responses (**A3**, **A4**) and action potentials (**B3**, **B4**) in the recorded granule cell. **D.** Timm's stain image of the same section in **C**. Note: mossy fiber sprouting surrounds the position of the recorded cell.

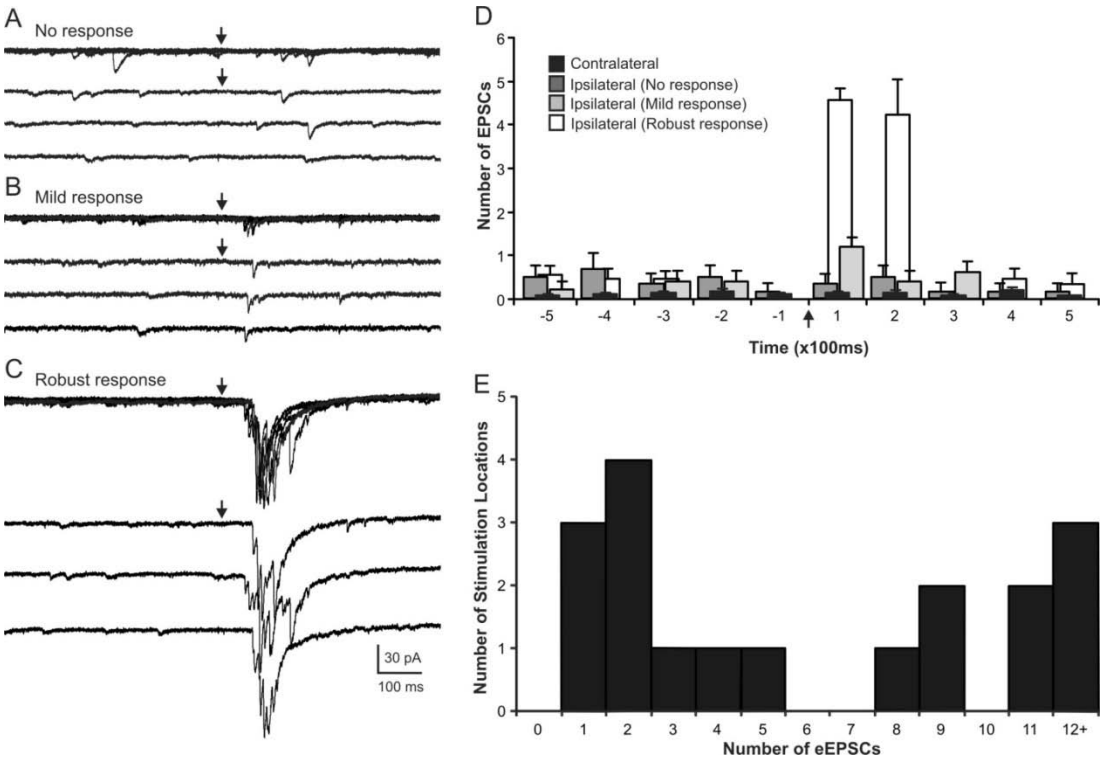

Figure 4.8. Variation in eEPSC responses in granule cells from slices ipsilateral to the lesion. A-C. Representative responses in a single neuron at three different stimulation locations of the granule cell layer. Each response shows five consecutive overlapping responses, with three consecutive individual traces separately shown below. **A.** Photostimulation did not evoke a response. **B.** A mild response of 1-2 EPSCs was consistently evoked in each of 5 trials. **C**. A more robust response that consisted of 5-9 eEPSCs in each of 5 trials after photostimulation at a different site in the granule cell layer. **D.** Number of EPSCs per 100ms before and after stimulation for each representative response in **A-C**. Contralateral responses are averaged across all stimulation locations in 5 neurons. Arrows indicate the time of stimulation. **E.** Frequency histogram shows the distribution of the average number of eEPSCs at 18 stimulation sites that had a positive response.

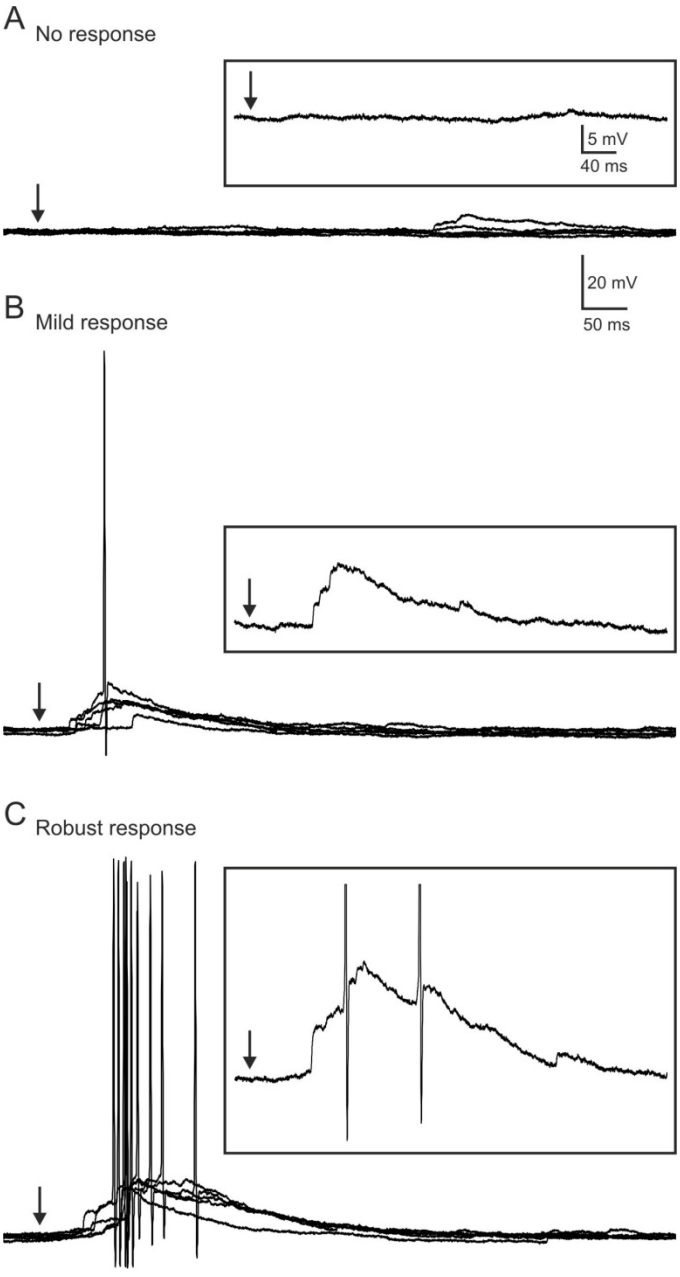
A
No response
5 mV
40 ms
20 mV
50 ms
B
Mild response
C
Robust response

Figure 4.9. Evoked EPSPs and action potentials in granule cells ipsilateral to CCI injury after photostimulation at distant locations in the granule cell layer. A-C. Representative responses in a single neuron at three different stimulation locations of the granule cell layer. Each response shows five consecutive overlapping responses. **A.** No response evoked by photostimulation. **B.** A mild response was evoked, with one of five responses reaching action potential threshold. Photostimulation at this location evoked an average of 3 EPSCs in voltage-clamp mode. **C.** A more robust evoked response that consisted of a small burst of action potentials in each of five trials. Photostimulation at this location evoked an average of 10 EPSCs in voltage-clamp mode. Insets show expanded portion of one trace. Arrows indicate the time of stimulation.

4.4 Discussion

Cellular mechanisms underlying the increased risk of epilepsy after head injury are not well understood. Here, I examined local network interactions in dentate granule cells from mice with posttraumatic mossy fiber sprouting and seizures. The goal of this study was to test the hypothesis that regionally localized mossy fiber sprouting after experimental cortical contusion injury was sufficient to produce a recurrent excitatory circuit in granule cells. An increase in excitatory input to individual granule cells was detected in slices with posttraumatic mossy fiber sprouting. In conditions of increased excitation and decreased inhibition, these cells displayed spontaneous epileptiform burst activity. Responses that reflect synaptic connections between granule cells were activated by glutamate photostimulation at some locations of the granule cell layer but never in the hilus or CA3. These data are consistent with the development of a local recurrent excitatory circuit (Traub and Wong, 1981; 1982; Miles et al., 1986; Miles and Wong, 1987; Lynch and Sutula, 2000; Waurin and Dudek, 2001; Winokur et al., 2004).

An important unresolved question regarding mossy fiber sprouting after TBI is whether it is associated with a relevant functional alteration in neuronal circuitry. A dominant hypothesis has been that mossy fiber sprouting after epileptogenic insult forms a positive feedback circuit between granule cells. Another hypothesis proposes that sprouted mossy fibers preferentially form synaptic connections with inhibitory interneurons, and may act to bolster recurrent inhibition (Sloviter, 1991, 1992; Kotti et

al., 1997). Studies that have examined chronic changes in excitability after TBI have primarily used extracellular field recordings and have not consistently identified synchronous network activity indicative of a recurrent excitatory circuit. This may be because many of these experiments were not performed in the presence of $GABA_A$-receptor antagonists (Reeves et al., 1997; Santhakumar et al., 2001), which is necessary for revealing recurrent excitatory circuits in the dentate gyrus (Cronin et al., 1992). However, Santhakumar et al (2001) reported that evoked population activity in the chronically injured dentate gyrus with mossy fiber sprouting after moderate fluid percussion injury was similar to controls, even in conditions of disinhibition. Because only minimal Timm granules are detected in the inner molecular layer months after moderate fluid percussion injury (Shumate et al., 1995; Santhakumar et al, 2001), the failure to detect an increase in recurrent excitability by extracellular recordings in granule cells may also be due to the paucity of new connections. A basic property of recurrent excitatory circuits is that there must be a sufficient number of excitatory interconnections between cells in order for activity to spread through the entire network (Traub and Wong, 1981, 1982; Miles and Wong, 1983). Other studies report that spontaneous electrographic seizures or mossy fiber sprouting do not develop until 7-12 months after *severe* fluid percussion injury in rats (Kharatishvili et al., 2006; 2007). On the other hand, in Chapter 3 I demonstrated spontaneous population activity indicative of synchronous network activation in slices with more robust mossy fiber sprouting after severe CCI (Hunt et al., 2009), a focal injury model.

In the present study, I provide relatively direct evidence for increased granule cell – granule cell connections after TBI. Several independent studies have indicated that recurrent excitatory circuits are normally masked by recurrent inhibitory circuits, even in animals with frequent spontaneous seizures, and can be revealed in conditions of reduced inhibition and/or increased excitation (Cronin et al., 1992; Waurin and Dudek, 1996, 2001; Patrylo and Dudek, 1998; Lynch and Sutula, 2000; Smith and Dudek, 2001; 2002; Winokur et al., 2004; Hunt et al., 2009). Therefore, reorganized circuits are proposed to form the basis from which functional electrical discharges periodically arise in context of other abnormalities. I used Mg^{2+}-free ACSF containing 100µM PTX in the present study to unmask NMDA-mediated excitatory synapses and block $GABA_A$-mediated inhibition.

These conditions were sufficient to reveal new excitatory connections in slices from injured animals with mossy fiber sprouting that were absent in control and injured slices without mossy fiber sprouting under identical recording conditions. It is unknown whether similar results would be obtained in the presence of PTX alone. Glutamate photostimulation is useful for identifing local synaptic connections, because it allows for focal stimulation of cell bodies and dendrites without activating axons of passage (Calloway and Katz, 1993). Evoked responses to photostimulation in some areas of the granule cell layer - but not in other areas - suggests an underlying local circuitry. Moreover, I observed variation in these responses (i.e., mild to robust responses), indicating that not all regions of the granule cell layer contribute equally to the newly formed network. Despite reports that indicate mossy cell-granule cell connections can sometimes be observed in slice preparations (Buckmaster et al., 1992; Scharfman, 1995), I did not find evidence of a photolysis-evoked excitatory synaptic connection between the hilus or CA3 region and any of the recorded granule cells. This is not surprising due to the relatively low probability of finding connections between the hilus and granule cells *in vitro* (Scharfman, 1995).

The degree of neuronal circuit reorganization necessary to produce a seizure focus remains unresolved. It seems reasonable to suggest that in a network configuration consisting of the appropriate principle cells interconnected by regionally localized recurrent excitatory connections, activating these particular circuits under appropriate conditions (e.g., a transient failure of inhibition) may engage an entire population of neurons and contribute to seizure generation (Traub and Wong, 1981; Miles and Wong, 1983). Activating nearby areas without interconnections may not lead to synchronous network activation. The presence of regionally localized mossy fiber sprouting and recurrent excitation in mice with spontaneous seizures after CCI injury is consistent with this proposed mechanism. More extensive synaptic reorganization may thus increase the probability of seizure generation or seizure severity. However, this relationship is likely indirect (Buckmaster and Dudek, 1997). Development of seizure foci in other susceptible brain regions, such as CA1 (Smith and Dudek 2001, 2002; Scheff et al., 2005) or neocortex (Salin et al., 1995), may also undergo synaptic reorganization independent of mossy fiber sprouting. Moreover, chronic injury-induced dysfunction of inhibitory

circuitry may compromise the ability of these circuits to mask new excitatory connections. The net effect of new localized recurrent excitatory circuits in combination with altered synaptic inhibition after head injury may contribute to the generation of spontaneous seizures. Interestingly, in Chapter 3 I reported an interval-specific alteration in extracellular paired-pulse responses, an indirect measure of synaptic inhibition, selective for ipsilateral slices with mossy fiber sprouting (Hunt et al., 2009). Future studies aimed at more thoroughly investigating altered inhibition after CCI are necessary to resolve this issue.

The abnormal electrophysiological responses in granule cells after head injury were qualitatively less robust and less widespread than reports at similar time-points after pharmacologically-induced status epilepticus (Waurin and Dudek 1996, 2001; Lynch and Sutula, 2000; Winokur et al., 2004). This may be due to less robust Timm staining in the inner molecular layer or less extensive synaptic network remodeling after head injury (i.e., only a portion of the dentate gyrus forms a recurrent excitatory circuit). Mechanisms other than mossy fiber sprouting and formation of new excitatory connections, such as altered glutamate receptor pharmacology (Meldrum et al., 1999) or altered ion channel function (Steinlein, 2004), could also contribute to the abnormal responses observed after injury and can not be ruled out. However, if these were sufficient features it would then be expected that epileptiform activity be present in the injured dentate gyrus independent of mossy fiber sprouting. I found a relationship between the degree of Timm granules in the inner molecular layer and EPSC frequency as previously reported after kainate-treatment in rats (Waurin and Dudek, 2001). Slices from injured animals that were devoid of mossy fiber sprouting in the inner molecular layer acted as internal controls, and responses in these slices were similar to those from uninjured controls, even in ipsilateral slices from animals with regionally localized sprouting in adjacent sections of the dentate gyrus. This supports the hypothesis that the presence of epileptiform activity is associated with mossy fiber spouting, rather than injury.

Structural damage and mossy fiber sprouting after CCI injury remains relatively localized to areas near the injury site, even in mice that have spontaneous seizures. This is different from induction paradigms that use status epilepticus and typically result in widespread damage that includes bilateral lesion of the hippocampus. Severe fluid

percussion injury, which primarily produces a concussive injury, also results in a variable degree of bilateral damage and mossy fiber sprouting (Kharatishvili et al., 2006). The present results suggest that widespread damage and synaptic reorganization is not an obligatory component of recurrent circuit formation or spontaneous seizure generation, but at least some degree of synaptic reorganization appears to be requisite for seizure generation. I report here a gross anatomical description of cortical damage after CCI injury to provide a qualitative representation of the hippocampal damage observed in mice used in this study. Other reports have provided more detailed analyses of the degree of injury and cell loss produced by severe CCI (Tong et al., 2002; Hall et al., 2005; Saatman et al., 2006). In the present study, a lesion to the granule cell layer at the injury site and mossy fiber sprouting was observed in nearly all mice. While mossy fiber sprouting is more robust after severe versus moderate contusion injury (Hunt et al., 2009), it is unlikely that a granule cell layer lesion is necessary to elicit mossy fiber sprouting after TBI (Kharatishvili et al., 2006).

Sprouting after CCI was typically most robust in sections just temporal to the injury site and became progressively less robust with increased distance away from the injury. In contrast, sprouting was generally absent in sections septal to the injury. While not always detected, granule cell loss has been reported in some temporal lobe epilepsy patients (Houser, 1990), and reductions in hippocampal volume have been reported after TBI (Bigler et al., 1997). Likewise, a recent study reported mossy fiber sprouting in at least a portion of the dentate gyrus - but not all areas - of resected tissue from all temporal lobe epilepsy patients with a history of head injury (Swartz et al., 2006). Therefore, localized mossy fiber sprouting is likely a relevant marker of TBI-induced epilepsy associated with mesial temporal lobe sclerosis.

Seizure detection was limited to infrequent behavioral monitoring, and many seizures likely went undetected. Moreover, non-convulsive seizures and other electrographic abnormalities (i.e., interictal spiking) cannot be accounted for. Statler et al. (2009) recently reported abnormal spontaneous electrographic activity and recurrent seizures in rats after CCI. Convulsive seizures were accompanied by behavioral manifestations similar to those described in the present study. Therefore, convulsive seizures associated with abnormal EEG activity are apparent in this model. While the

monitoring method employed in the present study is widely used and allows for comparison with earlier reports using models of status-epilepticus (Racine et al., 1979; Cronin and Dudek, 1988; Sloviter, 1992; Buckmaster and Dudek, 1997; Patrylo and Dudek, 1998; Waurin and Dudek, 2001; Shibley and smith, 2002), additional studies that use continuous EEG monitoring are necessary to provide more quantitative analyses of posttraumatic seizures. Regardless, spontaneous convulsive seizures are apparent in many mice after severe CCI injury.

The development of PTE in humans is highly variable and likely depends on injury characteristics such as severity, location, and injury type in addition to genetic background and acute and long-term treatment (Pitkanen and McIntosh, 2006). Therefore, it is impossible to experimentally reproduce all of the manifestations of human PTE. The lack of a reliable animal model in which PTE is easily and consistently reproducible has complicated studies aimed at elucidating cellular mechanisms of epileptogenesis after closed head TBI. The present study demonstrates that severe CCI injury is an advantageous model of PTE as many mice develop chronic seizures and localized synaptic circuit reorganization in the dentate gyrus.

Chapter 5

Increased local excitatory input to hilar GABAergic interneurons accompanies reduced synaptic inhibition of granule cells after traumatic brain injury

5.1 Introduction

Reorganization of dentate granule cell axons (i.e., mossy fibers) is associated with the emergence of a new recurrent excitatory circuit among granule cells after experimental TBI (Hunt et al., 2009, 2010) and in temporal lobe epilepsy (Dudek and Spitz, 1997). However, the input-output activity of granule cells is tightly regulated by hilar neurons, many of which are lost after experimental TBI (Lowenstein et al., 1992; Hall et al., 2005; Santhakumar et al., 2000; Grady et al., 2003; Kharatishvili et al., 2006) and in human posttraumatic epilepsy (Swartz et al., 2006). Consistent with fewer GABAergic synaptic contacts, hilar inhibitory neuron loss is accompanied by reduced mIPSCs in granule cells (Toth et al., 1997; Witgen et al., 2005) and increased evoked extracellular burst discharges in the granule cell layer *in vivo* (Lowenstein et al., 1992) one week after TBI. GABAergic cell loss presumably remains for several months (Santhakumar et al. 2000), but whether dysfunction of inhibitory circuits persists in the dentate gyrus after severe TBI is unresolved.

Hilar somatostatin-immunoreactive interneurons represent one subtype of local-circuit GABAergic interneuron in the dentate gyrus (Esclapez and Houser, 1995; Freund and Buzsáki, 1996). These neurons have dendrites that concentrate mostly in the hilus, and they receive inputs from the perforant pathway and mossy fibers (Leranth et al., 1990; Katona et al., 1999). Their axons synapse on granule cell dendrites opposite perforant pathway inputs in the outer molecular layer (Baskt et al., 1986; Leranth et al., 1990; Katona et al., 1999; Zhang et al., 2009). These neurons are uniquely positioned to restrict excitatory inputs to the dentate gyrus, but they are vulnerable to cell death after a variety of brain insults including ischemic injury (Johansen et al., 1987), alzheimer's disease (Ramos et al., 2006), repeated seizures (Sloviter et al., 1987; de Lanerolle et al., 1989; Mathern et al., 1995; Buckmaster and Dudek, 1997; Kobyashi and Buckmaster, 2003; Sun et al., 2007), and TBI (Lowenstein et al., 1992). Surviving hippocampal

GABAergic interneurons, including hilar somatostatin neurons, appear to sprout new axon collaterals to principal cells in epilepsy (Babb et al., 1989; Mathern et al., 1995; Cossart et al., 2001; Thind et al., 2009; Zhang et al., 2009), and they have increased soma size and dendritic branches (Tóth et al., 2007; Zhang et al., 2009). While these changes suggest a potentially compensatory increase of inhibitory influence over granule cell excitability after brain insult, excitatory drive to dentate basket cells and hilar border interneurons is reduced in epilepsy (Doherty and Dingledine, 2001; Zhang and Buckmaster, 2009). Therefore, injury-induced regional alterations specific to the hilar somatostatin interneuronal circuit may have critical pathological implications in the modulation of granule cell excitability.

Here, I performed whole-cell patch-clamp recordings of hilar GABA neurons and granule cells in mice which express enhanced green fluorescent protein (eGFP) in a subpopulation of somatostatin interneurons (Oliva et al., 2000). I tested whether surviving hilar eGFP neurons received increased excitatory inputs and whether synaptic inhibition of dentate granule cells is altered weeks after experimental brain injury.

5.2 Results

5.2.1 Mossy fiber sprouting

Mossy fiber sprouting into the inner molecular layer is a reliable marker of synaptic reorganization associated with posttraumatic epilepsy (Swartz et al., 2006; Kharatishvili et al., 2006; Hunt et al., 2009, 2010). Mossy fiber sprouting was present in sections of the dentate gyrus near the injury site (n=23 of 28 animals; Figure 1), but never in the contralateral hemisphere (n=0 of 28 animals; Figure 5.1) or in controls (n=0 of 10 animals). These findings verified the presence of axon sprouting in most animals, suggestive of network reorganization common to the injured dentate gyrus.

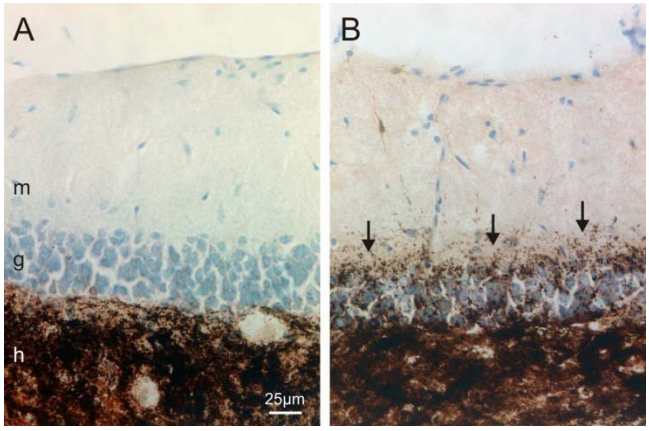

Figure 5.1. Mossy fiber sprouting in GIN mice after severe traumatic brain injury. A. Timm and Nissl-stained section from a slice contralateral to the injury. **B.** Timm and Nissl-stained section from a slice ipsilateral to the injury. Arrows indicate mossy fiber sprouting into the inner molecular layer. m, molecular layer; g, granule cell layer; h, hilus.

5.2.2 Increased excitatory inputs to hilar eGFP interneurons

To determine whether excitability of surviving GABAergic interneurons (Figure 2) was altered after TBI, eGFP-labeled hilar neurons were first recorded in the cell attached configuration to examine spontaneous action potential firing without intracellular disruption of the cell (Cossart et al., 2001; Jones and Baraban, 2007). A

significant difference in the mean unit firing frequency between treatment groups was detected by one-way ANOVA (control: 2.4 ± 1.4 Hz; contralateral: 3.9 ± 1.8 Hz, ipsilateral: 9.2 ± 6.1 Hz; $F_{(2,28)}$= 9.08, P<0.001; Figure 5.3). Post hoc comparisons revealed that interneurons from ipsilateral slices had a significantly higher action potential frequency versus other groups.

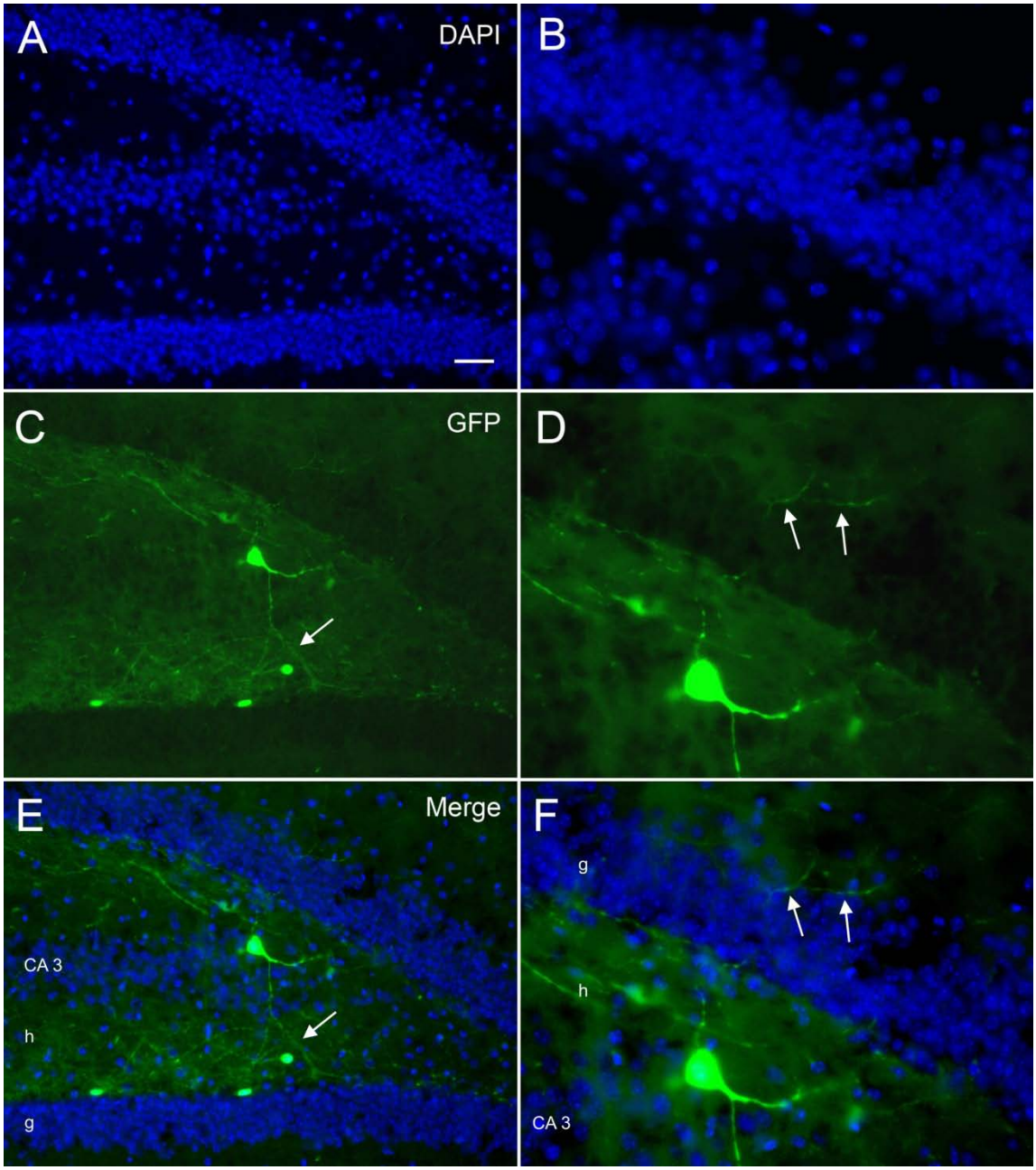

Figure 5.2. A hilar eGFP neuron in a slice ipsilateral to the injury. A. DAPI nuclear labeling in the dentate gyrus shows a tightly packed granule cell layer and the proximal pyramidal cell layer. **C.** In the same section, a single eGFP neuron is present in the hilus. Arrows indicate the dendrites of this neuron that are concentrated in the hilus but do not cross the granule cell layer. **E.** Merged image of (**A**) and (**C**). **B**, **D**, and **F.** High-magnification of the area containing the eGFP neuron in (**A**), (**C**), and (**E**). Note: the axon of the eGFP neuron projects through the granule cell layer into the molecular layer (arrows). Abbreviations: g, granule cell layer; h, hilus; CA3, CA3 pyramidal cell layer. Scale bar is 50µm in **A**, **C**, and **E** and 25µm in **B**, **D**, and **F**.

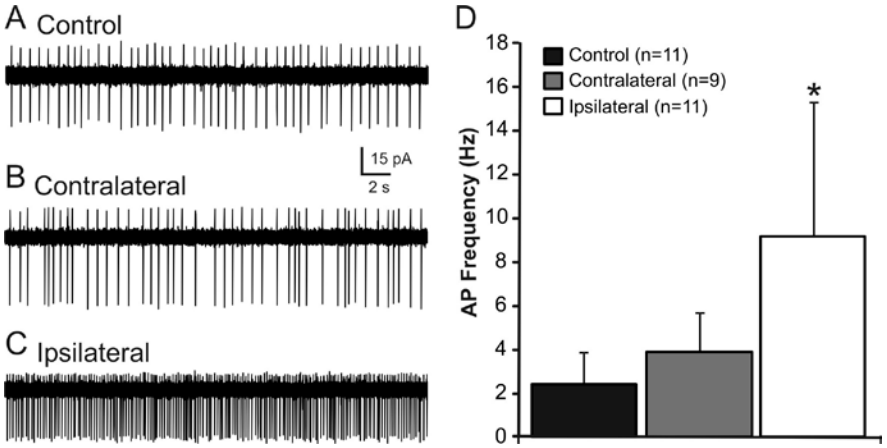

Figure 5.3. Increased spontaneous action potential firing in hilar eGFP interneurons ipsilateral to the injury. A-C. Cell-attached recordings of activity in a hilar eGFP interneuron in (**A**) a control slice, (**B**) a slice contralateral to the injury, and (**C**) a slice ipsilateral to the injury. **D.** Average action potential frequency for cells in each treatment group. Significance indicated by asterisk (*).

Excitatory synaptic input to hilar eGFP neurons was evaluated by whole-cell voltage-clamp recordings of sEPSCs at a holding potential of -60mV in controls (n= 21 cells from 13 animals) and in slices contralateral (n= 13 cells in 11 animals) and ipsilateral (n= 21 cells in 15 animals) to the injury. Representative recordings for each group are shown in Figure 5.4 A-C. A difference in the mean event frequency was detected by one-way ANOVA (control: 4.5 ± 1.8 Hz; contralateral: 5.3 ± 1.9 Hz; ipsilateral: 20.9 ± 12.9 Hz; $F_{(2,52)}$=25.5, P<0.001; Figure 5.4D). Post hoc comparisons revealed increased sEPSC frequency in hilar interneurons ipsilateral to the injury versus other groups. This 4-fold increase in event frequency is comparable to the increase

observed in granule cells after TBI (Hunt et al., 2010). The mean amplitude of sEPSCs for each treatment group was: control, -19.4 ± 6.7pA; contralateral, -18.8 ± 4.7pA; and ipsilateral, -20.9 ± 7.6pA. A significant difference between groups was not detected ($F_{(2,52)}$=0.43; P=0.65; Figure 5.4E). Kinetics of sEPSCs were comparable to reported values in cortical eGFP-somatostatin interneurons in these same transgenic mice (Halabisky et al., 2006). One-way ANOVA did not detect a difference between groups in mean 10-90% rise times (control: 1.6 ± 0.4ms; contralateral: 1.7 ± 0.5ms; ipsilateral: 1.7 ± 0.4ms; $F_{(2,52)}$= 1.0; P= 0.4) or decay time constant (control: 5.3 ± 2.0ms; contralateral: 6.6 ± 2.2ms; ipsilateral: 6.8 ± 0.4ms; $F_{(2,52)}$= 2.4; P= 0.11).

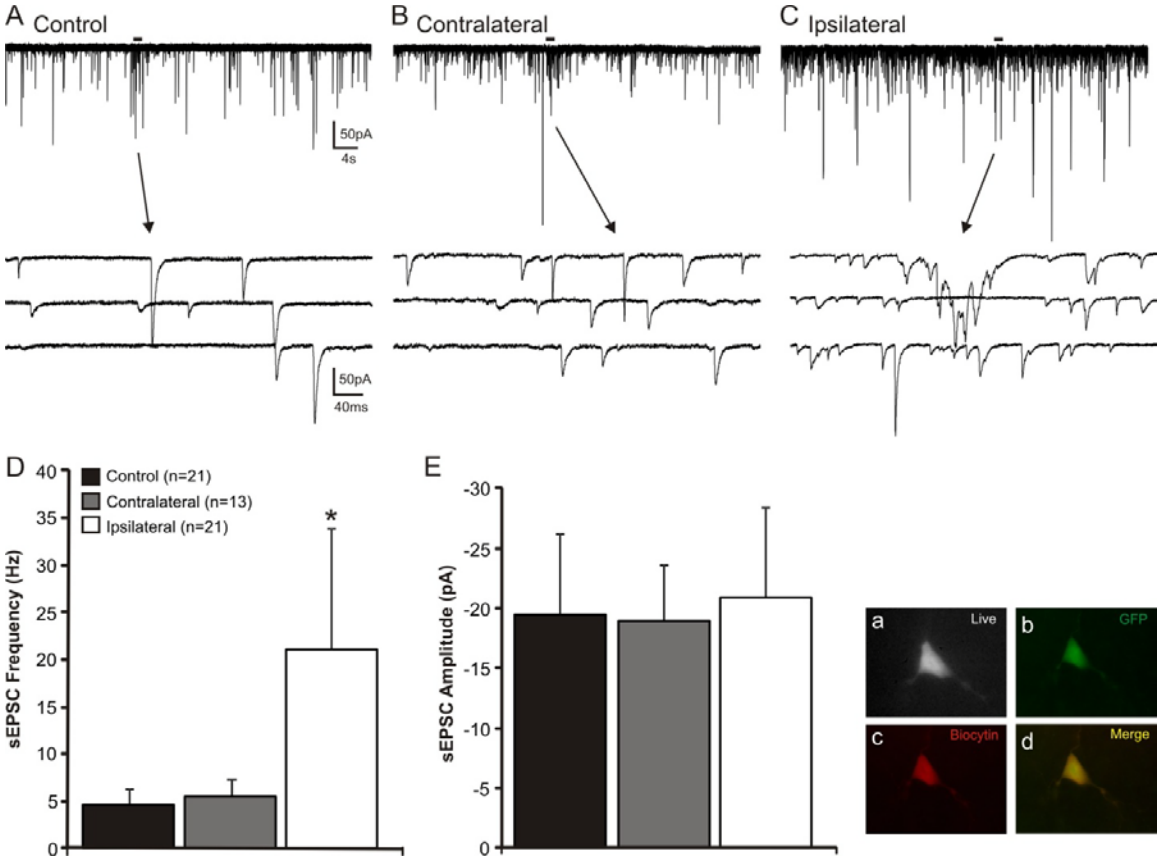

Figure 5.4. Increased sEPSC frequency in hilar eGFP interneurons in slices from the ipsilateral dentate gyrus. A-C. Example whole-cell patch-clamp recordings from eGFP-GABA neurons from (**A**) a control slice, (**B**) a slice contralateral to the injury, and (**C**) a slice ipsilateral to the injury. Line above each trace indicates area of the trace expanded below (arrows). **D.** Average sEPSC frequency for cells in each treatment group. Significance indicated by asterisk (*). **E.** Average sEPSC amplitude for cells in each treatment group. Inset shows example fluorescent illumination of a biocytin-filled eGFP neuron: **a.** eGFP-labeled neuron visualized in a live brain slice prior to recording; **b.** posthoc examination shows eGFP labeling; **c.** biocytin labeling of the same neuron (identified with an avidin Texas Red label); and **d.** merged image shows coexpression of eGFP and biocytin labeling.

Miniature EPSCs were recorded in the presence of 2µM TTX in some of the same cells used to examine spontaneous activity (controls, n=9; contralateral, n=8; ipsilateral, n=11). Representative recordings for each group are shown in Figure 5 A-C. Similar to spontaneous events, mEPSC frequency was significantly increased in hilar interneurons ipsilateral to the injury (control: 2.7 ± 1.3 Hz; contralateral: 3.1 ± 0.9 Hz; ipsilateral: 10.1 ± 6.5 Hz; $F_{(2,52)}$= 9.72, P<0.001; Figure 5.5D). The ratio of the frequency of mEPSCs to sEPSCs (mEPSC/sEPSC) was calculated to examine the relative contribution of network-driven inputs. The mEPSC/sEPSC ratio was significantly reduced in eGFP neurons ipsilateral to the injury (control: 0.71 ± 0.14; contralateral: 0.63 ± 0.17; ipsilateral: 0.44 ± 0.17; $F_{(2,25)}$= 7.6, P< 0.01; Figure 5.5E). Differences in mEPSC amplitude were not detected between groups by one-way ANOVA (control: 14.3 ± 7.0pA; contralateral: 13.4 ± 3.9pA; ipsilateral: 14.8 ± 4.3pA; $F_{(2,25)}$=0.18; P= 0.83; Figure 5.5F). Similarly, I did not detect a difference in mean event 10-90% rise times (control: 1.7 ± 0.5ms; contralateral: 1.9 ± 0.3ms; ipsilateral: 1.8 ± 0.4ms; $F_{(2,52)}$= 0.7; P= 0.5) or decay time constants (control: 6.0 ± 2.8ms; contralateral: 7.0 ± 1.7ms; ipsilateral: 6.5 ± 1.4ms; $F_{(2,52)}$= 0.6; P= 0.6).

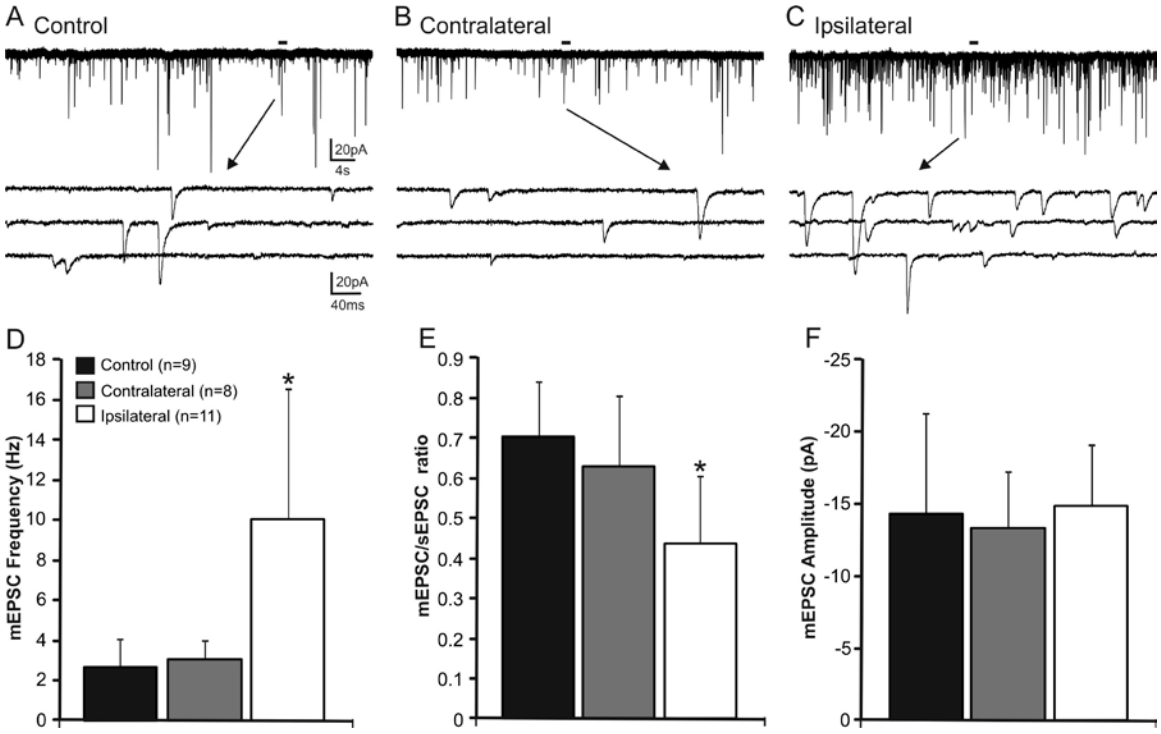

Figure 5.5. Increased mEPSC frequency in hilar eGFP interneurons of slices from the ipsilateral dentate gyrus. A-C. Example whole-cell patch-clamp recordings from eGFP neurons in (**A**) a control slice, (**B**) a slice contralateral to the injury, and (**C**) a slice ipsilateral to the injury. Line above each trace indicates area expanded below (arrows). **D.** Average mEPSC frequency for cells in each treatment group. **E.** Average mEPSC/sEPSC ratio for each treatment group. **F.** Average mEPSC amplitude for each treatment group. Significance indicated by asterisk (*).

5.2.3 Increased photostimulation-evoked activity in eGFP neurons after TBI

Nearly 60% of EPSCs in hilar eGFP neurons were action potential mediated, versus nearly 30% in cells from control slices. This suggests that excitatory synaptic input to eGFP neurons is enhanced due to greater local network activation of these neurons after injury, in addition to increased synaptic contacts. However, granule cells in slices ipsilateral to the injury did not fire spontaneous action potentials at rest in "normal" ACSF (n= 12), even in the presence of robust mossy fiber sprouting, because entorhinal inputs to granule cells were removed and recurrent excitatory circuits are normally masked by recurrent inhibition (Hunt et al., 2009, 2010). CA3 pyramidal cells are spontaneously active at rest in control animals (Spencer and Kandel, 1961; Wong et al.,

1979; Wong and Prince, 1981) and may form functional synaptic connections with hilar GABAergic interneurons (Kneisler and Dingledine, 1995; Doherty and Dingledine, 2001; Mangin et al., 2008). Therefore, I hypothesized that eGFP neurons receive increased excitatory inputs from both granule cells and CA3 pyramidal neurons.

Glutamate photostimulation applied to granule cells and CA3 pyramidal cells allowed for focal activation of cell bodies and dendrites but not axons of passage (Callaway and Katz, 1993; Hunt et al., 2010). After photostimulation of granule cells layer, an increase in evoked synaptic activity was observed in 2 of 6 eGFP cells from controls (3 of 71 stimulation sites) and 3 of 6 eGFP cells contralateral to the injury (3 of 50 stimulation sites). After photostimulation of the CA3 pyramidal neurons, an increase in synaptic activity was observed in 2 of 5 eGFP cells from controls (4 of 20 stimulation sites) and 1 of 6 eGFP cells contralateral to the injury (1 of 20 stimulation sites). Representative positive evoked responses observed in eGFP cells from controls and contrlateral to the injury are shown in Figure 5.6.

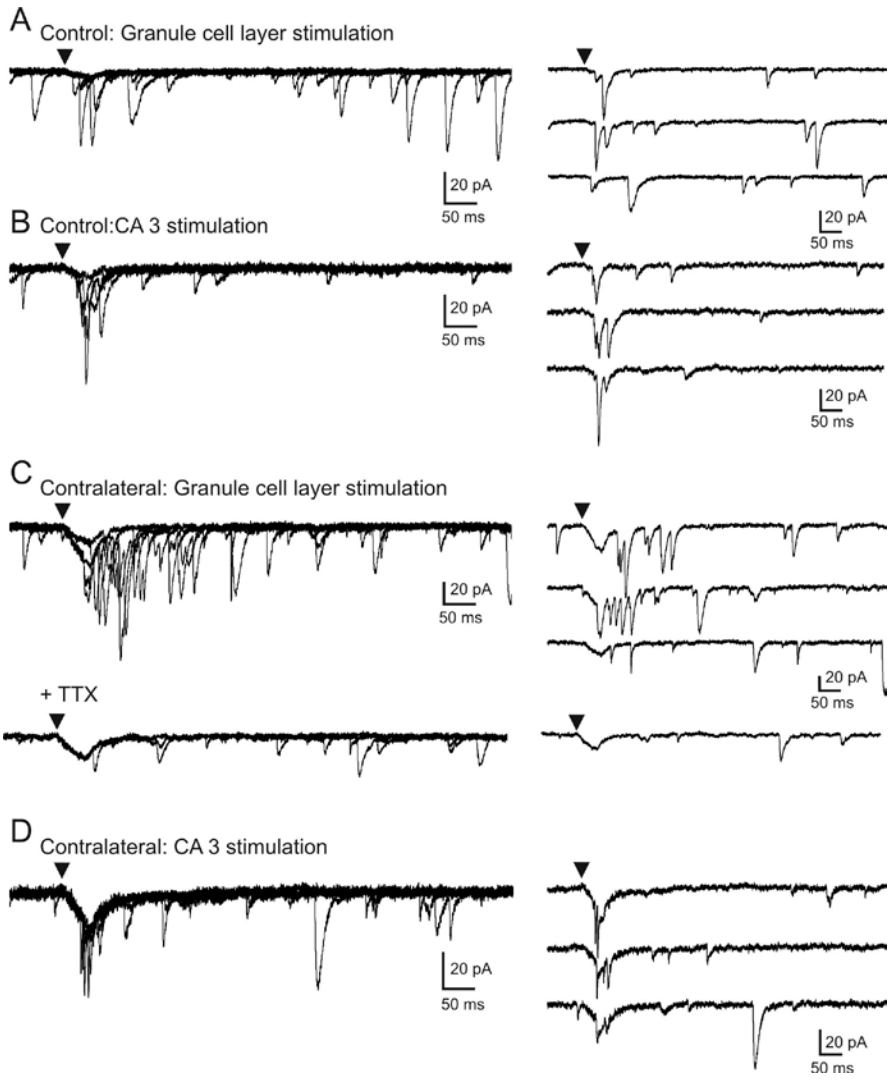

Figure 5.6. Responses in hilar eGFP neurons after glutamate photostimulation of the granule cell and pyramidal cell layers in control slices. A. Example positive evoked response to photostimulation of the granule cell layer in a control slice. **B.** Example positive evoked response to photostimulation of the CA3 pyramidal cell layer in a control slice. **C.** Example positive evoked response to photostimulation of the granule cell layer in a slice contralateral to the injury. Note: application of 2µM TTX blocked synaptic responses but not the direct current. **D.** Example positive evoked response to photostimulation of the CA3 pyramidal cell layer in a slice contralateral to the injury. For each response, a series of 5 consecutive stimulation trials are shown superimposed with 3 trials separated to the right. All example recordings were obtained from photostimulations applied to principal cells located relatively near the recorded cell.

Unlike the sparse local innervation detected in control slices, photostimulation of granule cells or CA3 pyramidal cells resulted in robust eEPSCs in hilar eGFP-GABA neurons ipsilateral to the injury (Figure 5.7). A synaptically-mediated response was observed in each of 7 cells after photostimulations applied to the granule cell layer (28 of 85 stimulation sites, 1-8 sites per cell) and in 5 of 7 cells after stimulations applied to area CA3 (12 of 36 stimulation sites, 1-4 sites per cell). Because relatively few positive responses were observed in cells from slices of controls and contralateral to the injury, data in these cells were combined for analysis against responses from cells ipsilateral to the injury. The total number of sites that had a positive versus negative response was greater in cells ipsilateral to the injury ($p<0.001$ for granule cell layer stimulation, $p<0.05$ for CA3 stimulation; Fisher's exact test). A frequency histogram was constructed to show the distribution of the average number of eEPSCs for each group (Figure 7 B and C). The range of the number of eEPSCs was increased in eGFP neurons ipsilateral to the injury after photostimulations applied to granule cells ($P<0.05$; two-tailed Mann-Whitney U,) and to CA3 pyramidal cells ($P<0.05$; two-tailed Mann-Whitney U). Therefore, both the number of stimulation sites with a positive response and the number of EPSCs evoked at each site were increased in eGFP neurons ipsilateral to the injury.

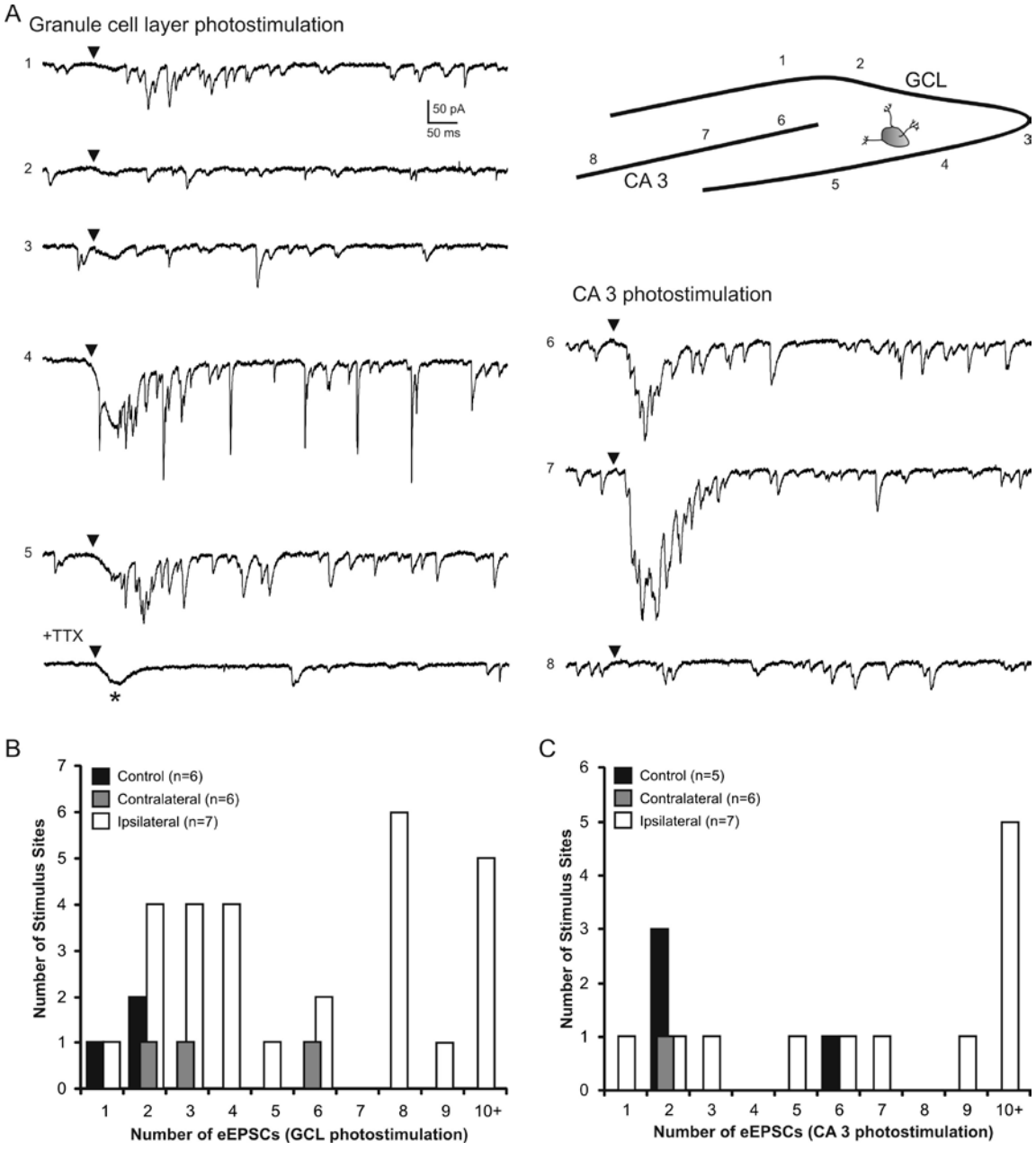
A
Granule cell layer photostimulation
50 pA
50 ms
+TTX
GCL
CA 3
CA 3 photostimulation
B
Control (n=6)
Contralateral (n=6)
Ipsilateral (n=7)
Number of Stimulus Sites
Number of eEPSCs (GCL photostimulation)
C
Control (n=5)
Contralateral (n=6)
Ipsilateral (n=7)
Number of Stimulus Sites
Number of eEPSCs (CA 3 photostimulation)

Figure 5.7. Increased synaptic connections to hilar eGFP interneurons from granule cells and CA3 pyramidal cells detected by glutamate photostimulation in a slice ipsilateral to the injury. A. Example responses to photostimulation of the granule cell and CA3 pyramidal cell layers. Numbers to the left of each trace indicate corresponding numbered stimulus position shown in the inset. Arrowheads above each trace indicate time of stimulation. Positive responses were observed at stimulation sites 1 and 4-7. Note: addition of 2μM TTX blocked photostimulation-evoked synaptic activity but not the current due to direct activation of the recorded neuron, indicated by the asterisk (*). **B** and **C.** Frequency histograms show the distribution of the average number of eEPSCs after photostimulation of (**B**) the granule cell layer and (**C**) the CA3 pyramidal cell layer.

5.2.4 Reduced synaptic inhibition of dentate granule cells after TBI

Increased excitatory synaptic inputs to hilar GABAergic interneurons may alter recurrent synaptic inhibition of granule cells. To test whether inhibitory synaptic input to dentate granule cells was altered after CCI injury, whole-cell voltage-clamp recordings of sIPSCs were obtained from granule cells in controls (n= 10 cells from 5 animals) and in slices contralateral (n= 12 cells in 11 animals) and ipsilateral (n= 20 cells in 11 animals) to the injury. Recordings were made from cells in the apex or outer blade regions of the granule cell layer in slices at or adjacent to the injury site. Spontaneous IPSCs were recorded at a holding potential of 0mV. At this potential, application of 30μM BMI completely blocked sIPSCs (n=5), indicating that these currents were mediated by $GABA_A$ receptors. Representative recordings for each group are shown in Figure 5.8A-C. The mean sIPSC frequency was significantly lower in granule cells ipsilateral to the injury versus other groups, as detected by one-way ANOVA with Tukey's post hoc test (control: 3.31 ± 0.5 Hz, contralateral: 3.38 ± 1.07Hz, ipsilateral: 1.55 ± 0.47Hz; $F_{(2,39)}$=34.5, P<0.001; Figure 5.8D).

To determine whether IPSCs were related to the presence of mossy fiber sprouting, event frequency from ipsilateral slices was assessed based on post hoc identification of the presence (Timm scores >1, n=13) or absence (Timm scores≤ 1, n=7) of mossy fiber sprouting in the inner molecular layer. A significant difference in sIPSC frequency was not found between slices with and without mossy fiber sprouting (P=0.84;

t-test; Figure 5.8E). One-way ANOVA did not detect a difference in sIPSC amplitudes between groups (control: 17.06 ± 3.8pA; contralateral: 18.04 ± 3.16pA; ipsilateral: 20.3 ± 6.11pA; $F_{(2,39)}$=1.7, P= 0.2; Figure 5.8F). However, one-way ANOVA found a significant difference in mean sIPSC 10-90% rise time (control: 1.5 ± 0.4ms; contralateral: 1.9 ± 0.5ms; ipsilateral: 2.5 ± 0.8ms; $F_{(2,39)}$= 7.4; P<0.01) and decay time constant (control: 13.2 ± 4.8ms; contralateral: 13.8 ± 4.1ms; ipsilateral: 18.6 ± 5.6ms; $F_{(2,39)}$= 5.8; P<0.01). While event kinetics in controls and contralateral slices were comparable to previously reported values for granule cells from controls (Kobyashi and Buckmaster, 2003; Shao and Dudek, 2005b), post hoc evaluations revealed slower sIPSC kinetics in granule cells ipsilateral to the injury.

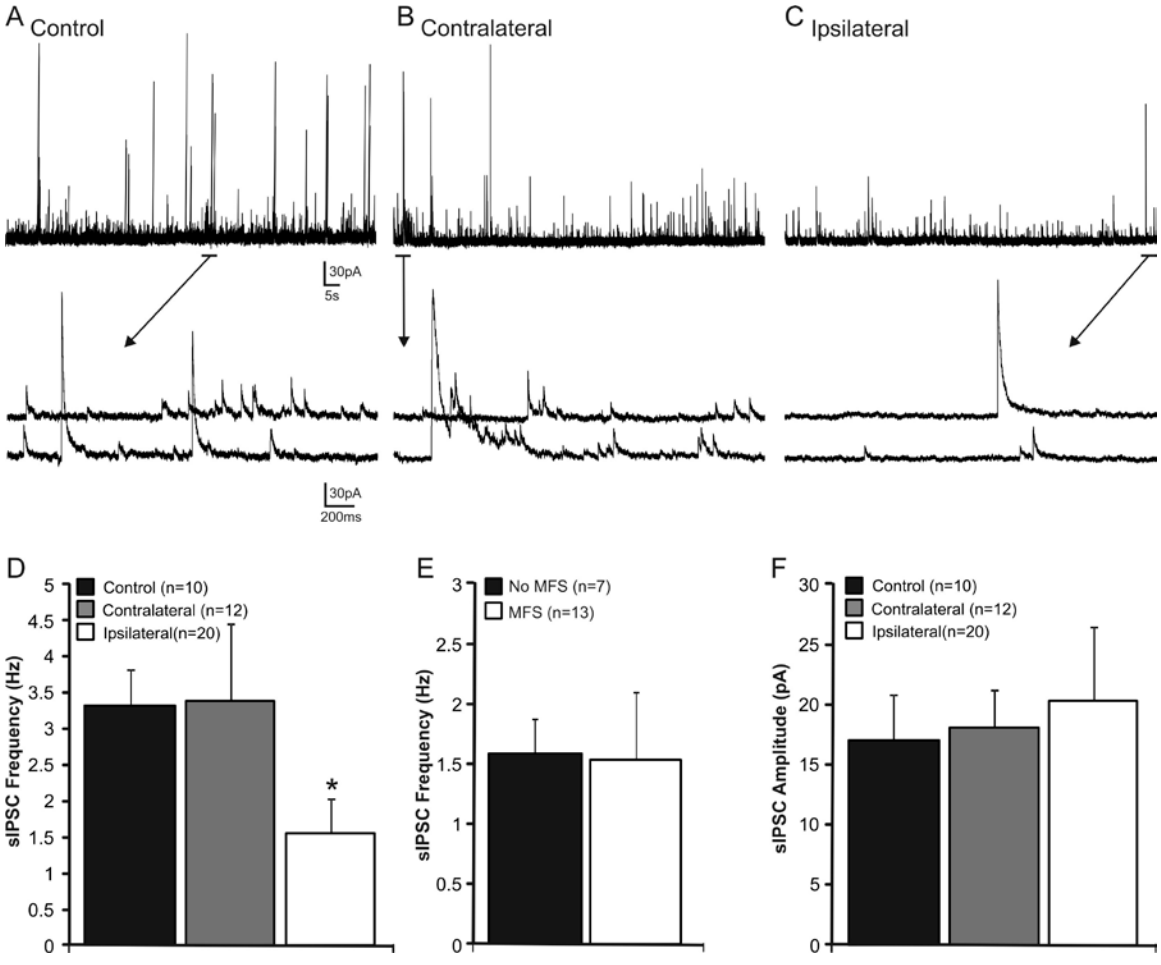

Figure 5.8. Reduced sIPSC frequency in granule cells in slices from the ipsilateral dentate gyrus. A-C. Example whole-cell patch-clamp recording from granule cells in (**A**) a control slice, (**B**) a slice contralateral to the injury, and (**C**) a slice ipsilateral to the injury. Line below each trace indicates region of the trace expanded below (arrows). **D.** Average sIPSC frequency for cells in each treatment group. Significance indicated by asterisk (*). **E.** Average sIPSC frequency for cells in ipsilateral slices in the presence and absence of mossy fiber sprouting (MFS). **F.** Average sIPSC amplitude for cells in each treatment group.

Miniature IPSCs were measured in the presence of 2μM TTX in some of the same granule cells used to measure sIPSCs. Representative recordings for each group are shown in Figure 5.9A-C. Similar to spontaneous events, mIPSC frequency was lower in granule cells ipsilateral to the injury (control: 2.56 ± 0.85 Hz; contralateral: 2.7 ± 1.08Hz; ipsilateral: 1.19 ± 0.42Hz; $F_{(2,31)}$= 14.3, P<0.001; Figure 5.9D). A significant difference in mIPSC frequency was not found between slices with mossy fiber sprouting (n= 9) versus those without sprouting (n= 6) (P=0.93; t-test; Figure 5.9E). Additionally, a difference in mIPSC amplitude was not detected between groups by one-way ANOVA (control: 12.05 ± 2.35pA; contralateral: 14.17 ± 2.2pA; ipsilateral: 14.14 ± 3.19pA; $F_{(2,31)}$= 2.0, P= 0.16; Figure 5.9F). Unlike spontaneous events, a significant difference was not detected in mean event 10-90% rise time (control: 1.7 ± 0.4ms; contralateral: 1.6 ± 0.3ms; ipsilateral: 1.9 ± 0.7ms; $F_{(2,39)}$= 0.85; P<0.85) or decay time constant (control: 13.2 ± 3.7ms; contralateral: 11.2 ± 2.4ms; ipsilateral: 14.9 ± 5.9ms; $F_{(2,39)}$= 2.0; P= 0.15).

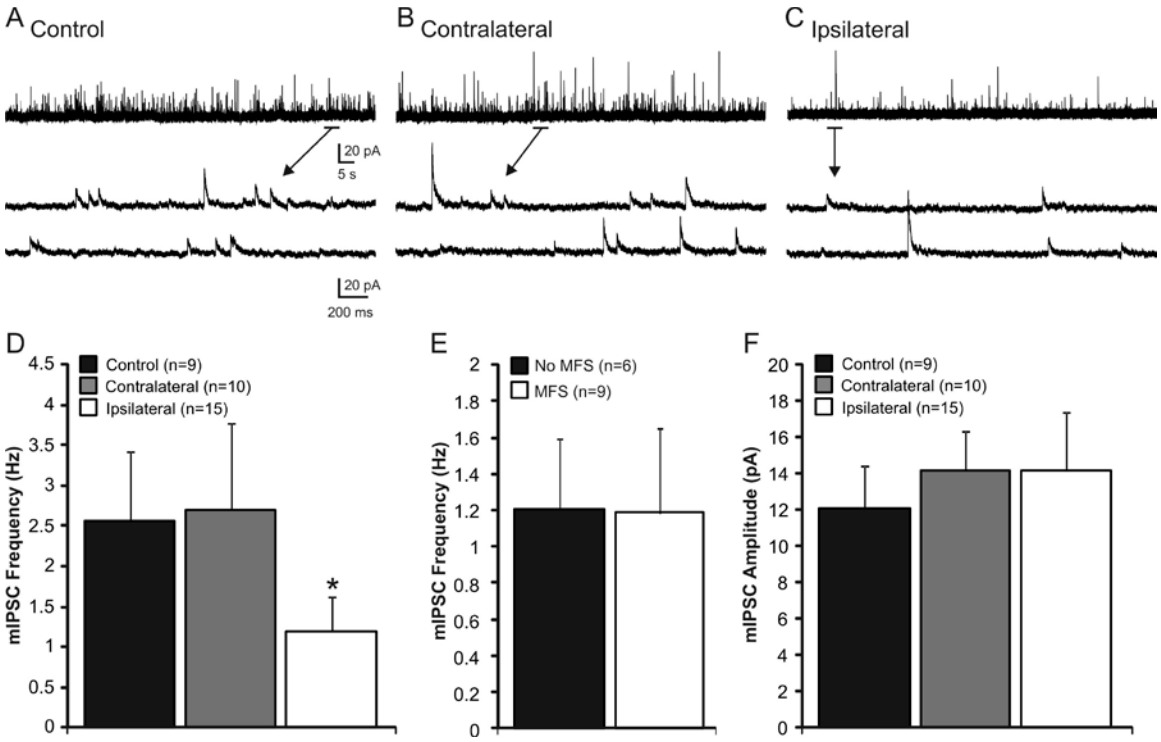

Figure 5.9. Reduced mIPSCs in granule cells of slices from the ipsilateral dentate gyrus. A-C. Example whole-cell patch-clamp recording from granule cells in **A**) a control slice, (**B**) a slice contralateral to the injury, and (**C**) a slice ipsilateral to the injury. Line below each trace indicates area of the trace expanded below (arrows). **D.** Average mIPSC frequency for cells in each treatment group. Significance indicated by asterisk (*). **E.** Average mIPSC frequency for cells in ipsilateral slices in the presence and absence of MFS. **F.** Average mIPSC amplitude for cells in each treatment group.

5.2.5 Hilar evoked PPRs are unchanged

Reduced mIPSC frequency in granule cells after head injury, despite increased activity of hilar eGFP neurons, could be due to dysfunction of GABAergic synaptic efficacy to granule cells or altered probability of vesicle release (Hirsch et al., 1999). To examine whether a change in presynaptic function of $GABA_A$ receptor-mediated feedback inhibition could be detected after TBI, paired stimuli were applied to the hilus at pairing intervals of 30, 60, 90, 120, and 200ms (50% maximum threshold, 80 µs, 0.1Hz) in the presence of 1mM kynurenic acid. Paired-pulse depression of eIPSC amplitudes was observed at all intervals (Figure 5.10), and application of 2µM TTX (n=3) or 30µM BMI (n=3) completely blocked hilar-evoked IPSCs. Two-way repeated

measures ANOVA detected a significant effect of pairing interval ($F_{(4, 116)}$= 3.56, P<0.01), but there was no effect of treatment group ($F_{(2, 29)}$= 0.48, P=0.63) or the pairing interval x treatment group interaction ($F_{(8, 116)}$= 0.71, P=0.68). These findings suggest there is no significant change in PPRs after injury.

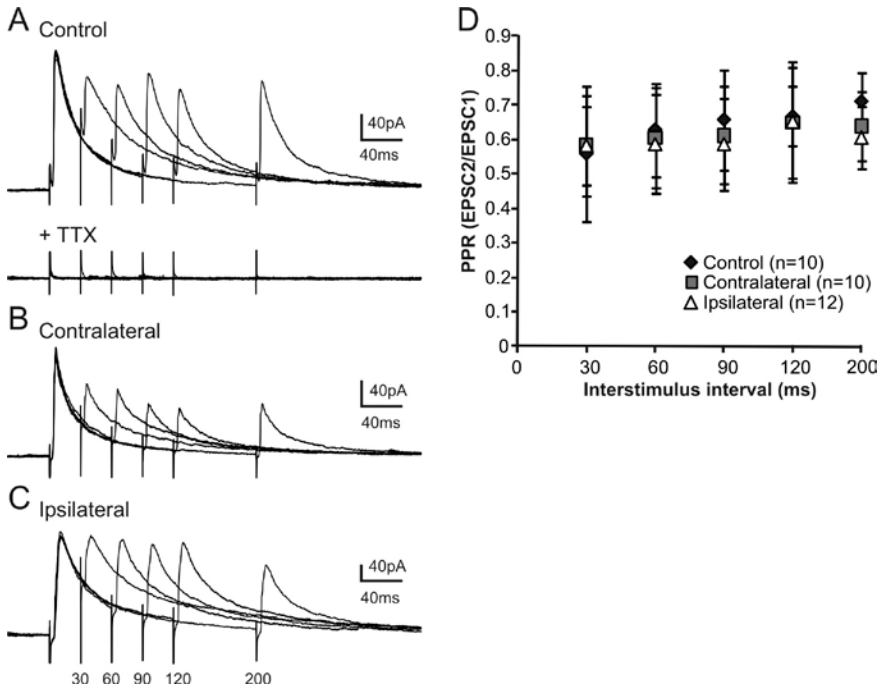

Figure 5.10. No change in paired-pulse ratios (PPRs) of hilar evoked $GABA_A$ receptor-mediated IPSCs in granule cells after brain injury. A-C. Superimposed pairs of eIPSCs at pairing intervals of 30, 60, 90, 120, and 200ms (average of 8-10 responses for each trial) in granule cells from (**A**) a control slice, (**B**) a slice contralateral to the injury, and (**C**) a slice ipsilateral to the injury. Note that application of 2μM TTX blocked hilar-evoked IPSCs. **D.** Average paired-pulse responses across cells for each treatment group showed no differences between groups.

5.3 Discussion

Reactive plasticity of glutamatergic mossy fiber circuits is a defining feature of the injured dentate gyrus (Dudek and Spitz, 1997; Hunt et al., 2009, 2010). However, excitatory networks are strongly modulated by distinct subtypes of GABAergic interneurons (Freund and Buzsáki, 1996), each having specialized functional roles to control neuronal excitability, synaptic efficacy, and synchronization. Perturbation of these circuitries after trauma may contribute to cognitive dysfunction (Witgen et al., 2003) or posttraumatic epileptogenesis (Toth et al., 1997; Hunt et al., 2009). Enhanced excitatory innervation of dentate GABAergic interneurons is a proposed cellular mechanism associated with injury-induced epileptogenesis (Chang and Lowenstein, 2003; Sloviter et al., 2003), but previous functional evidence suggests excitatory drive onto basket cells and hilar border interneurons is reduced in epilepsy (Doherty and Dingledine, 2001; Zhang and Buckmaster, 2009). In the present study I used mice in which a subset of somatostatin-GABAergic neurons express eGFP (i.e., GIN mice; Oliva et al., 2000). Frequencies of spontaneous, miniature, and photostimulation-evoked EPSCs were all increased in hilar eGFP neurons ipsilateral to the injury. Therefore, rewiring patterns of inhibitory circuits after brain injury may be specific to each GABA cell subtype.

Modifications of GABAergic networks may reflect a domain specific shift of inhibitory control over granule cells to stabilize excitatory networks after TBI. Increased excitability of eGFP neurons is consistent with larger soma size and increased axon and dendritic length in these neurons after pilocarpine-induced epilepsy (Zhang et al., 2009). These changes likely augment inhibitory shunting of excessive excitatory perforant pathway input into the dentate gyrus, which would tend to prevent the inadvertent activation of new recurrent excitatory circuits formed by mossy fiber sprouting. Whether hilar eGFP neurons also sprout axon collaterals to nearby CA3 pyramidal cells after injury is unknown, but this could help reestablish inhibitory tone in the hippocampus after injury. Alternatively, perisomatic inhibition provided by basket cells is important for synchronizing principal cell output (Lytton et al., 1991; Cobb et al., 1995; Miles et al., 1996). In the injured dentate gyrus, granule cell synchrony is augmented by the

emergence of new recurrent mossy fiber circuits (Dudek and Spitz, 1997; Hunt et al., 2009). This may diminish the role of inhibitory control provided by basket cells. Consistent with this hypothesis, dentate basket cells receive fewer excitatory synaptic inputs and a higher basket cell – to – granule cell transmission failure rate is observed in epilepsy (Zhang and Buckmaster, 2009). Therefore, the *global* loss, preservation, or enhancement of synaptic inhibition after TBI may not be as important to principal cell function as GABA cell-type specific modifications of inhibitory circuits.

Anatomical evidence indicates that mossy fibers normally make synaptic contacts with hilar somatostatin interneurons (Leranth et al., 1990; Katona et al., 1999), but functional CA3 pyramidal cell input to these neurons has not been well established (Wittner et al., 2006). I found that hilar eGFP interneurons receive input from both cell layers, and there is increased excitatory synaptic input from granule cells and CA3 neurons after head injury. The action potential-driven sEPSCs in eGFP neurons likely arise from CA3 pyramidal cells, because granule cells were rarely active in our slice preparations. Whether this network-driven activity is due to increased recurrent excitatory connections among CA3 neurons or another means of pyramidal cell activation is unknown. Hilar mossy cells could also contribute to enhanced excitability of inhibitory neurons and cannot be ruled out. However, this may not be a major contribution since nearly 50% of these neurons die after even *moderate* TBI (Tóth et al., 1997; Santhakumar et al., 2000).

Photostimulation-evoked synaptic connections between local principal cells and recorded eGFP neurons were sparse in control slices. To ensure uniformity, all recordings were made in slices with similar location (i.e., coronal sections in the transverse plane of the dorsal dentate gyrus), geometry, and under identical recording conditions. Individual granule cells often make only a single contact onto putative hilar somatostatin interneurons (Acsády et al., 1998), possibly making these inputs difficult to detect by the methods employed here. Difficulty in obtaining synaptic connections between granule cells and CA3 GABA cells in control slices has been acknowledged (Szabadics and Soltesz, 2009). Regardless, evoked activity that reflects synaptic connections onto eGFP neurons was significantly increased after TBI and could be evoked from relatively distant sites (e.g. the opposite blade of the granule cell layer, see Figure 5.7). Polysynaptic

activation of eGFP neurons after photostimulation is possible (e.g., granule cell –to– CA3 –to– eGFP neuron). However, onset latencies of eEPSCs after granule cell layer stimulation were often similar to evoked granule cell-to-granule cell synaptic connections after TBI (Hunt et al., 2010), and these responses sometimes occurred in the absence of positive evoked responses to CA3 stimulation. Therefore, increased synaptic input to eGFP neurons after TBI likely arise from both granule cells and CA3 pyramidal cells.

5.3.1 New connectivity patterns after injury could promote neuronal synchronization

Whether increased connectivity of hilar somatostatin-GABAergic neurons is compensatory or a pathogenic response remains unknown. These neurons have extensive axonal arborizations and large terminal fields in the dentate molecular layer (Leranth et al., 1990; Freund and Buzsáki, 1996; Katona et al., 1999; Buckmaster et al., 2002). Increased input-output relationships of surviving GABA cells allows for a single neuron to exert greater control over a larger number of principal cells. Inhibitory axon sprouting has long been a proposed mechanism for network synchronization in epilepsy (Babb et al., 1989), and modeling suggests that highly interconnected neurons may promote this activity (Traub and Wong, 1982; Morgan and Soltesz, 2008). Dendritically-projecting GABA neurons have been proposed to time rhythmic cortical cell discharges (Szabadics et al., 2001) and to drive ictogenesis (Wendling et al., 2002). With increased activity and presumably more divergent outputs (Zhang et al., 2009), there is greater risk that these cells will periodically coordinate synchronous activity in the dentate gyrus or hippocampus by restricting perforant pathway input simultaneously to larger groups of granule cells. Recently, Bonifazi et al. (2009) proposed that a small but morphologically heterogeneous subpopulation of GABAergic interneurons act as “superconnected hubs” to coordinate synchronous activation of CA3 neurons in the developing hippocampus. Perhaps eGFP neurons are converted into analogous “GABAergic hubs” that promote granule cell synchrony after injury. Moreover, fewer inhibitory neurons, each with greater influence over principal cells, implies that periodic failure of these neurons (e.g., transient inactivation during excessive or sustained excitation) may be more detrimental to restraining excitatory inputs to granule cells after injury than in controls.

5.3.2 Reduced synaptic inhibition after TBI

It seems likely that the substantial reduction in synaptic inhibition detected in granule cells after TBI is due to inhibitory neuron loss and the subsequent loss of synaptic contacts. Whether cell loss is preferential for certain subtypes of hilar neurons after TBI, as is often observed in temporal lobe epilepsy, remains unresolved. Parvalbumin-, cholecystokinin-, and somatostatin-immunoreactive cells are all reported to be reduced 1 week after moderate TBI (Lowenstein et al., 1992; Toth et al., 1997; Santhakumar et al., 2000), and numbers of parvalbumin and GAD-67 immunoreactive hilar interneurons remain reduced 5 months post-injury (Santhakumar et al., 2000). A recent study suggested reduced mIPSC frequency in granule cells contralateral to CCI in rats, but the ipsilateral dentate gyrus was unsuitable for patch-clamp recordings due to extensive damage after severe CCI (Mtchedlishvili et al., 2010). Our findings are not consistent with this result. Cortical cavitation as a result of the contusion injury produced by this model can occasionally extend into the hippocampus and dentate gyrus (Hall et al., 2005; Saatman et al., 2006; Hunt et al., 2010), but it does not normally ablate the ipsilateral hippocampus.

Slower sIPSC kinetics recorded at the granule cell soma is consistent with loss of perisomatically synapsing GABA neurons and increased activity or axon sprouting of dendritically projecting somatostatin-positive neurons (Pearce, 1993; Kobayashi and Buckmaster, 2003; Zhang et al., 2009). That no change in mIPSC kinetics was found may not be surprising as mIPSCs are reported to originate mostly from proximal synapses in granule cells (Soltesz et al., 1995). Altered IPSC kinetics have also been observed in epileptic animals (Kobayashi and Buckmaster, 2003; Shao and Dudek, 2005b; Sun et al., 2007). These changes could also be due to altered $GABA_A$ receptor subunits (Brooks-Kayal et al., 1998), altered ratio of dendritic versus perisomatic synapses (Cossart et al., 2001), or passive properties of granule cells. Surprisingly, I did not detect presynaptic changes in GABA release as reported in the pilocarpine model (Kobyashi and Buckmaster, 2003). This may be due to model specific differences, stimulator position (molecular layer versus hilus), stimulus intensity, or other technical differences.

Moreover, GABAergic cell subtype-specific changes in presynaptic function cannot be estimated by this method.

Increases in excitatory input to a subset of hilar GABA neurons arise from the granule cell layer and area CA3 after brain injury. These rewiring changes may be a key factor in restoring inhibitory control to granule cells in the injured dentate gyrus, or they may promote periodic granule cell synchrony in the presence of other excitatory and inhibitory circuit changes.

Chapter 6
General Discussion

6.1 Summary of findings

The principal findings of this dissertation research are: 1) mice develop posttraumatic seizures after moderate and severe CCI injury, 2) a recurrent excitatory circuit forms among granule cells in the dentate gyrus only when posttraumatic mossy fiber sprouting is present, 3) putative somatostatin GABAergic interneurons in the hilus receive increased excitatory synaptic input from granule cells and CA3 pyramidal cells after TBI, and 4) overall inhibitory synaptic input to dentate granule cells is reduced ipsilateral to the injury. These long-term structural and functional changes in neuronal circuitry are consistent with and expand upon findings in human and experimental epilepsy. Moreover, these results suggest that CCI injury may be an advantageous model of PTE in mice.

6.2 Models of posttraumatic epilepsy

Most of the information about cellular mechanisms of epileptogenesis has been derived from animal models. There is an ongoing debate over which experimental paradigms make for appropriate models of PTE, versus other forms of acquired epilepsy (Dichter, 2009). Pitkänen and McIntosh (2006) proposed the presence of spontaneous seizures in whole animals, versus slice or cell culture preparations, as necessary criteria for an epilepsy model. Relatively high numbers of animals in which the behavioral, anatomical, and physiological characteristics of epileptic pathology in humans is reproduced are essential to any epilepsy model. Additionally, models with low mortality and short but distinct latencies between initial injury and spontaneous seizure onset are also advantageous. The term “posttraumatic epilepsy” infers that a model also be considered a relevant model of experimental neurotrauma (i.e., spontaneous seizures are induced by mechanical injury). An ideal model will effectively reproduce the range of tissue deformation and damage observed in mild, moderate, and severe TBI so that the

dual pathology of cellular and molecular factors associated with injury severity and epileptogenesis can be dissociated. The ideal model should also invoke known risk factors for PTE.

Using these selection criteria, many traditional experimental epilepsy models, such as pharmacologically-induced status epilepticus, do not qualify as models of PTE, because they do not induce spontaneous seizures by a mechanical insult. This is not to negate these models, because they have provided valuable information about cellular mechanisms of epileptogenesis. Rather, these criteria provide a more restrictive and specific basis for differentiating between epileptogenesis mediated by a mechanically-induced lesion versus brain insults by other causes (e.g., pharmacological agents or electrical stimulation). It is important to make this distinction, because there is currently no effective treatement for PTE (Temkin, 2009; discussed below). Therefore, it is important to understand how the epileptogenic processes in experimental neurotrauma are similar, or different, in comparison with human PTE and other experimental epilepsy models (e.g., TLE induced by status epilepticus).

The presence of spontaneous behavioral seizures in mice after CCI is an important finding of the present study. Previously, posttraumatic electrographic activity, behavioral seizures, or hyperexcitability have only been examined in rats. The present finding that mice develop seizures after CCI injury is supported by a recent study which found that electrographic seizures accompany behavioral seizures after CCI in rats (Statler et al., 2009). That CCI is a widely used model of TBI suggests that it should also be considered as a model of PTE. Seizures after CCI are similar to spontaneous behavioral and electrographic seizures that have been described in rats after lateral FPI (Kharatashivilli et al., 2006) and in models of TLE (Racine et al., 1979; Cronin and Dudek, 1988; Sloviter, 1992; Buckmaster and Dudek, 1997; Patrylo and Dudek, 1998; Hellier and Dudek, 1999; Waurin and Dudek, 2001; Shibley and Smith, 2002). Spontaneous seizures after CCI occur with similar onset latency as pharmacologically-induced TLE (Hellier and Dudek, 1999; Shibley and Smith, 2002), which appears to be considerably shorter than the seizure onset latency after severe lateral FPI in rats (Kharatashivilli et al., 2006). The CCI model is currently the only mouse model of epilepsy after closed-head TBI.

It is difficult to compare PTE after CCI or lateral FPI injury with the rostral parasagittal FPI model used by D'Ambrosio and colleagues (2004, 2005, 2009). Rats injured by rostral parasagittal FPI do not generally develop tonic-clonic convulsive seizures (D'Ambrosio et al., 2004; 2005; 2009). The first study (D'Ambrosio et al., 2004) examined behavioral seizures based on the traditionally used modified Racine rating scale, but later studies (D'Ambrosio et al. 2005, 2009) developed a new seizure classification scale to describe the subtle behavioral abnormalities associated with electrographic activity in this model. The authors reasoned that posttraumatic seizures after rostral parasagittal FPI did not fit well with the Racine scale. The majority of electrographic abnormalities of injured rats in these studies was associated with behavioral inactivity or crouching and may not have been considered "seizure" activity in other studies (Kharatashivilli et al., 2006, 2007; Hunt et al., 2009, 2010; Statler et al., 2009). There are numerous benign variants of normal electrographic patterns that can morphologically reflect epileptiform activity but are not epileptic (Santoshkumar et al., 2009). Future studies that combine EEG monitoring with electromyogram (EMG) and electro-oculogram (EOG) may better distinguish ictal activity from interictal events or benign electrographic patterns.

6.3 Posttraumatic epileptogenesis

The term "epileptogenesis" refers to a transformation process by which the normal brain develops an increased propensity for generating spontaneous seizures (Lothman et al., 1991). That this process includes a latent period of variable time suggests a progressive series of cellular changes may be involved. Understanding the epileptogenic process after TBI should help to elucidate the importance of these cellular mechanisms in PTE and promote new therapeutic targets. Trauma sets into motion a multidimensional cascade of cellular and molecular events that involve three temporally overlapping responses in the brain: primary and secondary injuries and "self-repair" mechanisms (Mendelow and Crawford, 1997; Laurer et al., 2000; Graham et al., 2006; Figure 6.1). A key factor in future studies which investigate posttraumatic

epileptogenesis is to dissociate injury-induced cellular alterations that promote seizure generation from compensatory and "self-repair" responses.

Primary injury refers to the immediate tissue deformation and compression that occurs within seconds to minutes after mechanical brain insult (Mendelow and Crawford, 1997; Laurer et al., 2000; Graham et al., 2006). There is an immediate release of neurotransmitters, glutamate in particular, which is followed by ion channel activation and calcium influx. This can lead to excitotoxic injury, reflected by mitochondrial damage and energy depletion; neuronal and glial swelling; and cell death. Vascular damage and blood-brain barrier disruption can also occur in primary injury. Cortical structures such as the hippocampus are especially vulnerable to neuronal damage after moderate and severe TBI. Moreover, the presence of immediate seizures can further exacerbate initial damage and complicate injury management (Temkin, 2009). Strategies to protect against primary injury focus on preventive rather than therapeutic measures (e.g., wear a helmet when riding a bicycle).

Secondary injury involves a myriad of cellular and physiological factors associated with progressive tissue damage (Mendelow and Crawford, 1997; Teasdale and Bannan, 1997; Laurer et al., 2000; Graham et al., 2006). Over time, brain injury triggers inflammatory cascades, growth factor responses, edema, mitochondrial dysfunction, oxidative stress due to the build-up of free radicals and reactive oxygen species, delayed cell death, perturbation of cellular calcium homeostasis, and hypoxia and ischemia. The brain initiates "self-repair" mechanisms over the course of days to months concurrent with the development of secondary tissue damage. This period is characterized by synaptic circuit remodeling, axon sprouting, synaptic plasticity, gliosis, neurogenesis, and angiogenesis. As shown in the present study, time-dependant reorganization of synaptic circuitry can promote increased synchronous neuronal activity that may contribute to spontaneous seizure generation. Therefore, repair mechanisms may not always be beneficial. The primary goal of neuroprotective measures is to prevent or reduce secondary brain damage and to enhance beneficial "self-repair" mechanisms (Mendelow and Crawford, 1997; Teasdale and Bannan, 1997; Graham et al., 2006).

Genetic background, gender, age, acute medical treatments, and agent of injury all likely influence the epileptogenic processes, but the contribution of these personal traits

and injury dynamics in epilepsy have not been well established (Pitkanen and McIntosh, 2006). A better understanding of the importance of these factors in posttraumatic epileptogenesis will likely elucidate why some individuals develop PTE after TBI while others do not.

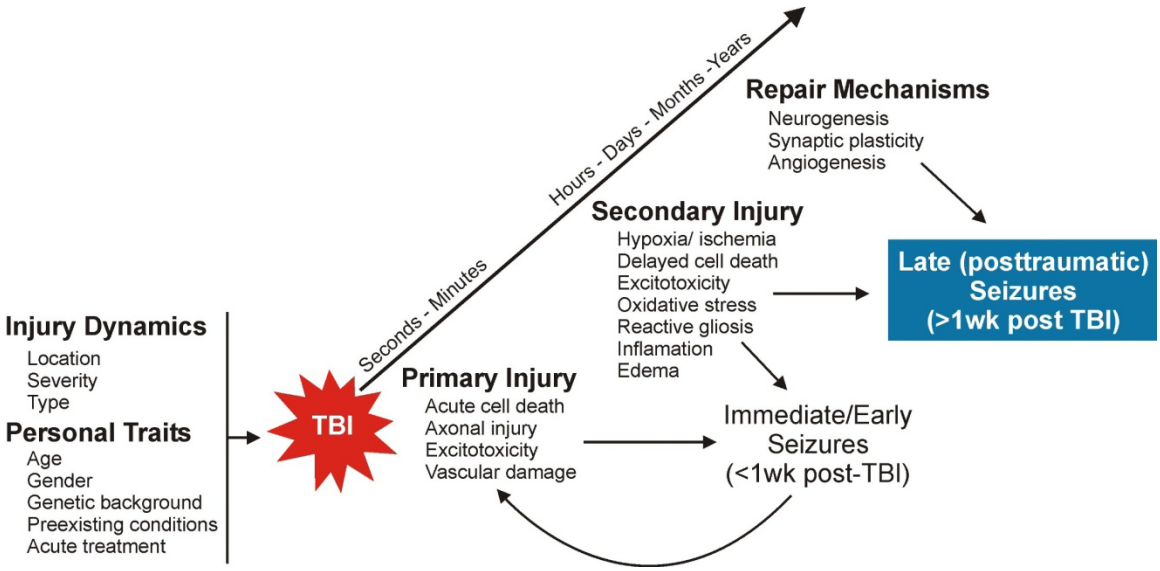

Figure 6.1. Cellular progression of neurotrauma.

6.4 Modified circuits may compromise dentate gyrus filtering

As shown in the present study, excitatory and inhibitory circuitries in the dentate gyrus undergo dramatic reorganization after TBI (Figure 6.2). A new interconnected network among granule cells, reorganization of inhibitory circuits, and a variety of other cellular changes may all promote seizure generation by compromising dentate gyrus filtering capability. Mossy fiber sprouting creates a means for granule cell synchrony that is not present in the normal dentate gyrus. Inhibitory control over granule cells may be unable to restrain excessive excitatory inputs from the the entorhinal cortex. This may be due to fewer GABAergic synaptic contacts, but it could also be due to a shift in domain specific inhibitory control over principle cells.

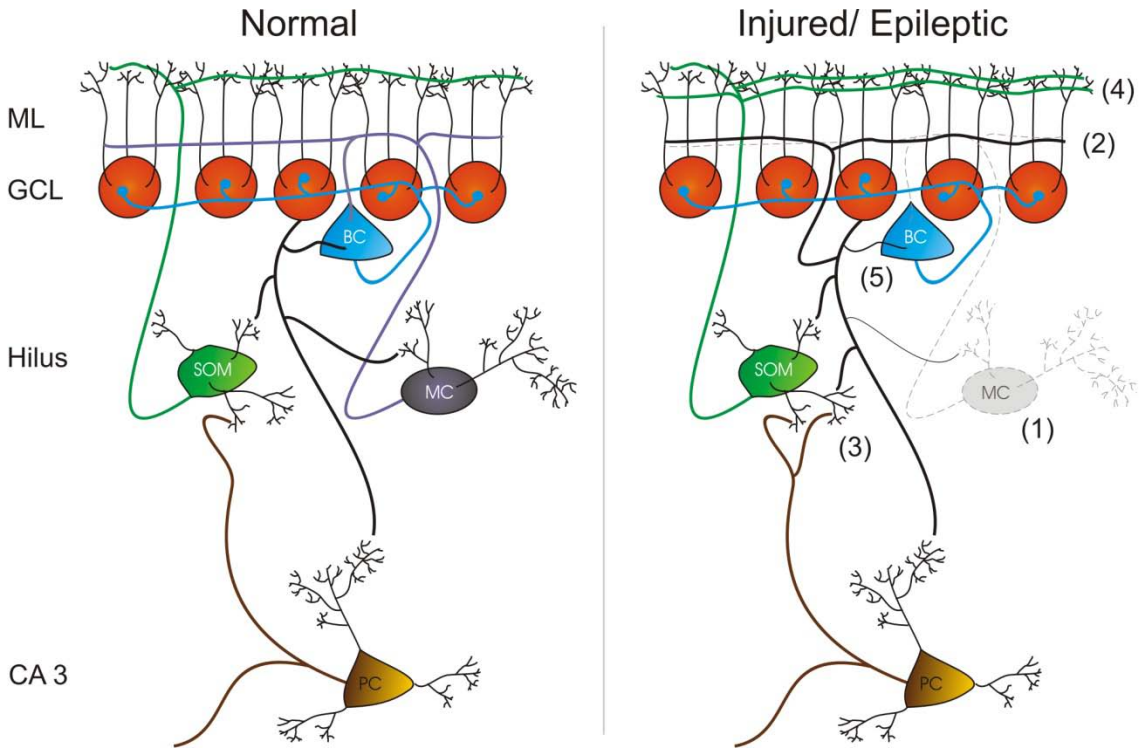

Figure 6.2. Reorganization of dentate gyrus circuitry after brain injury. 1. Within days after injury there are fewer mossy cells and GABA neurons in the hilus (Lowenstein et al., 1992; Toth et al., 1997; Santhakumar et al., 2000). **2.** Within weeks after TBI, mossy fibers sprout axon collaterals into the inner molecular layer and form a new recurrent excitatory circuit among granule cells (Chapters 3 and 4). **3.** Somatostatin-positive GABA neurons in the hilus receive increased excitatory inputs from granule cells and CA3 pyramidal cells (Chapter 5). **4.** These neurons also have increased axon length in the molecular layer in epilepsy (Zhang et al., 2009). **5.** In contrast, excitatory drive to basket cells is reduced after pilocarpine-induced status epilepticus (Zhang and Buckmaster, 2009). Abbreviations: ML, molecular layer; GCL, granule cell layer; CA3, CA3 pyramidal cell layer; BC, basket cell; MC, mossy cell; SOM, somatostatin-positive GABA neuron; and PC, pyramidal cell.

Spontaneous reverberating burst discharges in the injured dentate gyrus with mossy fiber sprouting after $GABA_A$-receptor blockade supports the hypothesis that a failure of inhibitory influences to regulate granule cell excitability may allow the inadvertent activation of recurrent mossy fiber circuits and permit synchronous activity in the dentate gyrus. Therefore, it is reasonable to suggest a transient failure of already fragile GABAergic circuitry may periodically promote granule cell synchrony. In the posttraumatic or epileptic dentate gyrus, a subopulation of surviving hilar GABA neurons receive an excessive amount of excitatory inputs (i.e., somatostatin-positive interneurons) while other GABA neurons may have a significant loss of inputs (i.e., basket cells). The effectiveness of inhibitory circuits to mask recurrent mossy fiber circuits likely depends on the ability of dendritic inhibition to properly shunt excitatory inputs and perisomatic inhibition to properly gate granule cells and prevent inappropriate synchrony in granule cells.

6.5 Is mossy fiber sprouting an epiphenomenon?

While mossy fiber sprouting is a consistent and reliable marker of the epileptic dentate gyrus, some propose that its functional contribution to epileptogenesis may be insignificant (Longo and Mello, 1997, 1998, 1999; Nissinen et al., 2001). The degree of mossy fiber sprouting in the inner molecular layer does not correlate well with seizure frequency or severity in epileptic rats (Buckmaster and Dudek, 1997). However, another study suggests that the degree of mossy fiber sprouting ipsilateral to lateral FPI is correlated with posttraumatic EEG spike activity (Kharatashivilli et al., 2007). Moreover, abnormal excitatory responses in epileptic tissue from humans and rodents are generally only observed when physiological conditions are perturbed (i.e., in the presence of $GABA_A$-receptor antagonists). This has led some to propose that mossy fiber sprouting does not contribute to seizure generation, because it is normally masked by inhibitory influences.

Treatment with the immunosuppressant, rapamycin, reduces the density of Timm's staining in the inner molecular layer of rats after pilocarpine-induced status epilepticus (Buckmaster et al., 2009) and in *Tsc1*$^{flox/flox}$-GFAP-Cre knock-out

(*Tsc1*^{GFAP}CKO) mice, a model of Tuberous sclerosis (Zheng et al., 2009). Zheng et al. (2009) reported a reduction in seizure frequency and duration that was associated with less robust mossy fiber sprouting. However, the Buckmaster laboratory reported that intraperitoneal administration of rapamycin did not reduce spontaneous seizures after pilocarpine-induced status epilepticus, despite less robust mossy fiber sprouting (Galanopoulou et al., 2010). These studies highlight the controversy over whether mossy fiber sprouting has functional significance in TLE.

There are several possible explanations for why spontaneous seizures may persist despite reduced mossy fiber sprouting after rapamycin treatment. Rapamycin treatment did not ablate mossy fiber sprouting in previous studies (Buckmaster et al., 2009; Zheng et al., 2009; Galanopoulou et al., 2010). There may be a plateau effect to any causal relationship between mossy fiber sprouting and seizure generation. Moreover, the findings in the present study suggest that robust, bilateral mossy fiber sprouting is not necessary for seizure generation. Perhaps rapamycin treatment also prevents GABA cell axon sprouting, in addition to blocking mossy fiber sprouting. This would be expected to reduce recurrent excitability but further compromise inhibitory control in the dentate gyrus. Another possibility is that rapamycin drug treatment has indirect actions or side effects that provoke seizures concurrent with preventing mossy fiber sprouting. If this were to occur, these non-epileptic seizures would be difficult, if not impossible, to dissociate from spontaneous seizures. For example, rapamycin inhibits the mammalian target of rapamycin (mTOR) which regulates insulin signaling pathways, and chronic rapamycin treatment promotes insulin resistance and a hyperglycemic state in humans (Di Paolo et al., 2006; Um et al., 2006) and in a *Psammomys obesus* model of type 2 diabetes (Fraenkel et al., 2008). Hyperglycemia can provoke seizures, and these non-epileptic seizures stop when hyperglycemia is corrected (Hennis et al., 1992). It is also possible that rapamycin treatment has different effects in different brain regions (e.g., there is a reduction in mossy fiber sprouting but an increase in CA1 pyrdamidal cell axon sprouting). Regardless, the relationship between mossy fiber sprouting and seizure generation is likely indirect, because synaptic network reorganization elsewhere in the brain may promote seizure generation independent of mossy fiber reorganization.

It is important to note that clinical seizures are infrequent episodic events that have identifiable beginning and ending points. Because synaptic reorganization likely occurs in other brain regions after injury (e.g., area CA1, Smith and Dudek, 2001, 2002; Scheff et al., 2005), it is unrealistic to expect mossy fiber sprouting to have a direct causal relationship with spontaneous seizure generation. It is also unrealistic to expect continuously detectable network synchronization or other electrophysiological abnormalities despite such a dramatic and permanent reorganization of excitatory and inhibitory circuitry. This is especially important when examining network function in acute brain slices - where many synaptic inputs have been surgically removed. Rather, reorganized circuits form the basis from which functional electrical discharges can periodically surface. Mossy fiber sprouting into the inner molecular layer is associated with an increase in sEPSC frequency in granule cells in normal ACSF (Wuarin and Dudek, 2001, Chapter 4) and new recurrent excitatory synaptic input to granule cells when inhibition is suppressed (Cronin et al., 1992; Wuarin and Dudek, 1996; 2001; Patrylo and Dudek, 1998; Lynch and Sutula, 2000; Winokur et al., 2004; Chapter 3 and 4). Increases in neuronal activity and network synchronization are widely hypothesized to be underlying factors in seizure generation. Therefore, the dentate gyrus acts as a model system for reactive plasticity in epilepsy.

6.6 Additional Future Directions

6.6.1 Synaptic reorganization of other cortical regions after TBI

There is an abundant literature describing the structural and functional reorganization of synaptic circuitry in the dentate gyrus in epilepsy (Lothman et al., 1991; McNamara, 1994; Dudek and Spitz, 1997; Nadler, 2003; Sutula and Dudek, 2007, Dudek and Sutula, 2007). This can lead inappropriately to a “dentate-centric” view of TLE. Focus was placed on the dentate gyrus in the present study, because of the abundant literature on this brain region, it is relatively easy to identify changes in mossy fiber circuitry, and it allowed for comparisons to easily be made versus traditional models of TLE (e.g., models of TLE after status epilepticus). Time-dependant reorganization of

excitatory and inhibitory circuits in other brain regions that are susceptible to neuronal injury after TBI is likely. For example, increased recurrent excitatory pyramidal cell connections have been reported in CA1 (Smith and Dudek, 2001, 2002; Calcagnotto and Baraban, 2005; Shao and Dudek, 2005a), neocortex (Salin et al., 1995), and thalamus (McCormick and Contreras, 2001) in a variety of experimental models. All of these brain regions are injured after experimental TBI (Hall et al., 2008), but whether an increase in recurrent excitation can be detected in these areas after TBI is unknown. The findings presented in Chapter 5 that eGFP neurons receive increased network-driven excitatory input after TBI may infer an injury-induced increase in recurrent CA3 pyramidal cell activity. Application of techniques similar to those performed in the present study will be useful in examining alterations in synaptic circuitry in other brain regions after TBI.

6.6.2 Synaptic circuit reorganization in area CA1 after TBI

Investigation of injury-induced synaptic reorganization in area CA1 after TBI is a particularly interesting future direction. Scheff et al. (2005) reported an initial loss of morphologically identified synapses in stratum radiatum two days post-CCI injury. This was followed by a progressive increase in the number of synapses out to 60 days post-injury, but the number of synapses was not restored to sham-control levels. These findings suggest that pyramidal cells undergo time-dependent synaptic plasticity changes, but whether these new synaptic contacts reflect excitatory or inhibitory synapses remains unknown. An injury-induced increase in recurrent excitatory connections among CA1 pyramidal cells is possible and may also contribute to seizure generation after CCI.

GABA cell subtype-specific reorganization of inhibitory circuitries may be different in area CA1 than in the dentate gyrus. There are fewer GABA neurons and inhibitory synaptic inputs to pyramidal cells in area CA1 after status epilepticus (Cossart et al., 2001; Smith and Dudek, 2001), in mutant mice with spontaneous seizures (Cobos et al., 2005), and in focal cortical dysplasia (Calcagnotto and Baraban, 2005). Cossart et al. (2001) suggested there is a reduction in dendritic inhibition but an increase in somatic inhibition of CA1 pyramidal cells after pilocarpine- and kainic acid-induced status epilepticus. These changes were accompanied by a preferential loss of dendritically

projecting stratum oriens interneurons and a global increase in excitatory drive to GABA neurons (i.e., perisomatic and dendritic projecting GABA neurons both had increased excitatory synaptic inputs). These findings are different from previous studies, including the present study, that have reported reduced synaptic inhibition of dentate granule cells (as measured from the soma) and GABA cell subtype-specific changes in excitability. Therefore, enhanced recurrent excitatory connections is widely believed to promote synchronous network activity and seizure generation, but domain specific reorganization of inhibitory circuits may vary in different brain regions. At least a subpopulation of hippocampal eGFP neurons survives severe CCI injury (Figure 6.3). Whether excitatory drive to these neurons is increased after TBI, as observed in hilar eGFP neurons, is unknown.

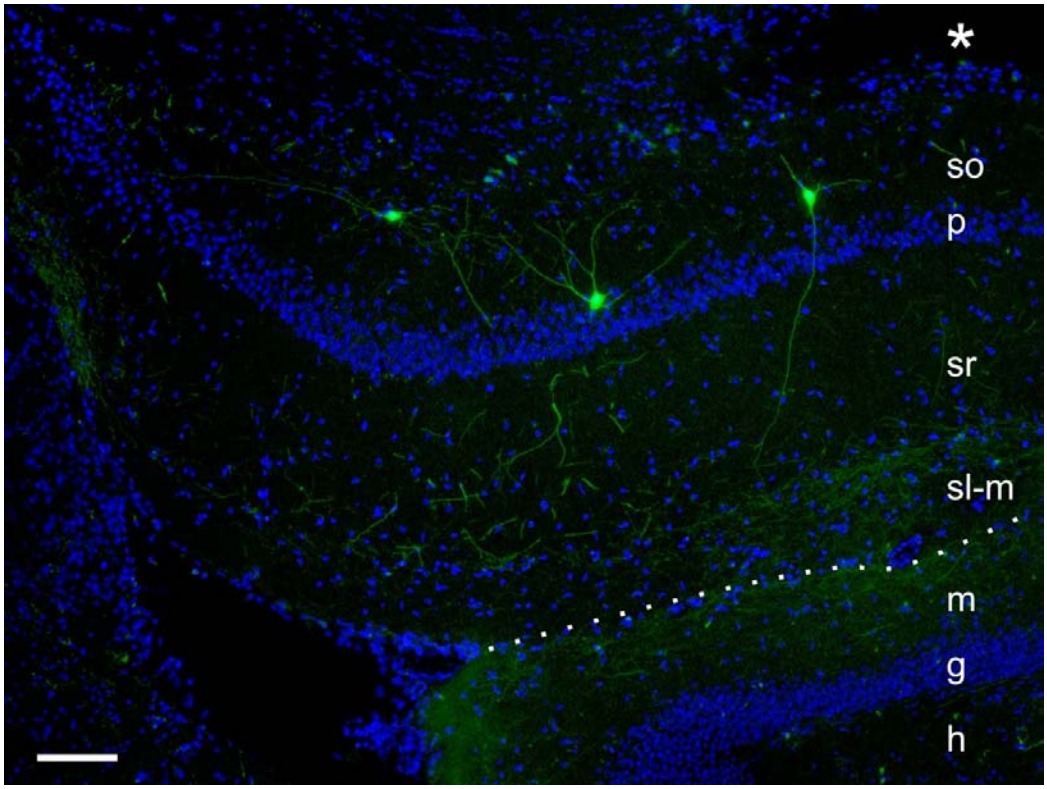

Figure 6.3. Surviving hippocampal eGFP neurons in a slice at the injury site. Merged image of DAPI nuclear labeling (blue) and eGFP fluorescent illumination. Abbreviations: so, stratum oriens; p, CA1 pyramidal cell layer; sr, stratum radiatum; sl-m, stratum lacunosum-moleculare; m, molecular layer; g, granule cell layer; h, hilus. Dotted line indicates hippocampal fissure. Asterisk (*) indicates cortical cavity produced by contusion injury. Note the dense plexus of eGFP in the molecular layers of CA1 and the dentate gyrus. Scale bar is 50μm.

6.6.3 Reorganization of dentate inhibitory circuits after TBI

There are a number of future experiments that can expand upon the present finding that excitatory drive to hilar GABA neurons is increased after TBI. The findings presented in Chapter 5 suggest an increase in excitatory input to hilar eGFP neurons but a decrease in overall synaptic inhibition of granule cells. Simultaneous dual somatic and dendritic recordings in granule cells will better reveal how domain specific synaptic inhibition of granule cells is altered after TBI. A shift in the normal balance between excitation and inhibition in principal cell dendrites has been speculated as an underlying factor driving ictogenesis (Szabadics et al., 2001; Wendling et al., 2002; El-Hassar et al., 2007). Moreover, dual recordings between synaptically connected eGFP neurons and granule cells may reveal the effectiveness of eGFP neurons to shunt electrically stimulated excitatory perforant pathway input after TBI. Preliminary evidence suggests that synapses of eGFP neurons with granule cells may be dysfunctional in epilepsy (Zhang et al., 2009).

An increased propensity of hilar GABA neurons to periodically inactivate after TBI was proposed in this study as a hypothetical mechanism for episodic failure of synaptic inhibition in the dentate gyrus. Future studies should examine whether this can be demonstrated in slice preparations. This could be tested by high frequency stimulations applied to the perforant pathway and/or by altering the ionic composition of ACSF (e.g., increase $[K^+]_o$ or remove Mg^{2+}). Excessive depolarization of hilar eGFP neurons – due to large numbers of excitatory inputs – may periodically lead to a transient inactivation of these neurons (e.g., after sodium channel inactivation in these cells). Inactivation of eGFP neurons would be expected to temporarily lessen dendritic synaptic inhibition of target neurons (i.e., granule cells). This may permit a “run” of synchronous

activity among granule cells and rhythmic discharges that propagate throughout the hippocampus, because hilar somatostatin interneurons innervate large portions of the dentate gyrus (Han et al., 1993; Buckmaster et al., 2002). Moreover, putative hilar somatostatin interneurons discharge only a single action potential in response to perforant pathway stimulation, versus a burst of action potentials evoked in basket cells (Buckmaster et al., 2002). This may reflect a higher threshold for activation or increased spike accommodation. Whether this threshold changes after TBI is unknown.

Excitability of other hilar GABA neuron subtypes should also be investigated to examine GABA cell subtype-specific reorganization of inhibitory circuitry after injury. Perisomatic inhibition provided by dentate basket cells is critical for controlling gating properties of principal cells (Cobb et al., 1995; Miles et al., 1996). These neurons have fewer excitatory inputs and a greater basket cell – to – granule cell transmission failure rate after pilocarpine-induced TLE (Zhang et al., 2009), but the function of these neurons after brain injury is unknown. The findings presented in Chapter 5 showing reduced spontaneous and miniature IPSCs suggests that basket cells and axo-axonic neurons may be differentially affected by TBI, versus hilar eGFP neurons. Changes in basket cell and axo-axonic neuronal circuits have been proposed to be especially important in preventing the spread of excitability throughout the hippocampus (Toth et al., 1997). Moreover, previous studies have suggested dysfunction in feed-forward inhibition of granule cells at one-week and several months after TBI (Lowenstein et al., 1992; Toth et al., 1997; Santhakumar 2000, 2001). It is unknown whether somatic or axonal projecting inhibitory neurons can effectively terminate synchronous granule cell discharges when they arise after TBI.

How specific subunits of postsynaptic and extrasynaptic $GABA_A$ receptors are chronically altered in granule cells after TBI remains to be established. The subunit composition of $GABA_A$ receptors – which consist of a family of heteropentimeric ionotropic membrane receptors with at least 16 different known subunits (α1-6, β1-3, γ1-3, ε, δ, π, and θ) (Sieghart, 2000) – can determine its kinetic properties. Moreover, there are alterations in $GABA_A$ receptor subunits in experimental and human TLE (Rice et al., 1996; Schwarzer et al., 1997; Brooks-Kayal et al., 1998; Fritschy et al., 1999; Loup et al., 2000; Houser and Esclapez, 2003; Peng et al., 2004; Zhang et al., 2007). In Chapter 5, I

found that sIPSCs in granule cells had slower decay time constants. This could reflect a change in the subunit composition of $GABA_A$ receptors that mediate synaptic (phasic) inhibition. For example, if postsynaptic $GABA_A$ receptors in granule cells have a α1 to α2 subunit switch after TBI, slower decay times of sIPSCs may be expected (Okada et al., 2000). An increased propensity for $GABA_A$ receptor reopening after desensitization may also prolong decay time after TBI (Jones and Westbrook, 1996). Moreover, little is known how extrasynaptic $GABA_A$ receptors, which mediate tonic inhibition, are altered in PTE (see Appendix 1).

6.7 Restorative & repair strategies for PTE

Posttraumatic epilepsy is difficult to treat, and therapeutic options for preventing or suppressing chronic seizures after trauma are limited and have been largely unsuccessful (Temkin et al., 1998; Temkin, 2001; Temkin, 2009). Prophylactic medication is generally prescribed only for patients with severe injuries or who have early seizures. Several drugs have been tested for antiepileptogenic effects; however, none have been consistently effective. Many of the current anitepileptic drugs act to increase GABAergic inhibition in the brain (e.g., benzodiazepines, barbiturates), but other drugs have mechanisms of action that include sodium channel blockade (e.g., lamotrigine, valproate, phenytoin, carbamazepine), calcium channel blockade (e.g., valproate), and hormones (e.g., progesterone). In most reports, antiepileptic drug treatments have little to no effect or even increase the rate of late seizures after trauma (Temkin, 2009). For example, Phenytoin and Carbamazepine have both been shown to suppress early seizures within a week of injury, but not epileptic seizures (Temkin et al., 1990; Glötzner et al., 1993). Little information is available with regard to the potential effect of other drugs on posttraumatic seizures (Temkin, 2009).

Because PTE is often intractable, the usual strategy is to evaluate the patient for resective surgery (Willmore, 2006). However, head injury sufficient to cause PTE can be accompanied by complications that influence the success of surgical resection. TBI often results in bilateral, multifocal tissue damage, making surgery ineffective. Challenges to the evaluation process include the unpredictable nature of lesion formation, the ability to

identify seizure foci in relation to lesion locations, and the ability to completely remove the epileptic tissue (Willmore, 2006).

The CCI injury model of PTE will be useful for testing a number of promising treatment options. The relatively short latency from injury to seizure onset is a clear advantage of CCI over other trauma models. Lateral FPI has a relatively long latency to seizure onset, which makes treatment studies laborious, and other models have not been shown to develop spontaneous seizures (e.g., weight drop, moderate FPI). The use of mice allows for examining the role of genetic manipulation in response to TBI and therapy. There is little to no mortality after CCI, and biomarkers of the epileptic dentate gyrus (i.e., hilar cell loss and mossy fiber sprouting) are reproduced in nearly all mice. The present findings demonstrate that the CCI injury model is a useful preclinical model for testing the effectiveness of treatment strategies on posttraumatic seizure generation, recurrent excitatory circuit formation, and alterations in synaptic inhibition in addition to cell loss and cognitive and motor function impairment.

Treatments for PTE will ultimately focus on preventing the epileptogenic process, restoring the normal balance of excitatory and inhibititory neurotransmission in the brain, or even reversing pathogenic synaptic network responses to a pre-injury state. To this end, there are three main hypothesized types of cell restoration or repair strategies for epilepsy: 1) ways to prevent mossy fiber sprouting and abnormal axon sprouting, 2) ways to promote cell survival, and 3) ways to replace dead or dysfunctional cells. Therapeutic studies will likely require the use of long-term EEG monitoring to examine whether electrographic and behavioral seizure activity is suppressed after treamtment.

6.7.1 Preventing mossy fiber sprouting

Prevention of mossy fiber sprouting has been proposed as a means to reduce abnormal recurrent excitatory circuit formation in the dentate gyrus and subsequently suppress seizure frequency or duration. Treatment with the protein synthesis inhibitor, cycloheximide, was reported to block pilocarpine- and kainic acid-induced mossy fiber sprouting but not spontaneous seizures in rats (Longo and Mello, 1997). However, these findings could not be replicated in rats after pilocarpine-induced status epilepticus

(Williams et al., 2002; Toyoda and Buckmaster, 2005). As discussed above, manipulation of the mTOR signaling pathway (e.g., by rapamycin treatment) may be a promising new approach to prevent mossy fiber sprouting, but the therapeutic potential of this pathway has not been well established.

Calcium is important for normal growth cone function (Henley and Poo, 2004), and the Ca^{2+}-calmodulin dependent phosphatase, calcineurin, stimulates neurite outgrowth when activated by increased calcium influx through voltage-gated calcium channels (Klee et al., 1979; Lautermilch and Spitzer, 2000). Therefore, Ca^{2+} homeostasis and Ca^{2+}-activated phosphatases have been examined as possible targets to prevent abnormal mossy fiber sprouting after injury. L-type calcium channel blockade with nicardipine was reported to suppress aberrant mossy fiber sprouting in hippocampal slice cultures (Ikegaya, 1999) and after pilocarpine-induced status epilepticus in mice (Ikegaya et al., 2000). Additionally, the immunosuppressant FK506, a calcineurin inhibitor, was reported to block mossy fiber sprouting in rats after amygdala kindling (Moriwaki et al., 1996). However, Ingram et al. (2009) reported that prolonged infusion of FK506, cyclosporin A, or nicardipine did not prevent mossy fiber sprouting after pilocarpine-induced status epilepticus in rats. Discrepancies between these studies could be due to model specific differences or different treatment protocols. Ikegaya et al. (2000) used very young mice, versus adult rats in the study by Ingram et al. (2009), and the extent of mossy fiber sprouting in positive controls was much less robust than that reported in adult mice after pilocarpine-induced TLE (Shibley and Smith, 2002). Additionally, it is unclear whether FK506 treatment in the study by Moriwaki et al. (1996) blocked mossy fiber sprouting by calcineurin inhibition or by indirect effects that reduced the kindling process, because FK506 was administered during kindling and treated rats reached less robust behavioral kindling stages. Moia et al., (1994) also found that treatment with FK506 or cyclosporin A inhibits kindling. In contrast, Ingram et al. (2009) began drug administration after induction of status epilepticus to ensure injuries were similar between treated and untreated animals.

6.7.2 Preventing cell death

Many studies are designed based on the hypothesis that preventing injury-induced cell death will improve cognitive and motor function, and cell survival strategies are a major focus of neurotrauma research (Teasdale and Bannan, 1997; Graham et al., 2006). There are two main mechanisms of cell death: necrosis and apoptosis. Necrosis occurs in response to acute traumatic injury and often involves excitotoxicity, metabolic failure, and ischemic/hypoxic tissue damage (Graham et al., 2006). Apoptosis refers to a process of programmed cell death (Raghupathi et al., 2000; Graham et al., 2006). Because of the complex neurobiology of TBI, there are numerous cellular and molecular targets for neuroprotection (Teasdale and Bannan, 1997; Graham et al., 2006). Neuroprotective strategies may also be useful to experimentally dissociate posttraumatic axon sprouting from cell death and to examine the role of each in seizure generation. However, whether cell survival strategies are beneficial in PTE is controversial. For example, the Soltesz laboratory has proposed that the survival – not the loss – of hilar mossy cells in TLE promotes abnormal discharge patterns in granule cells after TBI (i.e., "the irritable mossy cell hypothesis;" Santhakumar et al., 2000). Therefore, whether cell survival strategies will prevent posttraumatic seizure generation or promote pathogenic responses is unknown. The following is a brief description of cellular and molecular responses after TBI that may be important in regulating cell death or synaptic plasticity in PTE: calpain and caspase activation, mitochondrial dysfunction, and altered neurotrophin expression.

Calpain and caspase activation

TBI induces a massive release of glutamate from axon terminals of injured neurons and a subsequent increase of calcium ion influx into neurons via glutamate receptors and voltage-gated calcium channels (Graham et al., 2006). Persistent elevation of intracellular free calcium can activate calcium-dependent signaling pathways that promote necrotic cell death. Calcium-dependent proteases with papain-like activity, or calpains, are the primary mediators of necrosis (Graham et al., 2006). These are a family of ubiquitous cysteine proteases that are activated by calcium. Physiological calpain

activation by localized calcium influx allows for controlled proteolysis of target proteins and is essential for cell signaling and remodeling processes involved in normal neuronal function. However, persistent alterations in calcium ion homeostasis can lead to the pathological activation of calpain and induce proteolysis of the cytoskeleton, ion channels, and cell surface receptors (Kampfl et al., 1997; Graham et al., 2006). Therefore, pathological calpain activation has been proposed as a key mediator of necrotic cell death after TBI (Kampfl et al., 1997; Graham et al., 2006). Regulation of calpain activity – or its primary endogenous inhibitor, calpastatin – may be an important therapeutic target for neuroprotective strategies and for modulating synaptic circuit remodeling in PTE.

Apoptosis is a fundamental biological process that allows for programmed cell death in the normal brain (e.g., regulating cell numbers during development) or in the disease state (Raghupathi et al., 2000). While there are many proposed mechanisms for apoptosis after brain injury, the activation of a family of proteases called caspases, particularly caspase-3, is a major molecular pathway of programmed cell death (Raghupathi et al., 2000; Graham et al., 2006). Caspases are synthesized as proenzymes that undergo proteolytic processing to become activated. Once activated, caspases cleave other protein substrates within the cell and trigger apoptotic processes. These pro-apototic mechanisms include degradation of anti-apoptotic regulators, degradation of cytoskeletal proteins, chromatin condensation, and DNA fragmentation (Porter et al., 1999; Raghupathi et al., 2000). Growth factor deprivation, mitochondrial dysfunction, generation of free radicals, and hypoxia/ischemia can all activate caspase cascades (Raghupathi et al., 2000). Furthermore, release of cytochrome c from mitochondria can induce apoptosis via interaction with apoptosis protease activating factor-1 (Apaf-1), an upstream activator of caspase-3 (Porter et al., 1999; Kroemer and Reed, 2000; Raghupathi et al., 2000; Garrido et al., 2006). In contrast, activation of the Bcl-2 family of proteins promotes cell survival by inhibiting Apaf-1 activity or by preventing cytochrome c release from mitochondria (Kroemer and Reed, 2000). Therefore, molecular cascades of apoptosis provide numerous potential targets for neuroprotection.

Mitochondrial dysfunction

Mitochondria are the primary centers of energy production and aerobic metabolism in cells, but they can become dysfunctional after TBI (Kroemer and Reed, 2000; Sullivan et al., 2004; Graham et al., 2006). Additionally, mitochondria are important regulators of calcium ion homeostasis in cells, acting to sequester excessive intracellular calcium. After TBI, there is a massive increase of intracellular calcium in neurons. This triggers a cascade of events in mitochondria: the injury-induced increased intracellular calcium is presumably sequestered by mitochondria, the membrane potential generated by the electron transport chain across the inner mitochondrial membrane depolarizes, mitochondrial permeability transition pores open, and mitochondrial membrane permeability is increased (Sullivan et al., 2004). These actions disrupt ATP synthesis, increase free radical production, and promote cell death. Therefore, mitochondrial dysfunction after TBI may contribute to cell death by several mechanisms: reduced mitochondrial respiration, altered ATP production, oxidative stress, generation of reactive oxygen species which can damage DNA, increased permeability of the inner mitochondrial membrane, perturbation of calcium ion homeostasis, and release of cytochrome c (Kroemer and Reed, 2000; Sullivan et al., 2004). Additionally, mitochondrial dysfunction has recently been implicated as both a contributor and a consequence of seizures (Patel et al., 2004). Therefore, mitochondria are an intriguing therapeutic target for posttraumatic seizure management, especially in the acute phase.

Cyclosporin A is an immunosuppressant drug that inhibits the opening of the mitochondrial permeability transition pore (Scheff et al., 1999; Sullivan et al., 1999, Sullivan et al., 2004). While administration of cyclosporin A does not prevent mossy fiber sprouting into the inner molecular layer of epileptic animals (Ingram et al., 2009), a number of studies have suggested cylcosporin A treatment improved mitochondrial function and reduced tissue damage after experimental TBI (Scheff et al., 1999; Sullivan et al., 1999). Whether this treatment or similar drugs can be used as a cell survival strategy in PTE – regardless of its effects on mossy fiber sprouting – is unknown.

Neurotrophins

Neurotrophic factors are secreted peptides produced by neurons and glia that are important for the normal growth, survival, and differentiation of neurons (Lewin and Barde, 1996). They consist of a family of small proteins that include nerve growth factor (NGF), brain-derived neurotrophic factor (BDNF), and neurotrophins 3 and 4/5 (NT-3 and NT-4/5). Neurotrophins activate two types of cell surface receptors: the tropomyosin-related kinase (Trk) family of receptor tyrosine kinases, Trk A, B, and C, and the p75 low affinity neurotrophin receptor (Lewin and Barde, 1996; Amaral et al., 2007). Agonist binding to Trk receptors induces receptor dimerization and kinase activation; autophosphorylation of multiple intracellular tyrosine residues creates binding sites for target proteins; and G-proteins and other signaling cascades are activated. In the hippocampus, activation of Trk receptors promotes neuronal survival, axon growth, increased dendritic complexity, and induction of long-term potentiation; but the activation of p75 promotes neural apoptosis, axonal degeneration, reduced dendritic complexity, and induction of long-term depression (Amaral et al., 2007). Moreover, neurotrophic factor deprivation can trigger caspase activation and apoptotic cell death (Raghupathi et al., 2000; Graham et al., 2006).

Levels of NGF and BDNF mRNA and protein are elevated in the dentate gyrus of experimental epilepsy models (Lowenstein et al., 1993; Sato et al., 1996; Marcinkiewicz et al., 1997; Rudge et al., 1998), after CCI injury (Yang et al., 1996; DeKosky et al., 2004), and in resected brain tissue from human epileptic patients (Murray et al., 1994; Mathern et al., 1997; Takahashi et al., 1999). Interestingly, Yang et al. (1996) found that alterations in neurotrophin expression only occur in brain regions ipsilateral to CCI injury. Likewise, granule cell expression of trkB mRNA and protein, the high affinity receptor for BDNF, is upregulated after seizures (Rudge et al., 1998). In contrast, levels of NT-3 appear to be downregulated in epilepsy (Mathern et al., 1997) and after TBI (Yang et al., 1996). Protein and mRNA for the low affinity neurotrophin receptor, p75, is also upregulated in apoptotic neurons after pilocarpine-induced status epilepticus (Roux et al., 1999). Therefore, neurotrophin signaling via Trk and p75 receptors have been

proposed as key regulators of the structural reorganization and cell survival in the dentate gyrus during epileptogenesis (Jankowsky and Patterson, 2001; McNamara et al., 2006).

6.7.3 Exogenous cell transplantations

The regenerative capacity of the injured brain is limited. Exogenous cell transplants into the injured brain have been used as an attempt to replace neurons and glia lost to trauma, restore functional recovery, and improve cognitive and motor function (Schouten et al., 2004; Longhi et al., 2005). These strategies have had varying levels of success, but whether cellular transplantations can be developed as a therapeutic intervention to prevent or suppress posttraumatic seizures remains unknown. One approach that may work well is transplantation of embryonic median ganglionic eminence (MGE) precursor cells into the pericontusional area.

The MGE is a transitory protruding elevation of the ventricular cavity in the ventral telencephalon during embryonic and fetal stages of brain development (Figure 6.4). During development, these cells migrate throughout the cortex and differentiate into cortical GABAergic interneurons (Lavadas et al., 1999; Anderson et al., 2001). Transplanted early postnatal embryonic MGE precursor cells migrate widely throughout the host brain, differentiate into functional GABAergic interneurons, and increase synaptic inhibition of principle cells in the normal mouse brain (Wichterle et al., 1999; Alvarez-Dolado et al., 2006). Moreover, the duration and frequency of spontaneous seizures in Kv1.1 knock-out mice, a genetic model of epilepsy, are reduced after MGE transplants into the cortex (Baraban et al., 2009). Therefore, MGE cell grafts appear to be a promising cellular based approach to augment synaptic inhibition, mask abnormal recurrent excitatory circuits, and suppress seizures after TBI.

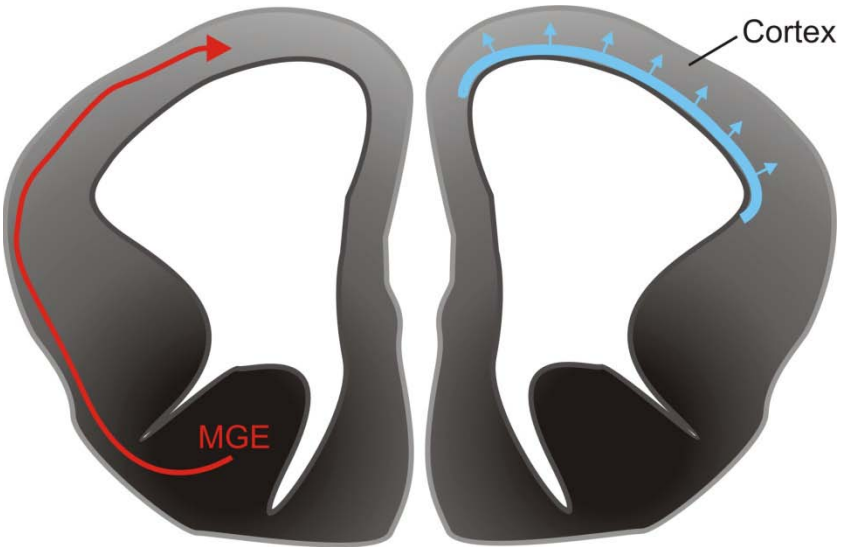

Figure 6.4. Illustration of a coronal section of a mouse forebrain at ~E12. Cells in the median ganglionic eminence (MGE) migrate to the cortex (red line) where they differentiate into GABA neurons. In contrast, glutamatergic cortical neurons are generated in the cortical ventricular zone (blue) and migrate radially (blue arrows) into the cortex.

Future studies should use MGE transplants into the contused area to examine whether replacement of GABA neurons after TBI can suppress posttraumatic seizures and restore synaptic inhibition to dentate granule cells. The relatively focal injury produced by CCI makes it an advantageous model for this type of procedure, because the injured area is known and is relatively localized to dorsal brain regions ipsilateral to the injury. This is in contrast to FPI, which has a large diffuse injury component. The relatively short but distinct latency to spontaneous seizure onset after CCI creates an amenable window for restorative strategies aimed at replacing GABA neurons in PTE. Transplants performed within days after injury may prevent PTE whereas transplants performed weeks later – after the onset of spontaneous seizures – may suppress PTE.

If MGE cell grafts are capable of preventing posttraumatic seizures, an interesting proof-of-principle study would be to then "silence" the transplanted neurons after they are integrated into synaptic circuits within the host brain to examine whether seizures subsequently emerge (or reemerge). Recent work has demonstrated how this might be feasible (Lechner et al., 1999; Wehr et al., 2009). The Calloway laboratory has created a line of transgenic mice which allows for the inducible expression of the *Drosophila*

allotostatin neuropeptide receptor (AlstR) when crossed with commercially available tet-transactivator lines (Wehr et al., 2009). Activation of AlstR in mammalian neurons activates G-protein-coupled inward rectifier K+ (GIRK) channels which hyperpolarize the neuron, thus inhibiting action potential firing in these neurons. Conceptually, transplantation of MGE cells from these animals into host brains from injured animals would allow for the inducible expression of this ligand-gated "silencer" transgene only in transplanted GABA neurons, because mammalian neurons do not have allotostatin or AlstR. Therefore, administration of allotostatin to brains of mice should allow only the transplanted GABA neurons which express AlstR to be "turned off." Unfortunately, receptor-associated AlstR mRNA is preferentially expressed in principal neurons, and it is rarely present in hippocampal interneurons (Wehr et al., 2009). However, if the AlstR was to be placed under the control of the G*ad1* gene, like eGFP in GIN mice, then it would be possible to "silence" eGFP neurons to examine their relative importance in posttraumatic seizure generation and regulating network excitability after TBI.

There are a number of important caveats to the use of embryonic precursor cells in treating epilepsy. Previous studies have performed MGE transplants only on very young animals (i.e., younger than postnatal day 7), and it is unknown whether grafted cells will survive in the adult brain, especially after injury-induced perturbation of the normal environment. Moreover, the migratory capacity of MGE precursor neurons in the injured brain is unknown. Precursor cells differentiate into somatostatin-, parvalbumin-, neuropeptide Y-, and calretinin-immunoreactive GABA neurons in the normal cortex and hippocampus (Alvarez-Dolado et al., 2006). This suggests grafted MGE cells are capable of differentiating into a wide variety of GABA neuron subtypes. This could have a restorative role to enhance synaptic inhibition of principle cells in the injured brain, or it could have a pathogenic role if neurons predominantly differentiate into "inappropriate" GABA cell subtypes.

6.8 Final conclusions

The findings in this dissertation suggest that CCI injury may be an advantageous mouse model of PTE. In the dentate gyrus, there is an increase in recurrent excitatory neurotransmission and dysfunction of synaptic inhibition. Future studies will examine time-dependant cellular and molecular mechanisms of epileptogenesis after CCI. There are also a number of cellular and molecular targets that may be useful for modulating synaptic circuitry, promoting cell survival, and suppressing seizures in PTE. Future studies are warrented to examine their role in posttraumatic epileptogenesis.

Appendix 1

Tonic $GABA_A$-receptor mediated inhibition is not altered after brain injury

A1.1 Introduction

$GABA_A$ receptors consist of a family of heteropentimeric ionotropic membrane receptors with at least 16 different known subunits (α1-6, β1-β3, γ1-γ3, ε, δ, π, and θ) (Sieghart, 2000; Mohler, 2006). The receptor subunit composition determines specific kinetic properties, affinity of the receptor for GABA and other pharmacological agents, and whether the receptor is concentrated at the synapse (synaptic) or away from the synapse (extrasynaptic or perisynaptic). Receptors that contain δ and α4 subunits are located mainly at perisynaptic and extrasynaptic locations where they are thought to mediate tonic inhibition (Nusser et al., 1998; Nuesser and Mody, 2002). In contrast, receptors that contain the γ2 subunit are typically found in postsynaptic $GABA_A$ receptors, where they mediate fast inhibitory neurotransmission (i.e., phasic inhibition) (Nusser et al., 1998; Nusser and Mody, 2002).

Alterations in $GABA_A$ receptor subunits occur in experimental and human TLE (Rice et al., 1996; Schwarzer et al., 1997; Brooks-Kayal et al., 1998; Fritschy et al., 1999; Loup et al., 2000; Houser and Esclapez, 2003; Peng et al., 2004; Zhang et al., 2007). In experimental TLE, there is a decrease in the δ subunit and an increase in γ2 and α4 subunits in granule cells (Zhang et al., 2007). Despite these receptor changes, previous studies have indicated that tonic inhibition of granule cells is maintained weeks after status epilepticus (Zhang et al., 2007; Zhan and Nadler, 2009). However, neurosteroid modulation of tonic currents may be enhanced after injury (Zhang et al., 2007). Whether tonic inhibition of granule cells is altered after TBI is not well established.

I tested whether a change in resting tonic inhibition could be detected in granule cells after CCI injury. An increase in tonic inhibition of granule cells may be an intrinsic response in granules cells to compensate for the reduction in synaptic inhibition after TBI. Alternatively, a reduction in tonic inhibition of granule cells may be a pathogenic response that further exacerbates the loss of inhibitory synaptic input to granule cells after injury.

A1.2 Methods

Tonic current. Resting tonic current (I_{tonic}) was calculated for each neuron as the amplitude difference between the holding current before and after application of 100µM BMI and was normalized to cell capacitance (i.e., pA/pF). The holding current was measured as the mean baseline amplitude of 30 epochs (100 ms/epoch; 1 epoch/s) (Nusser and Mody, 2002; Mtchedlishvili and Kapur, 2006; Zhang et al., 2007; Gao and Smith, 2009). Baseline measurements were taken 30 s before and 2-3 min after application of BMI (i.e., at the peak of the baseline shift in holding current). Tonic current was measured in granule cells from control animals and in injured animals contralateral and ipsilateral to the injury. Data were analyzed by one-way ANOVA. Significance was set at $P<0.05$.

A1.3 Results and Discussion

Whole-cell voltage-clamp recordings of sIPSCs were obtained from granule cells at a holding potential of 0 mV in ACSF containing 1mM kynurenic acid. Application of 100µM BMI resulted in a net inward current (Figure A1.1), revealing the tonic current (I_{tonic}) as a shift in holding current. Resting I_{tonic} was calculated for each neuron as the amplitude difference between the holding current before and after application of BMI and was normalized to cell capacitance (i.e., pA/pF). One-way ANOVA did not detect a difference in I_{tonic} ($F_{(2,25)}= 0.2$; $P= 0.82$) or cell capacitance ($F_{(2,25)}= 1.43$; $P= 0.3$). Therefore, these preliminary findings suggest there is no change in resting I_{tonic} in granule cells after CCI.

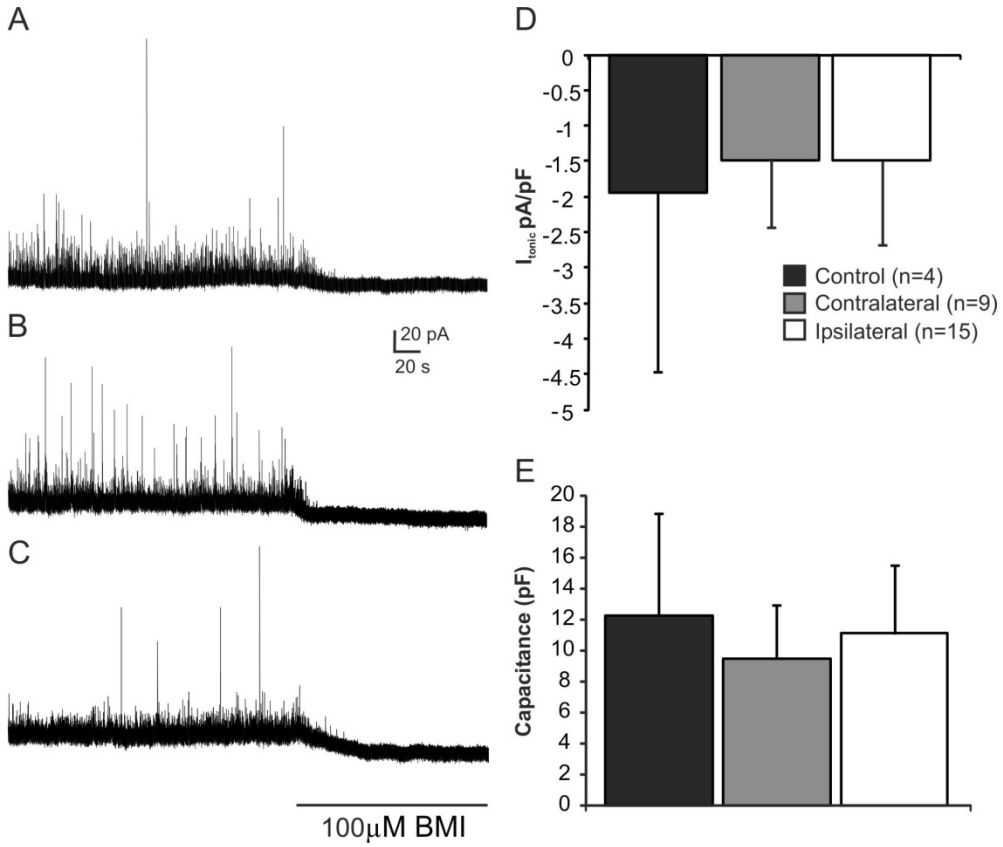

Figure A1.1. Resting tonic current in granule cells after TBI is similar to controls. Application of 100μM BMI revealed the tonic current (I_{tonic}) as a shift in baseline holding current in (**A**) a granule cell in a control slice, (**B**) a granule cell in a slice contralateral to the injury, and (**C**) a granule cell in a slice ipsilateral to the injury. **D.** Mean I_{tonic} normalized to cell capacitance (pA/pF) in granule cells for each treatment group. **E.** Mean whole-cell capacitance of granule cells in each treatment group.

The present result is consistent with previous findings from normotopic granule cells in epileptic rodents (Zhang et al., 2007; Zhan and Nadler, 2009) and preliminary findings from granule cells weeks to months after lateral FPI (Pavlov et al., 2009). However, preliminary studies from the Mtchedlishvili laboratory have suggested that tonic inhibition of granule cells may be increased after CCI in rats in the presence of 4,5,6,7-tetrahydroisoxazolo[5,4-c]pyridin-3-ol (THIP), a competitive agonist of $GABA_A$ receptors which contain δ-subunits; but δ-subunit immunoreactivity and neurosteroid modulation of I_{tonic} may be reduced in granule cells 90d after CCI (Mtchedlishvili et al., 2008a and b; Kharlamov et al., 2008; Mtchedlishvili et al., 2010). Therefore, a more

detailed examination of how tonic inhibition of granule cells and the subunit composition of extrasynaptic $GABA_A$ receptors may be altered after TBI is warranted. The functional consequences of $GABA_A$ receptor subunit changes after TBI will likely depend on the resulting subunit composition, the cell types involved, location of the receptor relative to the synapse (i.e., synaptic, perisynaptic, or extrasynaptic), and the cellular domain (i.e., somatic versus dendritic).

Appendix 2
Electrophysiology equipment for data acquisition

A2.1 List of Equipment

Vibration isolation table
Microscope (Olympus BX50WI)
Patch-clamp amplifier (Axopatch 200B or 700B)
Digitizer (Digidata 1320A or 1440A)
DR-484 Neuro-corder
Oscilloscope (Hitachi VC-6525)
Shutter (Uniblitz VMM-D1)
Signal timer (Master-8)
Micromanipulator (Sutter MP-225 or MPC-200)
Computer (Dell Precision T3400)
Pipette puller (Sutter P-87)

A2.2 Electrophysiology equipment setup

Cells were visualized and targeted for recording using an Olympus BX50WI upright fixed-stage water-immersion microscope. The current and voltage measured in patch or field recording electrodes were amplified with an Axopatch 200B (Figure A2.1 and A2.2) or 700B amplifier. Digital acquisition of bioelectric signals was made using the Digidata 1320A (Figure A2.3 and A2.4) or 1440A digitizer. These digitizers are 16 bit data acquisition systems that convert analog signals from the amplifier (i.e., Axopatch 200B or 700B) into a digital format that is recognized by the computer. Axon Instruments pClamp 8 data acquisition software was used to record data online. The DR-484 Neuro-corder (Figure A2.5) allowed for analog output from the Axopatch 200B amplifier to be simultaneously digitized at 88kHz and recorded on videotape. In addition to viewing signals online using pClamp software, the Hitachi VC-6525 oscilloscope allowed digitized electrical signals from Digidata 1320A and DR-484 Neuro-corder to be viewed.

The Master-8 (Figure A2.6) is a signal timer that was used to time electrical- or photostimulation-evoked responses. Data were later analyzed offline using pClamp 10.2 and Minianalysis 6 software.

Figure A2.7 shows how connections were made between the headstage, Axopatch 200B, Digidata 1320A, DR-484 Neuro-corder, and Master-8, and computer.

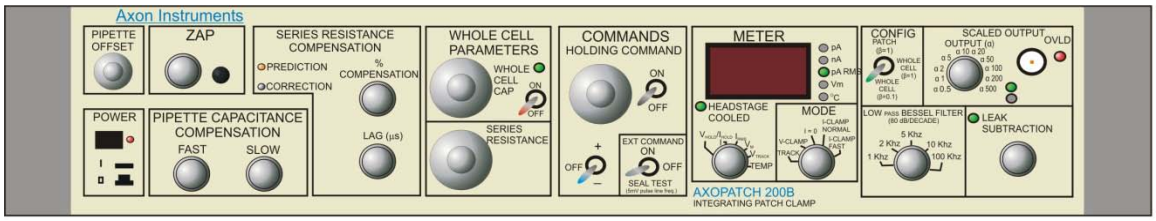

Figure A2.1. The Axopatch 200B Amplifier (front).

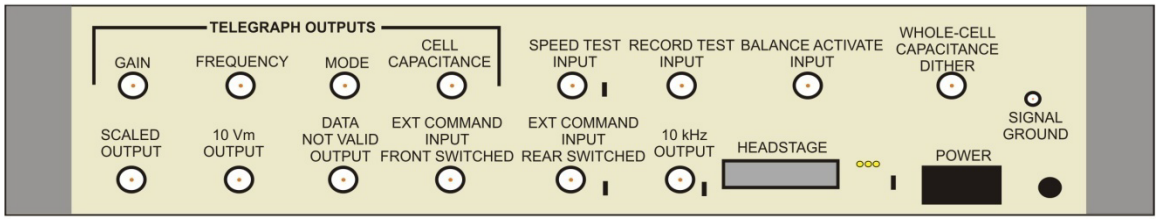

Figure A2.2. The Axopatch 200B Amplifier (back).

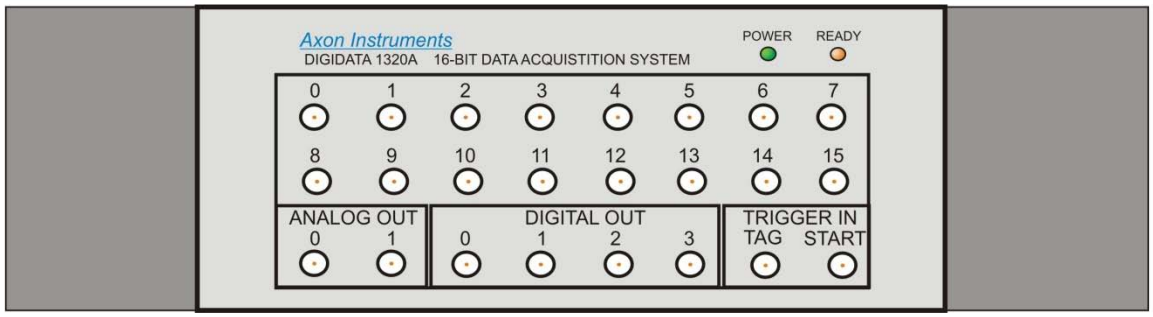

Figure A2.3. The Digidata 1320A digitizer (front).

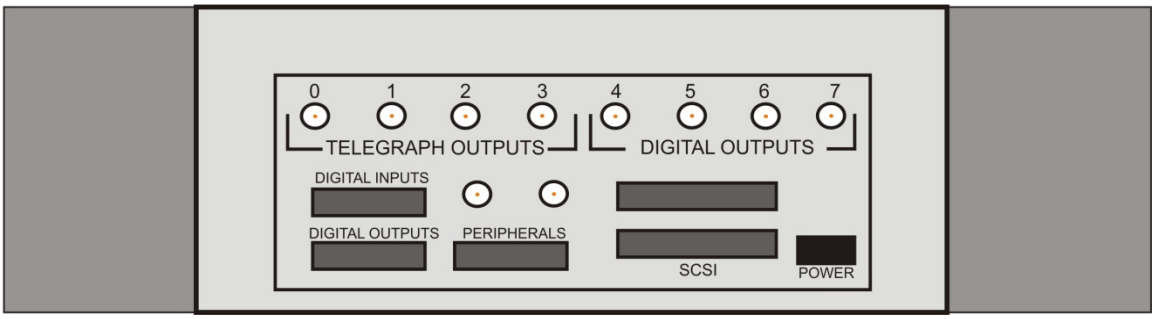

Figure A2.4. The Digidata 1320A digitizer (back).

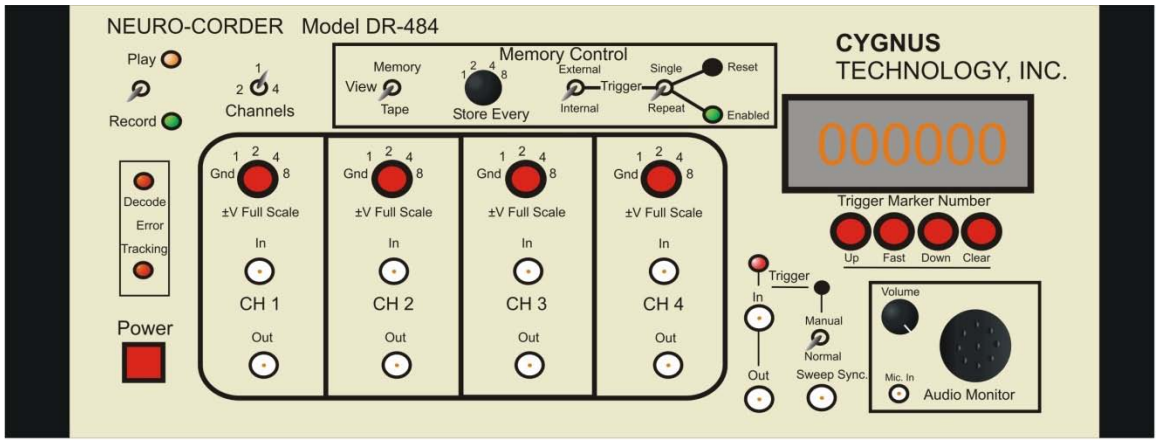

Figure A2.5. The DR-484 Neuro-corder.

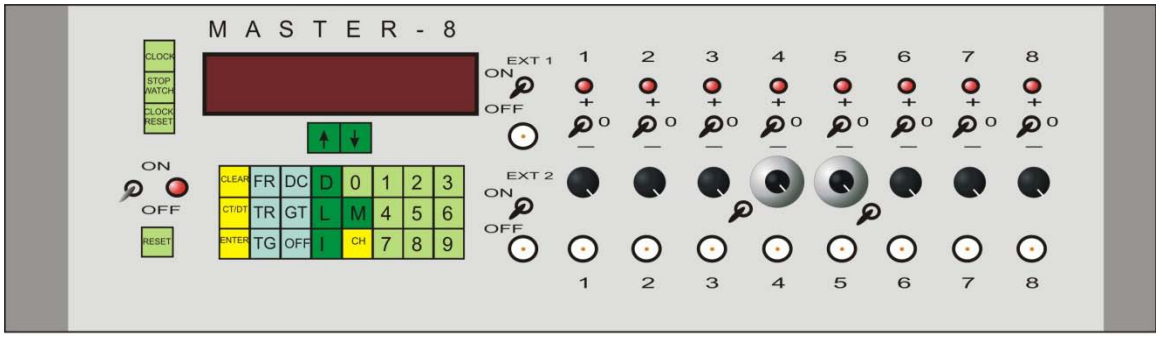

Figure A2.6. The Master -8 stimulator.

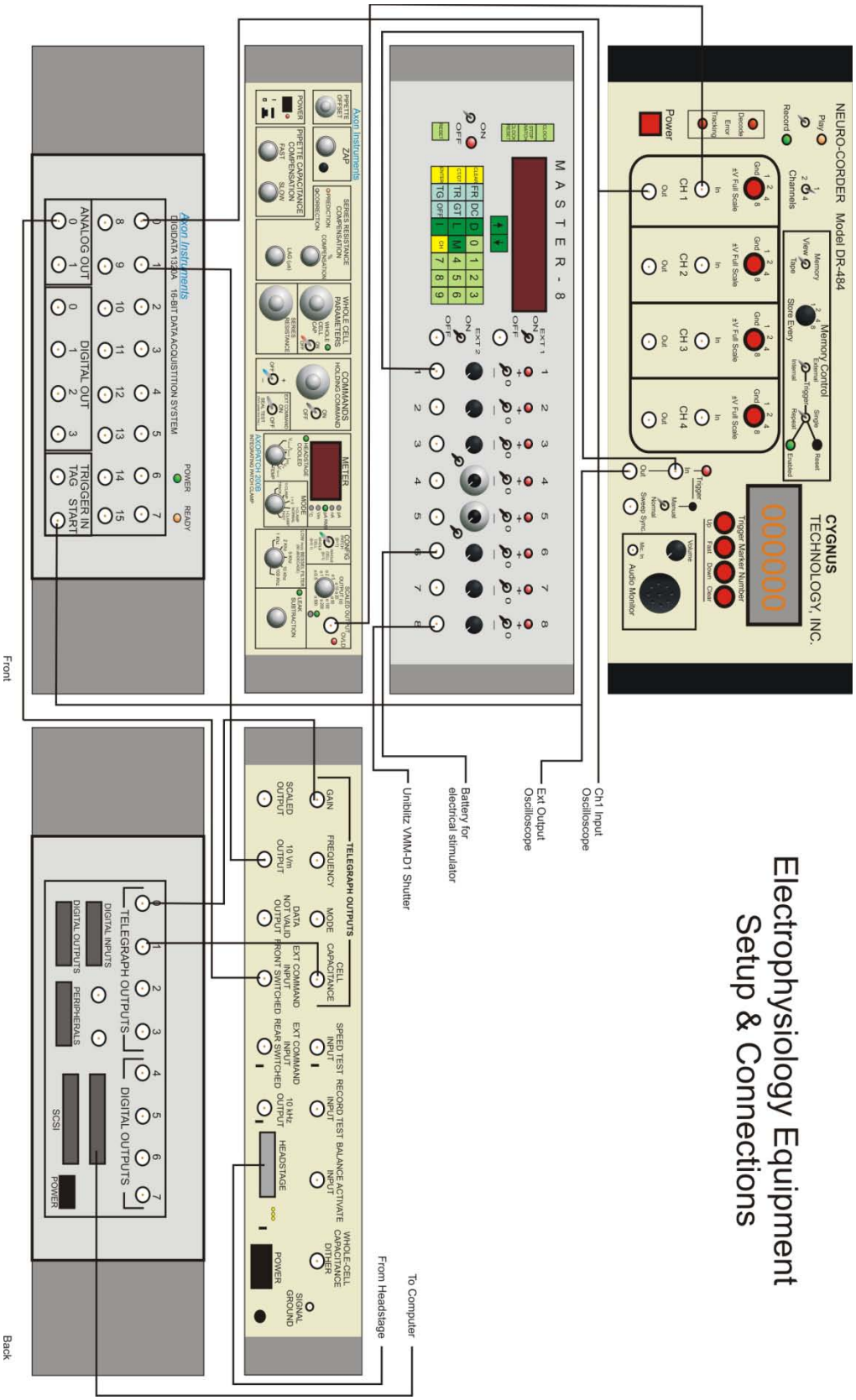

Figure A2.7. Electrophysiology Equipment Setup & Connections

Appendix 3

List of abbreviations

ACSF	Artificial cerebral spinal fluid
al	Alveus
APV	(2*R*)-amino-5-phosphonovaleric acid
BMI	Bicuculline methiodide
CA	Cornu Ammonis
DAPI	4',6-diamidino-2-phenylindole
DG	Dentate gyrus
EC	Entorhinal cortex
EEG	Electroencephalogram
eGFP	Enhanced green fluorescent protein
EPSC(P)	Excitatory postsynaptic current (potential)
	e- evoked
	m- miniature
	s- spontaneous
FPI	Fluid percussion injury
GABA	γ-aminobuteric acid
GAD	glutamic acid decarboxylase
GCL or g	Granule cell layer
GCS	Glasgow Coma Scale
GFP	Green flourescent protein
GIN	eGFP-expressing Inhibitory Neurons
H or h	Hilus
HICAP	Hilar commissural-associational pathway
HIPP	Hilar interneurons associated with the perforant pathway
HM	Henry Gustav Molaison
I	Current

IPSC(P)	Inhibitory postsynaptic current (potential)
	e- evoked
	m- miniature
	s- spontaneous
MFS	Mossy fiber sprouting
ML or m	Molecular layer
MOPP	Molecular layer interneurons associated with the perforant pathway
NINDS	National Institute of Neurological Disorders and Stroke
p	Pyramidal cell layer
Para	Parasubiculum
PBS	phosphate buffered saline
PDS	Paroxysmal depolarizing shift
PPR	Paired-pulse ratio
Pre	Presubiculum
PTE	Posttraumatic epilepsy
PTX	picrotoxin
PTZ	Pentylenetetrazol
sl	Stratum lucidum
sl-m	Stratum lacunosum-moleculare
so	Stratum oriens
sr	Stratum radiatum
Sub	Subiculum
TBI	Traumatic brain injury
TLE	Temporal lobe epilepsy
TRITC	Tetramethylrhodamine-5- (and 6)-isothiocyanate
TTX	Tetrodotoxin
Vm	Membrane potential

References

Acsády L, Kamondi A, Sík A, Freund T, Buzsá ki G (1998) GABAergic cells are the major postsynaptic targets of mossy fibers in the rat hippocampus. J Neurosci. 18(9): 3386-3403.

Agrawal A, Timothy J, Pandit L, Manju M (2006) Post-traumatic epilepsy: an overview. Clin Neurol Neurosurg. 108:433-439.

Alger BE, Teyler TJ (1976) Long-term and short-term plasticity in the CA1, CA3, and dentate regions of the rat hippocampal slice, *Brain Res.* 110: 463–480.

Alvarez-Buylla A, Ling CY, Kirn JR (1990) Cresyl violet: A red fluorescent Nissl stain. *J Neurosci Methods*. 33(2-3):129-33.

Alvarez-Dolado M, Calcagnotto ME, Karkar KM, Southwell DG, Jones-Davis DM, Estrada RC, Rubenstein JL, Alvarez-Buylla A, Baraban SC (2006) Cortical inhibition modified by embryonic neural precursors grafted into the postnatal brain. *J Neurosci.* 26: 7380-7389.

Amaral DG (1978) a Golgi study of cell types in the hilar region of the hippocampus in the rat. *J Comp Neurol.* 182: 851-914.

Amaral M. D., Chapleau C. A. and Pozzo-Miller L. (2007) Transient receptor potential channels as novel effectors of brain-derived neurotrophic factor signaling: potential implications for Rett syndrome. *Pharmacol. Ther.* 113: 394–409.

Amaral DG, Lavenex P (2007) Hippocampal neuroanatomy. In: The Hippocampus Book (Andersen P, Morris R, Amaral D, Bliss T, and O'Keefe J, eds.). Oxford University Press, New Y ork, p37-114, 133-242.

Andersen P, Bliss VP, Skrede KK (1971) Lamellar organization of hippocampal excitatory pathways. *Exp Neurol.* 13:222-238.

Anderson KJ, Miller KM, Fugaccia I, Scheff SW (2005) Regional distribution of Fluoro-Jade B staining in the hippocampus following traumatic brain injury. Exp Neurol. 193:125-130

Anderson RW, Brown CJ, Blumbers PC, McLean AJ, and Jones NR (2003) Impact mechanics and axonal injury in a sheep model, *J Neurotrauma* 20:961-974.

Anderson SA, Marín O, Horn C, Jennings K, Rubenstein JLR (2001) Distinct cortical migrations from the medial and lateral ganglionic eminences. *Development*. 128: 353-363.

Andrioli A, Alonso-Nanclares L, Arellano JI, DeFelipe J (2007) Quantitative analysis of parvalbumin-immunoreactive cells in the human epileptic hippocampus. *Neuroscience* 149:131–143.

Annegers JF, Hauser A, Coan SP, Rocca WP (1998) A population-based study of seizures and traumatic brain injuries. *N Eng J Med.* 338:20-24.

Asikainen I, Kaste M, Sarna S. (1999) Early and late posttraumatic seizures in traumatic brain injury rehabilitation patients: brain injury factors causing late seizures and influence of seizures on long-term outcome. *Epilepsia.* 40: 584–589.

Ayala G, Dichter M, Gumnit R, Matsumoto H, Spencer W (1973) Genesis of epileptic interictal spikes. *Brain Res.* 52: 1-17.

Babb, T.L., Kupfer, W.R., Pretorius, J.K., Crandall, P.H., Levesque, M.F. (1991) Synaptic reorganization by mossy fibers in human epileptic fascia dentata. Neuroscience 42:351-363.

Babb TL, Pretorius JK, Kupfer WR, Crandall PH (1989) Glutamate decarboxylase-immunoreactive neurons are preserved in human epileptic hippocampus. *J Neurosci.* 9(7): 2562-2574.

Baskt I, Avendano C, Morrison JH, Amaral DG (1986) An experimental analysis of the origins of somatostatin-like immunoreactivity in the dentate gyrus of the rat. *J Neurosci.* 6:1452-1462.

Ben-Ari, Y (1985) Limbic seizure and brain damage produced by kainic acid: mechanisms and relevance to human temporal lobe epilepsy. *Neurosci* 14:375-403.

Bernard C, Esclapex M, Hirsch JC, Ben-Ari T (1998) Interneurones are not so dormant in temporal lobe epilepsy: a critical reappraisal of the dormant basket cell hypothesis. *Epilepsy Res.* 32:93-103.

Bigler ED, Blatter DD, Anderson CV, Johnson SC, Gale SD, Hopkins RO, Burnett B (1997) Hippocampal volume in normal aging and traumatic brain injury. *Am J Neuroradiol*. 18:11-13.

Bonifazi P, Goldin M, Picardo MA, Jorquera I, Cattani A, Bianconi G, Represa A, Ben-Ari Y, Cossart R (2009) GABAergic hub neurons orchestrate synchrony in developing hippocampal networks. Science 326(5958): 1419-24.

Boyett JM, Buckmaster PS (2001) Somatostatin-immunoreactiv interneurons contribute to lateral inhibitory circuits in the dentate gyrus of control and epileptic rats. Hippocampus 11: 418-422.

Brooks-Kayal AR, Shumate MD, Jin H, Rikhter TY, Coulter DA (1998) Selective changes in single cell GABAA receptor subunit expression and function in temporal lobe epilepsy. *Nat Med.* 4:1166-1172.

Buckmaster PS, Dudek FE (1999) In vivo intracellular analysis of granule cell axon reorganization in epileptic rats. *J Neurophysiol.* 81:712-721.

Buckmaster PS, Dudek FE (1997a) Network properties of the dentate gyrus in epileptic rats with hilar neuron loss and granule cell axon reorganization. *J Neurophysiol* 77:2685-2596.

Buckmaster PS, Dudek FE (1997b) Neuron loss, granule cell axon reorganization, and functional changes in the dentate gyrus of epileptic kaintate treated rats. *J Comp Neurol.* 385:385:404.

Buckmaster PS, Jongen-Rêlo Al (1999) Highly specific neuron loss preserves lateral inhibitory circuits in the dentate gyrus of kainate-induced epileptic rats. *J Neurosci.* 19: 9519-9529.

Buckmaster PS, Stowbridge BW, Kunkel DD, Schmiege DL, Schwartzkroin PA (1992) Mossy cell axonal projections to the dentate gyrus molecular layer in the rat hippocampal slice. *Hippocampus*. 2(4):349-62.

Buckmaster, PS, Schwartzkroin PA (1994) Hippocampal mossy cell function: A speculative view. *Hippocampus* 4:393–402.

Buckmaster PS, Wentzel HJ, Kunkel DD, Schwartzkroin PA (1996) Axon arbors and synaptic connections of hippocampal mossy cells in the rat in vivo. *J Comp Neurol.* 366: 270-292.

Buckmaster PS Yamawaki R, Zhang GF (2002) Axon arbors and synaptic connections of a vulnerable population of interneurons in the dentate gyrus in vivo. J comp Neurol. 445:360-373.

Buhl EH, Han ZS, Lorinczi Z, Stezhka W, Karnup SV, Somogyi P (1994) Physiological properties of anatomically identified axo-axonic cells in the rat hippocampus. *J Neurophysiol.* 71:1289-1307.

Bullock R (1997) Injury and cell function. In: *Head Injury*. (Reilly P, Bullock R, eds.). London: Chapman & Hall. pp 121- 141.

Calloway EM and Katz LC (1993) Photostimulation using caged glutamate reveals functional circuitry in living brain slices. *PNAS*. 90 (16): 7661-65.

Cavazos JE, Das I, Sutula TP (1994) Neuronal loss induced in limbic pathways by kindling: evidence for induction of hippocampal sclerosis by repeated brief seizures. *J Neurosci.* 14: 3106-3121.

Cavazos JE, Sutula TP (1990) Progressive neuronal loss induced by kindling: a possible mechanism for mossy fiber synaptic reorganization and hippocampal sclerosis. *Brain Res.* 527:1-6.

Caveness WF, Meirowski AM, Rish BL, Mohr JP, Kistler JP, Dillon JD, Weiss GH (1979) The nature of posttraumatic epilepsy. *J Neurosurg* 50:545-553.

Chang BS, Lowenstein DH (2003) Epilepsy. N Engl J Med. 349:1257-1266.

Cobb SR, Buhl EH, Halasy K, Paulsen O, Somogyi P (1995) Synchronisation of neuronal activity by individual hippocampal GABAergic interneurons. Nature. 378:75-78.

Cossart R, Dinocourt C, Hirsch JC, Merchan-Perez A, De Felipe J, Ben-Ari Y, Esclapez M, Bernard C (2001) Dendritic but not somatic GABAergic inhibition is decreased in experimental epilepsy. *Science.* 4(1): 1419-1424.

Coulter DA, Carlson GC (2007) Functional regulation of the dentate gyrus by GABA-mediated inhibition. *Prog Brain Res.* 163:235-243.

Cronin, J, Dudek, FE (1988) Chronic seizures and collateral sprouting of dentate mossy fibers after kainic acid treatment in rats. *Brain Res*. 474:181-184.

Cronin J, Obenaus A, Houser CR, Dudek FE (1992) Electrophysiology of dentate granule cells after kainite-induced synaptic reorganization of the mossy fibers. *Brain Res*. 573:305-310.

D'Alessandro R, Tinuper P, Ferrara R, Cortelli P, Pazzaglia P, Sabattini L, Frank G, Lugaresi E (1982) CT scan prediction of late post-traumatic epilepsy. *J Neurol Neurosurg Psychiatry.* 45:1153-55.

D'Ambrosio R, Fairbanks JP, Fender JS, Born DE, Doyle DL, Miller JW (2004) Post-traumatic epilepsy following fluid percussion injury in the rat. *Brain*. 127:304–314.

D'Ambrosio R, Fender JS, Fairbanks (2005) Progression from frontal-parietal to mesial-temporal epilepsy after fluid percussion injury in the rat. *Brain*. 128:174-188**.**

D'Ambrosio R, Hakimian S, Stewart T, Verley DR, Fender JS, Eastman CL, Sheerin AD, Gupta P, Diaz-Arrastia R, Ojemann J, Miller JW (2009) Functional definition of seizure provides new insight into post-traumatic epileptogenesis. *Brain.* 132: 2805-2821.

Dantzker JL, Callaway EM (2000) Laminar sources of synaptic input to cortical inhibitory interneurons and pyramidal neurons. *Nature Neurosci.* 3(7):701-707.

DeKosky ST, Taffe KM, Abrahamson EE, Dixon CE, Kochanek PM, Ikonomovic MD (2004) Time course analysis of hippocampal nerve growth factor and antioxidant enzyme activity following lateral controlled cortical impact brain injury in the rat. *J Neurotrauma.* 24: 491-500.

de Lanerolle NC, Kim JH, Robbins RJ, Spencer DD (1989) Hippocampal interneuron loss and plasticity in human temporal lobe epilepsy. Brain Res 495:387-395.

Diaz-Arrastia R, Agostini MA, Frol AB, Mickey B, Fleckenstein J, Bigio E, Van Ness PC (2000) Neurophysiologic and neuroradiologic features of intractable epilepsy after traumatic brain injury in adults. *Arch Neurol* 57:1611-1616.

Dichter MA (2009) Posttraumatic epilepsy: the challenge of translating discoveries in the laboratory to pathways to a cure. *Epilepsia.* 50(s2): 41-45.

Dichter MA, Ayala GF (1987) Cellular mechanisms of epilepsy: a status report. *Science*. 237: 157-164.

Di Paolo S, Teutonico A, Leogrande D, Capobianco C, Schena PF (2006) Chronic inhibition of mammalian target of rapamycin signaling downregulates insulin receptor substrates 1 and 2 and AKT activation: a crossroad between cancer and diabetes? *J Am Soc Nephrol*. 17: 2236-2244.

Dixon CE, Clifton GL, Lighthall JW, Yaghmai AA, Hayes L (1991) A controlled cortical impact model of traumatic brain injury in the rat. *J Neurosci Methods* 3:253-262.

Dixon CE, Kline AE (2009) Controlled cortical impact injury model. In: Animal models of acute neurological injuries (Chen J, Xu ZC, Xu XM, Zhang JH, eds.). Totowa, NJ: Humana Press. pp. 385-391.

Doherty J, Dingledine R (2001) Reduced excitatory drive onto interneurons in the dentate gyrus after status epilepticus. *J Neurosci.* 21:2048-2057.

Dudek FE, Hellier JL, Williams PA, Ferraro DJ, Staley KJ (2002) The course of cellular alterations associated with the development of spontaneous seizure after status epilepticus. *Prog Brain Res.* 135:53-65.

Dudek FE, Spitz M (1997) Hypothetical mechanisms for the cellular and neurophysiologic basis of secondary epileptogenesis: proposed role of synaptic reorganization. J. Clin. Neurophysiol. 14:90-101.

Dudek FE, Sutula TP (2007) Epileptogenesis in the dentate gyrus: a critical perspective. *Prog Brain Res.* 163:755-773.

Eadie MJ, Bladin PF (2001) A Disease Once Sacred: A History of the Medical Understanding of Epilepsy. England: John Libbey and Co., LTD.

Echegoyen J, Armstrong C, Morgan RJ, Soltesz I (2009) Single application of a CB1 receptor antagonist rapidly following head injury prevents long-term hyperexcitability in a rat model. *Epilepsy Res.* 85:123-127.

El-Hassar L, Milh M, Wendling F, Ferrand N, Esclapez M, Bernard C (2007) Cell domatin-dependent changes in the glutamatergic and GABAergic drives during epileptogenesis in the rat CA1 region. *J Physiol.* 518(Pt 1): 193-211.

Englander JE, Bushnik T, Duong TT, Cifu DX, Zafonte R, Wright J, Hughes R, Bergman W (2003) Analyzing the risk factors for late posttraumatic seizures: a prospective, multicenter investigation. *Arch Phys Med Rehabil* 84:365-373.

Engel Jr J (1987) New concepts of the epileptic focus. In: Current Problems in Epilepsy, Vol. 3. The Epileptic Focus (eds Wiser HG, Speckmann EJ, Engel Jr J). John Libbey: London. Pp. 83-94.

Engel Jr J, Williamson PD, Wieser HG (1997) Mesial temporal lobe epilepsy. In: Epilepsy: a comprehensive textbook (Engel Jr J, Pedley TA, eds). Philadelphia: Lippincott-Raven. pp 2417-2426.

Esclapez M, Houser CR (1995) Somatostatin neurons are a subpopulation of GABA neurons in the rat dentate gyrus: evidence from colocalization of pre-prosomatostatin and glutamate decarboxylase messenger RNAs. *Neurosci*. 64:339-355.

Farrant M, Nusser Z (2005) Variations on an inhibitory theme: phasic and tonic activation of $GABA_A$ receptors. *Nat Rev Neurosci*. 6:215-229.

Faul M, Xu L, Wald MM, Coronado VG (2010) Traumatic brain injury in the United States: emergency department visits, hospitalizations, and deaths. Atlanta (GA): Centers for Disease Control and Prevention, National Center for Injury Prevention and Control.

Fox GB, Fan L, Levasseur RA, Faden AI (1998) Sustained sensory/motor and cognitive deficits with neuronal apoptosis following controlled cortical impact brain injury in the mouse. *J Neurotrauma* 15: 599–614.

Fisher RS, van Emde Boas W, Blume W, Elger C, Genton P, Lee P, Engel Jr J (2005) Epileptic seizures and epilepsy: definitions proposed by the International League Against Epilepsy (ILAE) and the International Bureau for Epilepsy (IBE). *Epilepsia.* 46:470-72.

Fraenkel M, Ketzinel-Gilad M, Ariav Y, Pappo O, Karaca M, Castel J, Berthault MF, Magnan C, Cerasi E, Kaiser N, Leibowitz G (2008) mTOR inhibition by rapamycin prevents β-cell adaptation to hyperglycemia and exacerbates the metabolic state in type 2 diabetes. *Diabetes*. 57: 945-957.

Freund TF, Buzsáki G (1996) Interneurons of the hippocampus. *Hippocampus.* 6: 347-470.

Frey LC (2003). Epidemiology of posttraumatic epilepsy: a critical review. Epilepsia 44: S11–S17.

Fricke RA and Prince DA (1984) Electrophysiology of dentate granule cells. *J Neurophysiol*. 51(2): 195-209.

Fritschy J-M, Kiener T, Bouilleret V, Loup F (1999) GABAergic neurons and $GABA_A$-receptors in temporal lobe epilepsy. *Neurochem Int.* 34:435–445.

Frotscher M, Zimmer J (1983a) Commissural fibers terminate on nonpyramidal neurons in the guinea pig hippocampus-a combined Golgi/EM degeneration study. Brain Res 265:289-293.

Frotscher M, Zimmer J (1983b) Lesion-induced mossy fibers to the inner molecular layer of the rat fascia dentata: identification of postsynaptic granule cells by the Golgi-EM technique. J Comp Neurol 215:299-311.

Galanopoulou A, Crino P, Wong M, Buckmaster P, Raffo E (2010) Rapamycin: from tuberous sclerosis and beyond. [Abstract] *Epilepsia* 50 (s7).

Gao H, Smith BN (2010) Tonic GABAA receptor-mediated inhibition in the rat dorsal motor nucleus of the vagus. *J Neurophysiol.* 103: 904-914.

Garrido C, Galluzzi L, Brunet M, Puig PE, Didelot C, Kroemer G (2006) Mechanisms of cytochrome c release from mitochondria. *Cell Death and Differentiation.* 13: 1423-1433.

Golarai G, Greenwood AC, Feeney DM, Connor JA (2001) Physiological and structural evidence for hippocampal involvement in persistent seizure susceptibility after traumatic brain injury. J. Neurosci. 21(21):8523-37.

Goldsmith W (1966) The physical processes producing head injury. In: Head Injury, Conference Proceedings (Cavaness WF, Walker AE, eds). Philadelphia: Lippincott.

Goodman JC, Cherian L, Bryan Jr RM, Robertson CS (1994) Lateral cortical impact injury in rats Pathologic effects of varying cortical compression and impact velocity, *J Neurotrauma* **11:**587–597.

Grady MS, Charleston JS, Maris D, Witgen BM, Lifshitz J (2003) Neuronal and glial cell number in the hippocampus after experimental traumatic brain injury: analysis by stereological estimation. *J Neurotrauma* 20: 929-941.

Graham DI, Saatman KE, Marklund N, Conte V, Morales D, Royo N, McIntosh TK (2006) Neuropathology of Trauma. In: Neurology and Trauma, 2nd ed (Evans RW, ed.) New York. Oxford University Press. pp.45-94.

Griesemer D, Mautes AM (2007) Closed head injury causes hyperexcitability in rat hippocampal CA1 but not in CA3 pyramidal cells. J Neurotrauma 24:1823-32.

Gurkoff GG, Giza CC, Shin D, Auvin S, Sankar R, Hovda DA (2009) Acute neuroprotection to pilocarpine-induced seizures is not sustained after traumatic brain injury in the developing rat. Neurosci. 164:862-876.

Halabisky B, Shen F, Huguenard JR, Prince DA (2006) Electrophysiological classification of somatostatin-positive interneurons in mouse sensorimotor cortex. *J Neurophysiol*. 96:834-845.

Halasy K, Somogyi P (1993b) Subdivisions in the multiple GABAergic innervation of granule cells in the dentate gyrus of the rat hippocampus. Eur J Neurosci 5:411-429.

Hall ED, Sullivan PG, Gibson TR, Pavel KM, Thompson BM, Scheff SW (2005) Spatial and temporal characteristics of neurodegeneration after controlled cortical impact in mice: more than a focal brain injury. *J Neurotrauma*. 22(2):252-65.

Hall ED, Bryant YD, Cho W, Sullivan PG (2008) Evolution of post-traumatic neurodegeneration after controlled cortical impact traumatic brain injury in mice and rats as assessed by the de Olmos silver and fluorojade staining methods. J Neurotrauma. 25:235-247.

Haltiner AM, Temkin NR, Dikmen SS (1997) Risk of seizure recurrence after the first late posttraumatic seizure. *Arch Phys Med Rehabil*. 78:835-840.

Han ZS, Buhl EH, Lorinczi Z, Somogyi P (1993) A high degree of spatial selectivity in the axonal and dendritic domains of physiologically identified local-circuit neurons in the dentate gyrus of the rat hippocampus. Eur J Neurosci. 5:395-410.

Hannay HJ, Feldman z, Phan P, Keyani A, Panwar N, Goodman JC, Robertson CS (1999) Validation of a controlled cortical impact model of head injury in mice. J Neurotrauma 16:1103-1114.

Hauser WA, Annegers JF, Kurland LT (1991) Prevalence of epilepsy in Rochester, Minnesota: 1940-1980. *Epilepsia* 32: 429-445.

Hauser WA, Hesdorffer DC (1990) Epilepsy: frequency, causes, and consequences. New York: Demos.

Heinemann U, Beck H, Dreier JP, Ficker E, Stabel J, Zhang CL (1992) The dentate gyrus as a regulated gate for the propagation of epileptiform activity. *Epilepsy Res. Suppl.* **7**:273–280.

Hellier JL, Patrylo PR, Buckmaster PS, Dudek FE (1998) Recurrent spontaneous motor seizures after repeated low-dose systemic treatment with kainate: assessment of a rat model of temporal lobe epilepsy. *Epilepsy Res.* 31:73-84.

Hennis A, Corbin D, Fraser H (1992) Focal seizures and non-ketotic hyperglycaemia. *J Neurol Neurosurg Psychiatry.* 55:195-197.

Herman ST (2002) Epilepsy after brain insult: targeting epileptogenesis. *Neurology* 59: S21–S26.

Hirota K, Roth SH (1997). The effects of sevoflurane on population spikes in CA1 and dentate gyrus of the rat hippocampus in vitro. Anesth Analg. 85:426-30.

Hirsch JC, Agassandian C, Merchán-Pérez A, Ben-Ari Y, DeFelipe J, Esclapez M, Bernard C (1999) Deficit of quantal release of GABA in experimental models of temporal lobe epilepsy.

Holtzman DM, Lowenstein DH. (1995) Selective inhibition of axon outgrowth by antibodies to NGF in a model of temporal lobe epilepsy. *J Neurosci* 15:7062–7070

Houser CR (1990) Granule cell dispersion in the dentate gyrus of humans with temporal lobe epilepsy. Brain Res. 535:195-204.

Houser CR, Esclapez M (2003) Downregulation of the α5 subunit of the $GABA_A$ receptor in the pilocarpine model of temporal lobe epilepsy. *Hippocampus* 13:633–645.

Houser CR, Miyashiro JE, Swartz BE, Walsh GO, Rich JR, Delgado-Escueta AV (1990) Altered patterns of dynorphin immunoreactivity suggest mossy fiber reorganization in human hippocampal epilepsy. *J Neurosci.* 10:267-282.

Hsu D (2007) The dentate gyrus as a filter or gate: a look back and a look ahead. Prog Brain Res. 163:601-613.

Hudak AM, Trivedi K, Harper CR, Booker K, Caesar RR, Agostini M, Van Ness PC, Diaz-Arrastia R (2004) Evaluation of seizure-like episodes in survivors of moderate and severe traumatic brain injury. J Head Trauma Rehabil. 19: 290-295.

Hunt RF, Scheff SW, Smith BN (2009) Posttraumatic epilepsy after controlled cortical impact injury in mice. Exp Neurol. 215(2): 243-252.

Hunt RF, Scheff SW, Smith BN (2010) Regionally localized recurrent excitation in the dentate gyrus of a cortical contusion model of posttraumatic epilepsy. J Neurophysiol.

Hudak AM, Trivedi K, Harper CR, Booker K, Caesar RR, Agostini M, Van Ness PC, Diaz-Arrastia R (2004) Evaluation of seizure-like episodes in survivors of moderate and severe traumatic brain injury. *J Head Trauma Rehabil* 19:290-295.

Iijima T, Witter MP, Ichikawa M, Tominaga T, Kajiwara R, Matsumoto G (1996) Entorhinal-hippocampal interactions revealed by real-time imaging, *Science* 272: 1176–1179.

Ikegaya Y. (1999) Abnormal targeting of developing hippocampal mossy fibers after epileptiform activities via L-type Ca^{2+} channel activation in vitro. *J Neurosci* 19: 802–812.

Ikegaya Y, Nishiyama N, Matsuki N. (2000) L-type Ca^{2+} channel blocker inhibits mossy fiber sprouting and cognitive deficits following pilocarpine seizures in immature mice. *Neuroscience* 98: 647–659.

Ingram EA, Toyoda I, Wen X, Buckmaster PS (2009) Prolonged infusion of inhibitors of calcineurin or L-type calcium channels does not block mossy fiber sprouting in a model of temporal lobe epilepsy. *Epilepsia.* 50:56-64.

Ishizuka N, Weber J, Amaral DG (1990) Organization of intrahippocampal projections originating from CA3 pyramidal cells in the rat. J Comp Neurol. 295:580-623.

Jiao Y, Nadler JV (2007). Stereological analysis of GluR2-immunoreactive hilar neurons in the pilocarpine model of temporal lobe epilepsy: correlation of cell loss with mossy fiber sprouting. Exp Neurol 205:569-82.

Johansen FF, Zimmer J, Diemer NH (1987) Early loss of somatostin neurons in dentate hilus after cerebral ischemia in the rat precedes CA-1 pyramidal cell loss. *Acta Neuropathol*. 73:110-114.

Jones DL, Baraban SC (2007) Characterization of inhibitory circuits in the malformed hippocampus of Lis1 mutant mice. *J Neurophysiol.* 98(5):2737-46.

Jones MV, Westbrook GL (1996) Impact of receptor desensitization on fast synaptic transmission. *Trends in Neurosci.* 19: 96-101.

Kampfl A, Posmantur RM, Zhao X, Schmutzhard E, Clifton GL, Hayes RL (1997) Mechanisms of calpain proteolysis following traumatic brain injury: implications for pathology and therapy: a review and update. *J Neurotrauma.* 14: 121-34.

Katona I, Acsády L, Freund TF (1999) Postsynaptic targets of somatostatin-immunoreactive interneurons in the rat hippocampus. *Neurosci.* 88(1):37-55.

Keller BU, Konnerth A, Yaari Y (1991) Patch clamp analysis of excitatory synaptic currents in granule cells of rat hippocampus. *J Physiol*. 435:275-293.

Kharatishvili I, Immonen R, Gröhn O, Pitkänen A (2007) Quantitative diffusion MRI of hippocampus as a surrogate marker for post-traumatic epileptogenesis. *Brain.* 130: 3155-3158.

Kharatishvili I, Nissinen JP, McIntosh TK, Pitkänen A (2006) A model of posttraumatic epilepsy induced by lateral fluid-percussion brain injury in rats. Neuroscience. 140:685-97.

Kirby MT, Hampson RE, Deadwyler SA (1995) Cannabinoids selectively decrease paired-pulse facilitation of perorant path synaptic potentials in the dentate gyrus in vitro. Brain Res. 688:114-120.

Klee CB, Crouch TH, Krinks MH. (1979) Calcineurin: a calcium- and calmodulin-binding protein of the nervous system. *Proc Natl Acad Sci* 76: 6270–6273.

Kneisler TB, Dingledine R (1995) Synaptic input from CA3 pyramidal cells to dentate basket cells in rat hippocampus. J Physiol. 487 (Pt.1): 125-146.

Kobayashi M, Buckmaster PS (2003) Reduced inhibition of dentate granule cells in a mouse model of temporal lobe epilepsy. *J Neurosci.* 23(6): 2440-2452.

Kochanek PM, Vagni VA, Janesko KL, Washington CB, Crumrine PK, Garman RH, Jenkins LW, Clark RS, Homanics GE, Dixon CE, Schnermann J, Jackson EK (2006) Adenosine A1 receptor knock-out mice develop lethal status epilepticus after experimental traumatic brain injury. J Cerebral Blood Flow Met 26:565-575.

Kotti T, Reikkinen PJ, Miettinen R (1997) Characterization of target cells for aberrant mossy fiber collaterals in the dentate gyrus of epileptic rat. Exp Neurol. 146(2):323-30.

Kroemer G, Reed JC (2000) Mitochondrial control of cell death. Nat Med. 6:513-519.

Laurer H, Lenzlinger PM, McIntosh TK (2000) Modles of traumatic brain injury. Eur J Trauma. 26: 95-100.

Lautermilch NJ, Spitzer NC. (2000) Regulation of calcineurin by growth cone calcium waves controls neurite extension. *J Neurosci* 20: 315–325.

Lavadas AA, Grigoriou M, Pachnis V, Parnavelas JG (1999) The medial ganglionic eminence gives rise to a populayion of early neurons in the developing cerebral cortex. J Neurosci. 19:7881-7888.

Lechner HAE, Lein ES, Callaway EM (2002) A genetic method for selective and quickly reversible silencing of mammalian neurons. J Neurosci. 22: 5287-5290.

Leranth C, Malcolm AJ, Frotscher M (1990) Afferent and efferent synaptic connections of somatostatin-immunoreactive neurons in the rat fascia dentata. *J Comp Neurol.* 295:111-122.

Lewin GR, Barde YA (1996) Physiology of the neurotrophins. *Ann Rev Neurosci.* 19: 289-317.

Lewis FT (1922) The significance of the term hippocampus. J Comp Neurol 35:213–230.

Lifshitz J (2009) Fluid percussion injury model, Ch 32. In: Animal models of acute neurological injuries (Chen J, Xu ZC, Xu XM, Zhang JH, eds.). Totowa, NJ: Humana Press. pp. 369-384.

Lighthall, JW (1988). Controlled cortical impact: a new experimental brain injury model. *J Neurotrauma* 5:1-15.

Li X-G, Somogyi P, Ylinen A, Buzsáki G (1994) The hippocampal CA3 network: an in vivo intracellular labeling study. J Comp Neurol. 339:181-208.

Longo BM, Mello LEAM (1997) Blockade of pilocarpine- or kainite-induced mossy fiber sprouting by cycloheximide does not prevent subsequent epileptogenesis in rats. Neurosci Lett. 226:163-166.

Lorente de No R (1934) Studies on the structure of the cerebral cortex. II. Continuation of the study of the ammonic system. *J. Psychol. Neurol.* 46: 113-177.

Lothman EW, Bertram III EH, Stringer JL (1991) Functional anatomy of hippocampal seizures. *Prog Neurobiol.* 37:1-82.

Lothman EW, Stringer JL, Bertram III EH (1992) The dentate gyrus as a control point for seizures in the hippocampus and beyond, *Epilepsy Res. Suppl.* **7**:301–313.

Loup F, Wieser HG, Yonekawa Y, Aguzzi A, Fritschy J-M (2000) Selective alterations in $GABA_A$ receptor subtypes in human temporal lobe epilepsy. J Neurosci 20: 5401–5419.

Lowenstein DH, Seren MS, Longo FM (1993) Prolonged increases in neurotrophic activity associated with kainite-induced hippocampal synaptic reorganization. *Neurosci.* 56:597-604.

Lowenstein DH, Thomas MJ, Smith DH, McIntosh TK (1992) Selective vulnerability of dentate hilar neurons following traumatic brain injury: a potential mechanistic link between head trauma and disorders of the hippocampus. *J Neurosci*. 12:4846–4853.

Lynch M, Sutula T (2000) Recurrent excitatory connectivity in the dentate gyrus of kindled and kainic acid-treated rats. J. Neurophysiol. 83:693-04.

Lytton WW, Sejnowski TJ (1991) Simulations of cortical pyramidal neurons synchronized by inhibitory interneurons. J Neurophysiol. 66:1059-1079.

Maglóczky Z (2010) Sprouting in human temporal lobe epilepsy: Excitatory pathways and axons of interneurons. Epilepsy Res. doi:10.1016/j.eplepsyres.2010.01.002.

Mangin JM, Kunze A, Chittajallu R, Gallo V (2008) Satellite NG2 progenitor cells share common glutamatergic inputs with associated interneurons in the mouse dentate gyrus. J Neurosci. 28(30):7610-23.

Marcinkiewicz M, Nagao T, Day R, Seidah NG, Chretein M, Avoli M (1997) Pilocarpine-induced seizures are accompanied by a transient elevation in the messenger RNA expression of the prohormone convertase PC1 in rat hippocampus: comparison with nerve growth factor and brain-derived neurotrophic factor expression. Neurosci. 76: 425-439.

Marmarou CR, Prieto R, Taya K, Young HF, Marmarou A (2009) Marmarou weight drop injury model, Ch 34. In: Animal models of acute neurological injuries (Chen J, Xu ZC, Xu XM, Zhang JH, eds.). Totowa, NJ: Humana Press.

Mathern GW, Babb TL, Micevych PE, Blanco CE, Pretorius JK (1997) Granule cell mRNA levels for BDNF, NGF, and NT-3 correlate with neuron losses or supragranular mossy fiber sprouting in the chronically damaged and epileptic human hippocampus. *Mol Chem Neuropathol.* 30: 53-76.

Mathern GW, Babb TL, Pretorius JK, Leite JP (1995) Reactive synaptogenesis and neuron densities for neuropeptide Y, somatostatin, and glutamate decarboxylase immunoreactivity in the epileptogenic human fascia dentata. *J Neurosci*. 15:3990-4004.

Matsumota AH, Ajmone-Marsan C (1964a) Cortical cellular phenomena in experimental epilepsy: interictal manifestations. *Exp Neurol*. 9:286-304.

Matsumota AH, Ajmone-Marsan C (1964b) Cortical cellular phenomena in experimental epilepsy: ictal manifestation. *Exp Neurol*. 9:305-326.

McBain CJ, Fisahn A (2001) Interneurons unbound. *Nat Rev Neurosci.* 2:11-23.

McCormick DA, Contreras D (2001) On the cellular and network bases of epileptic seizures. *Annu Rev Physiol.* 63:815-846.

McLean AJ, Anderson RWG (1997) Biomechanics of closed head injury. In: *Head Injury*. (Reilly P, Bullock R, eds.). London: Chapman & Hall. pp 25-37.

McNamara JO (1994) Cellular and molecular basis of epilepsy. *J Neurosci.* 14:3413-3425.

McNamara JO (2006) Molecular signalling mechanisms underlying epileptogenesis. *Sci STKE*. 2006(356): re12.

Meldrum BS, Akbar MT, Chapman AT (1999) Glutamate receptors and transporters in genetic and acquired models of epilepsy. *Epilepsy Res*. 36(2-3):189-204.

Mendelow DA, Crawford PJ (1997) Primary and secondary brain injury. In: *Head Injury*. (Reilly P, Bullock R, eds.). London: Chapman & Hall. pp 71-88.

Miles R, Tóth K, Gulyás AI,k Hájos N, Freund TF (1996) Differences between somatic and dendritic inhibition in the hippocampus. Neuron. 16:815-823.

Miles R, Wong RKS, Traub RD (1986) Synchronized afterdischarges in the hippocampus: contribution of local synaptic interactions. *Neurosi*. 12(4):1179-89.

Miles R and Wong RKS (1987). Inhibitory control of local excitatory circuits in the guinea-pig hippocampus. *J Physiol*. 388:611-629.

Miles R and Wong RKS (1983). Single neurons can initiate synchronized population discharge in the hippocampus. *Nature*. 306:397-418.

Mohler H (2006) $GABA_A$ receptor diversity and pharmacology. *Cell Tissue Res.* 326: 505-516.

Moia LJMP, Matsui H, de Barros GAM, Tomizawa K, Miyamoto K, Kuwata Y, Tokuda M, Itano T, Hatase O. (1994) Immunosuppressants and calcineurin inhibitors, cyclosporin A and FK506, reversibly inhibit epileptogenesis in amygdaloid kindled rat. *Brain Res* 648: 337–341.

Molnar P, Nadler JV (1999) Mossy fiber-granule cell synapses in the normal and epileptic rat dentate gyrus studied with minimal laser photostimulation. *J Neurophysiol*. 82:1883-94.

Morgan TA, Soltesz I (2008) Nonrandom connectivity of the epileptic dentate gyrus predicts a major role for neuronal hubs in seizures. Proc. Natl. Acad. Sci. 105:6179-6184.

Moriwaki A, Lu Y-F, Hayashi Y, Tomizawa K, Tokuda M, Itano T, Hatase O, Matsui H. (1996) Immunosuppressant FK506 prevents mossy fiber sprouting induced by kindling stimulation. *Neurosci Res* 25: 191–194.

Mtchedlishvili Z, Kapur J (2006) High-affinity, slowly desensitizing $GABA_A$ receptors mediate tonic inhibition in hippocampal dentate granule cells. *Mol Pharmacol.* 69: 564-575.

Mtchedlishvili Z, Kharlamov E, Lu B, Kelly KM (2008a) Altered of GABAAR-mediated tonic and phasic inhibition and δ subunit-containing receptor expression in hippocampal dentate granule cells after traumatic brain injury. [Abstract] *Epilepsia.*

Mtchedlishvili Z, Kharlamov E, Lu B, Kelly KM (2008b) Increase of $GABA_A$ receptor-mediated tonic inhibition in hippocampal dentate granule cells after traumatic brain injury. [Abstract]. *Soc Neurosci Abstr*. 34:647.17.

Mtchedlishvili Z, Lepsveridze E, Xu H, Kharlamov E, Lu B, Kelly KM (2010) Increase of $GABA_A$ receptor-mediated tonic inhibition in dentate granule cells after traumatic brain injury. *Neurobiol Dis.* doi:10.1016/j.nbd.2010.03.012.

Murray KD, Roper SN, Eskin TA, King MA (1997) Altered mRNA expression for brain-derived neurotrophic factor and calcium/calmodulin-dependent protein kinase type II in hippocampi from patients with intractable temporal lobe epilepsy. *Epilepsia.* 35 (s8): 65.

Nadler JV (2003) The recurrent mossy fiber pathway of the epileptic brain. *Neurochem Res.* 28:1649-1658.

Nadler, J.V., Perry, B.W., Cotman, C.W. (1980) Selective reinnervation of hippocampal area CA1 and the fascia dentata after destruction of CA3-CA4 afferents with kainic acid. Brain Res. 182:1-9.

Nusser Z, Mody I (2002) Selective modulation of tonic and phasic inhibitions in dentate gyrus granule cells. J Neurophysiol 87:2624–2628.

Nilsson P, Ronne-Engstrom E, Flink R, Ungersted U, Carlson H, Hillered L (2004) Epileptic seizure activity in the acute phase following cortical impact trauma in rat. Brain Res 637:227–232.

Nusser Z, Sieghart W, Somogyi P (1998) Segregation of different $GABA_A$ receptors to synaptic and extrasynaptic membranes of cerebellar granule cells. *J Comp Neurol* 18:1693–1703.

Obenaus A, Esclapez M, Houser CR (1993) Loss of glutamate decarboxylase mRNA-containing neurons in the rat dentate gyrus following pilocarpine-induced seizures. *J Neurosci*. 13:4470–4485.

Okada M, Onodera K, Renterghem CV, Sieghart W, Takahashi T (2000) Functional correlation of GABAA receptor α subunits expression with the properties of IPSCs in the developing thalamus. *J Neurosci.* 20: 2202-2208.

Okazaki MM, Evenson DA, Nadler JV (1995) Hippocampal mossy fiber sprouting and synapse formation after status epilepticus in rats: visualization after retrograde transport of biocytin. J Comp Neurol 352:515-534.

Oliva AA Jr, Jiang M, Lam TT, Smith KL, Swann JW (2000) Novel hippocampal interneuronal subtypes identified using transgenic mice that express green fluorescent protein in GABAergic interneurons. *J Neurosci.* 20: 3354-3368.

Olry R, Haines DE (1998) Cerebral mythology: a skull stuffed with gods. Journal of the History of the Neurosciences **7**:82–83.

Patel M (2004) Mitochondrial dysfunction and oxidative stress: cause and consequence of epileptic seizures. *J Free Rad Biomed.* 37: 1951-1962.

Patrylo, PR, Dudek, FE (1998) Physiological unmasking of new glutamatergic pathways in the dentate gyrus of hippocampal slices from kainate-induced epileptic rats. J. Neurophysiol. 79:418-429.

Patrylo PR; Browning RA; Cranick S (2006) Reeler homozygous mice exhibit enhanced susceptibility to epileptiform activity. *Epilepsia* 47:257-266.

Pavlov I, Huusko N, Nissinen J, Sperk G, Pitkänen A, Walker MC (2009) Phasic but not tonic inhibition is decreased in dentate gyrus granule cells in fluid-percussion brain

injury model of posttraumatic epilepsy in rats. [Abstract] *Soc for Neurosci Abstr.* 35:241.3

Pearce RA (1993) Physiological evidence for two distinct $GABA_A$ responses in rat hippocampus. *Neuron.* 10:189-200.

Peng Z, Huang CS, Stell BM, Mody I, Houser CR (2004) Altered expression of the δ subunit of the $GABA_A$ receptor in a mouse model of temporal lobe epilepsy. *J Neurosci* 24:8629–8639.

Pitkanen A and McIntosh TK (2006) Animal models of posttraumatic epilepsy. *J Neurotrauma*. 23(2): 241-61.

Pitkanen A, Sutula TP (2002) Is epilepsy a progressive disorder? Prospects for new therapeutic approaches in temporal lobe epilepsy. *Lancet Neurol* 1:173-181.

Porter AG, Jänicke RU (1999) Emerging roles of caspase-3 in apoptosis. *Cell Death and Differentiation.* 6:99-104.

Racine RJ (1972) Modification of seizure activity by electrical stimulation: II. Motor seizures. Electrorencephalogr. Clin. Neurophysiol. 32, 281–294.

Raghupathi R, Graham DI, McIntosh TK (2000) Apoptosis after traumatic brain injury. *J Neurotrauma.* 17: 927-938.

Ramón y Cajal S (1995) General Organization of the Cortex. In: Histology of the Nervous System of Man and Vertebrates, Vol 2 (Swanson N, Swanson LW, translators). New York: Oxford University Press.

Ramos B, Baglietto-Vargas D, del Rio JC, Moreno-Gonzalez I, Santa-Maria C, Jimenez S, Caballero C, Lopez-Tellez JF, Khan ZU, Ruano D, Gutierrez A, Vitorica J (2006) Early neuropathology of somatostatin/NPY GABAergic cells in the hippocampus of a PS1 x APP transgenic model of Alzheimer's disease. *Neurobiol Ag.* 27:1658-1672.

Ribak CE, Nitsch R, Seress L (1990) Proportion of parvalbumin-positive basket cells in the GABAergic innervations of pyramidal and granule cells of the rat hippocampal formation. *J Comp Neurol.* 300:449-461.

Ribak CE, Seress L, Amaral DG (1985) The development, ultrastucture and synaptic connections of the mossy cells of the dentate gyrus. *J Neurocytol.* 14:835-857.

Ribak CE, Seress L (1983) Five types of basket cells in the hippocampal dentate gyrus; a combined Golgi and electron microscopic study. *J Neurocytol.* 12:577-597.

Rice A, Rafiq A, Shapiro SM, Jakoi ER, Coulter DA, DeLorenzo RJ (1996) Long-lasting reduction of inhibitory function and gamma-aminobutyric acid type A receptor subunit mRNA expression in a model of temporal lobe epilepsy. *Proc Natl Acad Sci* USA 93:9665–9669.

Reeves TM, Lyeth BG, Phillips LL, Hamm RJ, Povlishock JT (1997) The effects of traumatic brain injury on inhibition in the hippocampus and dentate gyrus. *Brain Res.* 1:119-132.

Rola R, Mizumatsu S, Otsuka S, Morhardt DR, Noble-Haeusslein LJ, Fishman K, Potts MB, Fike JR (2006) Alterations in hippocampal neurogenesis following traumatic brain injury in mice. Exp Neurol. 202:189-199.

Rosene DL, van Hosen GW (1987) The hippocampal formation of the primate brain. A review of some comparative aspects of cytoarchitecture and connections. In: Cerebral Cortex: Further Aspects of Cortical Function, Including Hippocampus, Vol. 6. (Jones EG, Peters A, eds.). Plenum Press: New York. pp. 345-457.

Roux PP, Colicos MA, Barker PA, Kennedy TE (1999) p75 neurotrophin receptor expression is induced in apoptotic neurons after seizure. *J Neurosci.* 19: 6887-6896.

Rudge JS, Mather PE, Pasnikowski EM, Cai N, Corcoran T, Acheson A, Anderson K, Lindsay RM, Wiegand SJ (1998) Endogenous BDNF protein is increased in adult rat hippocampus after a kainic acid induced excitotoxic insult but exogenous BDNF is not neuroprotective. *Exp Neurol.* 149: 398-410.

Saatman KE, Duhaime AC, Bullock R, Maas AI, Valadka A, Manley GT; Workshop Scientific Team and Advisory Panel Members (2008) Classification of traumatic brain injury for targeted therapies. *J Neurotrauma*. 25:719-38.

Saatman KE, Feeco KJ, Pape RL, Raghupathi R (2006) Differential behavioral and histopathological responses to graded cortical impact injury in mice. *J Neurotrauma* 23:1241-1253.

Salazar AM, Jabbari B, Vance SC, Grafman J, Amin D, Dillon JD (1985) Epilepsy after penetrating head injury. I. Clinical correlates: a report of the Vietnam Head Injury Study. *Neurology*. 1985 35:1406-14.

Salin P, Tseng GF, Hoffman S, Parada I, Prince DA (1995) Axonal sprouting in layer V pyramidal neurons of chronically injured cerebral cortex. *J Neurosci.* 15(2)8234-45.

Santhakumar V, Bender R, Frotscher M, Ross ST, Hollrigel GS, Toth Z, Soltesz I (2000) Granule cell hyperexcitability in the early post-traumatic rat dentate gyrus: the 'irritable mossy cell' hypothesis. *J Physiol.* 524 (Pt1): 117-134.

Santhakumar V, Ratzliff ADH, Jeng J, Toh Z, Soltesz I (2001) Long-term hyperexcitability in the hippocampus after experimental head trauma. Ann Neurol 50:708-717.

Santoshkumar B, Chong JJ, Blume WT, McLachlan RS, Young GB, Diosy DC, Burneo JG, Mirsattari SM (2009) Prevelence of benign epileptiform variants. *Clin Neurophysiol.* 120: 856-861.

Sato K, Kashihara K, Morimoto K, Hayabara T (1996) Regional increases in brain-derived neurotrophic factor and nerve growth factor mRNAs during amygdaloid kindling, but not in acidic and basic fibroblast growth factor mRNAs. *Epilepsia.* 37:6-14.

Scharfman HE (1995) Electrophysiological evidence that dentate hilar mossy cells are excitatory and innervate both granule cells and interneurons. *J Neurophysiol*. 74(1):179-94.

Scharfman HE, Sollas AL, Berger RE, Goodman JH (2003) Electrophysiological evidence of monosynaptic excitatory transmission between granule cells after seizure-induced mossy fiber sprouting. *J Neurophysiol* 90:2536-2547.

Scharfman HE, Schwartzkroin PA (1990) Responses of cells of the rat fascia dentate to prolonged stimulation of the perforant path: sensitivity of hilar cells and changes in granule cell excitability. *Neurosci.* 35:491-504.

Scharfman HE (2007) The CA3 "backprojection" to the dentate gyrus. *Prog Brain Res.* 163: 627-637.

Scheff SW, Baldwin SA, Brown RW, Kraemer PJ (1997) Morris water maze deficits in rats following traumatic brain injury: lateral controlled cortical impact. *J Neurotrauma* 14:615-627.

Scheff SW, Price DA, Hicks RR, Baldwin SA, Robinson S, Brackney C (2005). Synaptogenesis in the Hippocampal CA1 Field following Traumatic Brain Injury. J Neurotrauma 22:719-32

Schubert D, Staiger JF, Cho N, Kotter R, Ziles K, Luhmann HJ (2001) Layer-specific intracolumnar and transcolumnar functional connectivity of layer V pyramidal cells in rat barrel cortex. J Neurosci. 21: 3580-92.

Schwarzer C, Tsunashima K, Wanzenbock C, Fuchs K, Sieghart W, Sperk G (1997) $GABA_A$ receptor subunits in the rat hippocampus II: altered distribution in kainic acid-induced temporal lobe epilepsy. *Neuroscience* 80:1001–1017.

Schwartzkroin PA, Prince DA (1978) Cellular and field potential properties of epileptogenic hippocampal slices. *Brain Res.* 147:117-130.

Scoville WB, Milner B (1957) Loss of recent memory after bilateral hippocampal lesions. *J Neurol Neurosurg Psychiatry*. 20:11-21.

Semah F, Picot MC, Adam C, Broglin D, Arzimanoglou A, Bazin B, Cavalcanti D, Baulac M (1998) Is the underlying cause of epilepsy a major prognostic factor for recurrence? *Neurology.* 51:1256-1262.

Seress L, Ribak CE (1984) Direct commissural connections to the basket cells of the hippocampal dentate gyrus: anatomical evidence for feed-forward inhibition. *J Neurocytol.* 13:215-225.

Shao LR, Dudek FE (2005a) Changes in mIPSCs and sIPSCs after kainite treatment: evidence for loss of inhibitory input to dentate granule cells and possible compensatory responses. *J Neurophysiol.* 94:952-960.

Shao LR, Dudek FE (2005b) Detection of increased local excitatory circuits in the hippocampus during epileptogenesis using focal flash photolysis of caged glutamate. *Epilepsia.* 46(s5): 100-106.

Shibley H, Smith BN (2002) Pilocarpine-induced status epilepticus results in mossy fiber sprouting and spontaneous seizures in C57BL/6 and CD-1 mice. Epilepsy Res., 49:109-120.

Shima K, Marmarou A (1991) Evaluation of brain-stem dysfunction following severe fluid-percussion head injury to the cat. *J Neurosurg.* 74: 270-277.

Shumate M, Rafiq A, Lyeth B, Gong QZ, Coulter DA (1995) Traumatic brain injury produces loss of neurons in hilus and CA3 but no significant mossy fiber sprouting in hippocampus. Epilepsia. 36(S4):118.

Sieghart, W (2000) Unraveling the function of $GABA_A$ receptor subtypes. *Trends in Pharm Sci.* 21: 411-413.

Sloviter RS, Zappone CA, Harvey BD, Bumanglag AV, Bender RA, Frotscher M (2003) "Dormant basket cell" hypothesis revisited:relative vulnerabilities of dentate gyrus mossy cells and inhibitory interneurons after hippocampal status epilepticus in the rat. *J comp Neurol.* 459:44-76.

Sloviter RS (1987) Decreased hippocampal inhibition and a selective loss of interneurons in experimental epilepsy. *Science.* 269:977-981.

Sloviter RS (1991) Permanently altered hippocampal structure, excitability, and inhibition after experimental status epilepticus in the rat: the "dormant basket cell" hypothesis and its possible relevance to temporal lobe epilepsy. Hippocampus. 1(1):41-66.

Sloviter RS (1992) Possible functional consequences of synaptic reorganization in the dentate gyrus of kainite-treated rats. Neurosci Lett. 137:91-96.

Sloviter RS (1994) On the relationship between neuropathology and pathophysiology in the epileptic hippocampus of humans and experimental animals. Hippocampus. 4:250-253.

Smith and Dudek (2002) Network interactions mediated by new excitatory connections between CA1 pyramidal cells in rats with kainite-induced epilepsy. *J Neurophysiol* 87:1655-1658.

Smith BN, Dudek FE (2001) Short- and long-term changes in CA1 network excitability after kainate treatment in rats. J Neurophysiol 85:1-9.

Smith DH, Soares HD, Pierce JES, Perlman KG, Saatman KE, Meaney DF, Dixon CE, McIntosh TK (1995) A model of parasagittal controlled cortical impact in the mouse cognitive and histopathologic effects, J Neurotrauma 12:169-178.

Soltesz I, Smetters DK, Mody I (1995) Tonic inhibition originates from synapses at the soma. Neuron. 14:1273-1283.

Soriano E, Frotscher M (1993) GABAergic innervation of the rat fascia dentata: a novel type of interneuron in the granule cell layer with extensive axonal arborization in the molecular layer. *J Comp Neurol.* 334:385-396.

Soriano E, Frotscher M (1989) A GABAergic axo-axonic cell in the fascia dentata controls the main excitatory hippocampal pathway. *Brain Res.* 503:170-174.

Spencer WA, Kandel ER (1961) Electrophysiology of hippocampal neurons. IV. Fast pre-potentials. J Neurophysiol. 24:272-285.

Staley KJ, Dudek FE (2006) Interictal spikes and epileptogenesis. *Epilepsy Curr*. 6:199-202.

Staley KJ, Otis TS, Mody I (1992) Membrane properties of dentate gyrus granule cells: Comparison of sharp microelectrodes and whole cell recordings. *J Neurophysiol*. 67(5): 1346-57.

Statler KD, Swank S, Abildskov T, Bigler ED, White HS (2008) Traumatic brain injury during development reduces minimal clonic seizure thresholds at maturity. *Epilepsy Res.* 80:163-170.

Statler KD, Scheerlinck P, Pouliot W, Hamilton M, White HS, Dudek FE (2009) A potential model of pediatric posttraumatic epilepsy. *Epilepsy Res.* 86(2-3): 221-3.

Steinlein OK (2004) Genetic mechanisms that underlie epilepsy. *Nat Rev Neurosci*. 5(5):400-08.

Stringer JL, Lothman EW (1992) Reverberatory seizure discharges in hippocampal-parahippocampal circuits, *Exp. Neurol.* 116: 198–203.

Stringer JL, Williamson JM Lothman EW (1989) Induction of paroxysmal discharges in the dentate gyrus: frequency dependence and relationship to afterdischarge production, *J. Neurophysiol.* 62: 126–135.

Sullivan PG, Bruce-Keller AJ, Rabchevsky AG, Christakos S, St. Clair DK, Mattson MP, Scheff SW (1999) Exacerbation of damage and altered NFkB activation in mice lacking tumor necrosis factor receptors following traumatic brain injury. *J Neurosci* 19:6248-6256.

Sullivan PG, Rabchevsky AG, Waldmeier PC, Springer JE (2004) Mitochondrial permeability transition in CNS trauma: cause or effect of neuronal cell death? *J Neurosci Res.* 79: 231-239.

Sun C, Mtchedlishvili Z, Bertram EH, Erisir A, Kapur J (2007) Selectrive loss of dentate hilar interneurons contributes to reduced synaptic inhibition of granule cells in an

electrical stimulation-based animal model of temporal lobe epilepsy. J Comp Neurol. 500:876-893.

Sutula T, Cascino G, Cavazos J, Parada I, Ramirez L (1989) Mossy fiber synaptic reorganization in the epileptic human temporal lobe. Ann Neurol. 26:321-30.

Sutula TP, Dudek FE (2007) Unmasking recurrent excitation generated by mossy fiber sprouting in the epileptic dentate gyrus: an emergent property of a complex system. *Prog Brain Res.* 163:541-63.

Swanson TH, Sperlin MR, O'Connor MJ (1998). Strong paired pulse depression of dentate granule cells in slices from patients with temporal lobe epilepsy. *J Neural Transm* 105:613-625.

Swartz BE, Houser CR, Tomiyasu U, Walsh GO, DeSalles A, Rich JR, Delgado-Escueta A (2006) Hippocampal cell loss in posttraumatic human epilepsy. Epilepsia. 47 (8): 1373-82.

Szabadics J, Lorincz A, Tamás G (2001)β and γ frequency synchronization by dendritic GABAergic synapses and gap junctions in a network of cortical neurons. J Neurosci. 21: 5824-5831.

Szabadic Z, Soltesz I (2009) Functional specificity of mossy fiber innervations of GABAergic cells in the hippocampus. J Neurosci. 29(13): 4239-4251.

Takahashi M, Hayahi S, Kakita A, Wakabayashi K, Fukuda M, Kameyama S, Tanaka R, Takahashi H, Nawa H (1999) Patients with temporal lobe epilepsy show an increase in brain-derived neurotrophic factor protein and its correlation with neuropeptide Y. Brain Res. 818: 579-582.

Támas G, Buhl EH, Lörincz, Somogyi P (2000) Proximally targeted GABAergic synapses and gap junctions synchronize cortical interneurons. *Nat Neurosci.* 3:366-371.

Tauck DL, Nadler JV (1985) Evidence of functional mossy fiber sprouting in hippocampal formation of kainic acid-treated rats. *J. Neurosci*. 5:1016-1022.

Teasdale GM, Bannan PE (1997) Neuroprotection in head injury. In: *Head Injury*. (Reilly P, Bullock R, eds.). London: Chapman & Hall. pp 423-438.

Teasdale G, Jennett B (1976) Assessment and prognosis of coma after head injury. *Acta Neurochir.* 34: 45-55.

Temkin NR (2001) Antiepileptogenesis and seizure prevention trials with antiepileptic drugs meta-analysis of controlled trials, *Epilepsia* 42: 515–524.

Temkin NR, Dikmen SS, Winn HR (1998) Clinical trials for seizure prevention. Adv Neurol. 76:179-88.

Temkin NR (2009) Preventing and treating posttraumatic seizures: the human experience, *Epilepsia* 50(s2): 10-13.

Toth Z, Hollrigel GS, Gorcs T, Soltesz I (1997) Instantaneous perturbation of dentate interneuronal networks by a pressure wave-transient delivered to the neocrotex. *J Neurosci.* 17(21): 8106-8117.

Tóth K, Wittner L, Urbán Z, Doyle WK, Buzsáki G, Shigemoto R, Freund TF, Maglóczkzy Z (2007) Morphology and synaptic input of substance P receptor-immunoreactive interneurons in control and epileptic human hippocampus. *Neurosci.* 144:495-508.

Tong W, Igarashi T, Ferreiro DM, Noble LJ (2002) Traumatic brain injury in the immature mouse brain: characterization of regional vulnerability. *Exp Neurol.* 176:105-116.

Toyoda I, Buckmaster PS. (2005) Prolonged infusion of cycloheximide does not block mossy fiber sprouting in a model of temporal lobe epilepsy. *Epilepsia* 46: 1017–1020.

Traub RD and Wong RKS (1982) Cellular mechanisms of neuronal synchronization in epilepsy. *Science*. 216:745-47.

Traub RD and Wong RKS (1981) Penicillin induced epileptiform activity in the hippocampal slice: A model of synchronization of CA3 pyramidal cell bursting. *Neurosci*. 6:223-230.

Traumatic brain injury: hope through research (2009, March 15) Retrieved February 25, 2010, from National Institute of Neurological Disorders and Stroke.
Website: http://www.ninds.nih.gov/disorders/tbi/detail_tbi.htm

Tuff LP, Racine RJ, Adamec R (1983) The effects of kindling on GABA-mediated inhibition in the dentate gyrus of the rat. I. Paired pulse depression. *Brain Res* 277:79-90.

Teyler TJ, Alger BE (1976) Monosynaptic habituation in the vertebrate forebrain: the dentate gyrus examined in vitro, *Brain Res.* 115: 413–425.

Um SH, D'Alessio D, Thomas G (2006) Nutrient overload, insulin resistance, and ribosomal protein S6 kinase 1, S6K1. *Cell Metab*. 3: 393-402.

Vespa PM, Nuwer MR, Nenov V, Ronne-Engstrom E, Hovda DA, Bergsneider M, Kelly DF, Martin NA, Becker DP (1999) Increased incidence and impact of nonconvulsive and convulsive seizures after traumatic brain injury as detected by continuous electroencephalographic monitoring. J. Neurosurg., 91:750-60.

Waldbaum S, Dudek FE (2008) Increased paired-pulse suppression after slight increases in excitability or reductions in GABAA-receptor mediated inhibition: does the paired-pulse technique provide artifactual evidence for "hyperinhibition" during epileptogenesis? [Abstract] In: American Epilepsy Society National Meeting, 2007; Philadelphia, PA; *Epilepsia.*

Waldbaum S, Dudek FE (2007) Parametric assessment of the consistency of the paired-pulse protocol for studying hippocampal inhibition and hyperexcitability. [Abstract] In: Society for Neuroscience National Meeting, 2005; Washington, DC; *J Neurosci*; 276.12.

Wehr M, Hostick U, Kyweriga M, Tan A, Weible AP, Wu H, Wu W, Callaway EM, Kentros C. Transgenic silencing of neurons in the mammalian brain by expression of the allatostatin receptor (AlstR). *J Neurophysiol.* 102:2554-2562.

Wendling F, Bartolomei F, Bellanger JJ, Chauvel P (2002) Epileptic fast activity can be explained by a model of impaired GABAergic dendritic inhibition. *Eur J Neurosci.* 15:1499-1508.

Wenzel HJ, Woolley CS, Robbins CA, Schwartzkroin PA (2000) Kainic acid-induced mossy fiber sprouting and synapse formation in the dentate gyrus of rats. Hippocampus 10:244-260.

Wichterle H, Garcia-Verdugo JM, Herrera DG, Alvarez-Buylla A (1999) Young neurons from medial ganglionic eminence disperse in adult and embryonic brain. *Nat Neurosci.* 2: 461–466.

Williamson A, Spencer SS, Spencer DD (1995) Depth electrode studies and intracellular dentate granule cell recordings in temporal lobe epilepsy. Ann Neurol 38:778–787.

Williamson A, Patrylo PR, Spencer DD (1999) Decrease in inhibition in dentate granule cells from patients with temporal lobe epilepsy. Ann Neurol 45:92–99.

Williams PA, Wuarin JP, Dou P, Ferraro DJ, Dudek FE (2002) Reassessment of the effects of cycloheximide on mossy fiber sprouting and epileptogenesis in the pilocarpine model of temporal lobe epilepsy. *J Neurophysiol.* 88:2075-2087.

Willmore LJ (2006) Posttraumatic epilepsy. In: Neurology and Trauma, 2nd ed (Evans RW, ed.) New York. Oxford University Press. pp. 146-155.

Winokur RS, Kubal T, Liu D, Davis SF, Smith, BN (2004) Recurrent excitation in the dentate gyrus of a murine model of temporal lobe epilepsy. Epilepsy Res. 58:93-105.

Witgen BM, Lifshitz J, Smith ML, Schwarzbach E, Liang SL, Grady MS, Cohen AS (2005) Regional hippocampal alteration associated with cognitive deficit following experimental brain injury: a systems, network and cellular evaluation. *Neurosci*. 133:1-15.

Witter L, Henze DA, Záborszky L, Buzsáki G (2006) Hippocampal CA3 pyramidal cells selectively innervate aspiny interneurons. *Eur J Neurosci*. 24: 1286-1298.

Wong RKS, Prince DA (1981) Afterpotential generation in hippocampal pyramidal cells. J Neurophysiol. 45:86-97.

Wong RKS, Prince DA, Basbaum A (1979) Intradendritic recordings from hippocampal neurons. Proc. Natl. Acad. Sci. 76: 986-990.

Wuarin JP, Dudek FE (1996) Electrographic seizures and new recurrent excitatory circuits in the dentate gyrus of hippocampal slices from kainate-treated epileptic rat. J. Neurosci. 16:4438-4448.

Wuarin JP, Dudek FE (2001) Excitatory synaptic input to granule cells increases with time after kainate treatment. J. Neurophysiol. 85:1067-1077.

Yang K, Perez-Polo JR, Mu XS, Yan HQ, Xue JJ, Iwamoto Y, Liu SF, Dixon CE, Hayes RL (1996) Increased expression of brain-derived neurotrophic factor but not neurotrophin-3 mRNA in rat brain after cortical impact injury. *J Neurosci Res.* 44: 157-164.

Zhang N, Houser CR (1999) Ultrastructural localization of dynorphin in the dentate gyrus in human temporal lobe epilepsy: a study of reorganized mossy fiber synapses. *J Comp Neurol*. 405:472-490.

Zhang N, Wei W, Mody I, Houser CR (2007) Altered localization of $GABA_A$ receptor subunits on dentate granule cell dendrites influences tonic and phasic inhibition in a mouse model of epilepsy. *J Neurosci.* 27: 7520-7531.

Zhang W, Buckmaster PS (2009) Dysfunction of the dentate basket cell circuit in a rat model of temporal lobe epilepsy. *J Neurosci.* 29: 7846-7856.

Zhang W, Yamawaki R, Wen X, Uhl J, Diaz J, Prince DA, Buckmaster PS (2009) Surviving hilar somatostatin interneurons enlarge, sprout axons, and form new synapses with granule cells in a mouse model of temporal lobe epilepsy. *J Neurosci.* 29(45): 14247-14256.

Zhan RZ, Nadler JV (2009) Enhanced tonic GABA current in normotopic and hilar ectopic dentate granule cells after pilocarpine-induced status epilepticus. *J Neurophysiol.* 102: 670-81.

Zhu ZQ, Armstrong DL, Hamilton WJ, Grossman RG (1997) Disproportionate loss of CA4 parvalbumin-immunoreactive interneurons in patients with Ammon's horn sclerosis. *J Neuropathol Exp Neurol.* 56:988–998.

Zipp F, Nitsch R, Soriano E, Frotscher M (1989) Entorhinal fibers form synaptic contacts on pawalbumin-immunoreactive neurons in the rat fascia dentata. Brain Res 495:161-166.

Zola-Morgan S, Squire LR (1993) Neuroanatomy of memory. *Ann Rev Neurosci.* 16:547-563.

Vita
Robert F. Hunt, III

Born August 23, 1982; Portland, ME

EDUCATION

2006- *present* **PhD Candidate (Physiology)**
University of Kentucky Medical College, Lexington, KY
Advisor: Bret N. Smith, PhD
Thesis Committee: Stephen W. Scheff, PhD; Kathryn E. Saatman, PhD; Steven Estus, PhD

2005- 2006 **Doctoral Coursework**
Department of Cell & Molecular Biology
Tulane University, New Orleans, LA
Advisor: Bret N. Smith, PhD

Doctoral Coursework
Department of Anatomy & Neurobiology
Virginia Commonwealth University- Medical College of Virginia, Richmond, VA
Attendance due to Hurricane Katrina

2000- 2005 **BS (Biology with Chemistry Minor)**
Liberty University, Lynchburg, VA

SELECTED HONORS & AWARDS

2008	Epilepsy Foundation of America Pre-doctoral Fellowship; *Posttraumatic epileptiform activity following controlled cortical impact*
2008	Graduate Student Incentive Program Award, University of Kentucky Graduate School
2007-08	Student support travel awards, University of Kentucky Graduate
2001, 2002	Big South Conference Presidential Scholar
2001, 2002	Big South Track & Field All Conference
2000-2002	Liberty University Men's Cross Country, Indoor, and Outdoor Track & Field Teams
2000- 2005	Liberty University Academic Scholarship
2000	The Graustein Scholar Award
2000	Gretchen B. Hatch Memorial White Mountain Milers Scholarship

PUBLICATIONS

Manuscripts

Hunt RF, Scheff SW, Smith BN (2009). Posttraumatic epilepsy after controlled cortical impact injury in mice. *Exp Neurol*. 215 (2): 243-252.

Hunt RF, Scheff SW, Smith BN. (2010) Regionally localized recurrent excitation in the dentate gyrus of a cortical contusion model of posttraumatic epilepsy. *J Neurophysiol*. 103 (3): 1490-1500.

Submitted

Hunt RF, Scheff SW, Smith BN. Increased local excitatory input to hilar GABAergic interneurons accompanies reduced synaptic inhibition of granule cells after traumatic brain injury. Submitted to *J Neurosci*.

In Preparation

Hunt RF, Haselhorst LA, Bach EC, Rios-Pelier J, Schoch KM, Scheff SW, Saatman KE, and Smith BN. Region-specific mossy fiber sprouting is associated with the degree of cortical damage after controlled cortical impact injury. In preparation for *Epilepsia*.

Abstracts

Hunt RF, Scheff SW, Smith BN (2010) Excitatory input to hilar GABAergic interneurons is enhanced after traumatic brain injury. *Neurotrauma Soc Abstr*.

Hunt RF, Scheff SW, Smith BN (2009) Localized recurrent excitation in the dentate gyrus of a cortical contusion model of posttraumatic epilepsy. *Epilepsia* 50 (S7). Selected for platform presentation.

Smith BN, **Hunt RF**, Haselhorst LA, Bach EC, Rios-Pilier J, Schoch KM, Scheff SW, and Saatman KE (2009) Posttraumatic epileptogenesis is associated with injury severity after cortical contusion head injury. *Epilepsia* 50 (S7).

Hunt RF, Haselhorst LA, Bach EC, Rios-Pilier J, Schoch KM, Scheff SW, Saatman KE, and Smith BN (2009) Relationship between injury severity and posttraumatic epileptogenesis after controlled cortical impact in mice. Soc Neurosci Abstr.

Hunt RF, Scheff SW, Smith BN (2008) Seizures and recurrent excitatory connections in the dentate gyrus of mice after controlled cortical impact injury. *Epilepsia* 49 (S7).

Hunt RF, Scheff SW, Smith BN (2008) Seizures and long-term changes in network excitability in the dentate gyrus of mice after experimental brain injury. *Soc Neurosci Abstr*. 34:250.1

Hunt RF, Bhaskaran MD, Stephens LB, Smith BN (2007) Epileptiform activity with low to moderate mossy fiber sprouting in the dentate gyrus of FVB/N mice following pilocarpine-induced status epilepticus. *Epilepsia* 48(S6): 296.

SEMINARS

Mar 2008 "Controlled cortical impact: a mouse model of posttraumatic epilepsy." Department of Physiology, University of Kentucky Medical College.

TEACHING ACTIVITIES

2006 **Graduate Teaching Assistant**
Dept of Cell & Molecular Biology, Tulane University
Course: General Biology
Role: Help session instructor, hold office hours and proctor examinations

2005 **Teaching Assistant**
Dept of Biology & Chemistry, Liberty University
Course: Biochemistry I
Role: Laboratory Assistant

2005 **Undergraduate Tutor**
Bruckner Learning Center, Liberty University
Role: Tutor undergraduate students in Biology, Chemistry, and Math courses

PROFESSIONAL ACTIVITIES

Professional Memberships

2009-*present* American Physiological Society
2006-*present* American Epilepsy Society
2006-*present* Society for Neuroscience
2006-2010 Bluegrass Chapter Society for Neuroscience

University/ Department Service

2009 Student Advisory Committee, University of Kentucky Medical College